National Institute of Public Health and Environmental Protection, Bilthoven
DLO Winand Staring Centre for Integrated Land, Soil and Water Research, Wageningen
DLO Institute for Forestry and Nature Research, Wageningen

Report no. 733001003

Application of three Forest-Soil-Atmosphere models to the Speuld experimental forest.

A. Tiktak[+], J.J.M. van Grinsven[+], J.E. Groenenberg[◊],
C. van Heerden[+], P.H.M. Janssen[+], J. Kros[◊], G.M.J. Mohren[o],
C. van der Salm[◊], J.R. van de Veen[o] and W. de Vries[◊].

February 1995

+ National Institute of Public Health and Environmental Protection, Dep. Soil and Groundwater research, P.O. Box 1, 3720 BA, Bilthoven, Netherlands

◊ DLO Winand Staring Centre for Integrated Land, Soil and Water Research, P.O. Box 125, 6700 AC WAGENINGEN, Netherlands.

o DLO Institute for Forestry and Nature Research, P.O. Box 23, 6700 AA WAGENINGEN, Netherlands

This investigation has been carried out on behalf of and for account of the Directorate-General Environment (DGM/LE) within the framework of the 3rd phase of the Dutch Priority Programme of Acidification (DPPA), theme II: 'Modelling for policy analysis.

MAILING LIST

1	Directeur Lucht en Energie	Drs. G.J.A. Al
2	Directeur Generaal Milieubeheer	H.A.P.M. Pont
3	Plv. DG Milieubeheer	Dr. Ir. B.C.J. Zoeteman
4	Plv. DG Milieubeheer	Mr. G.J.R. Wolters
5	Plv. DG Milieubeheer	Drs. P.E. de Jongh
6	Mr. V.G. Keizer (DGM/LE)	
7	Drs. H. Marseille (DGM/LE)	
8	Ir. B.A. Kleinbloesem (SEP)	
9	Drs. Z. Jeuring (EZ)	
10	Dr. R. van Venetië (LNV)	
11	Prof. Dr. K. Verhoeff (LNV)	
12	Ir. F.C. Zuidema (LNV)	
13	Drs. M.M. Dorenbosch (VROM/L)	
14	Prof. Dr. J.D. Aber (Univ. New Hampshire)	
15	Dr. G.I. Ågren (Swedish Agric. Univ., Uppsala)	
16	Dr. P. Arp (Univ. New Brunswick, Fredericton)	
17	Dr. K. Bellman (PIK, Potsdam)	
18	Dr. J.J.M. Berdowski (TNO)	
19	Prof. Dr. F. Berendse (Agricultural University, Wageningen)	
20	Ir. F.J. Bianchi (IBN-DLO, Wageningen)	
21	Dr W. Bleuten (Univ. Utrecht)	
22	Prof. Dr. H. Bossel (Univ. Kassel)	
23	Drs. F.C. Bosveld (KNMI, De Bilt)	
24	Dr. W.J. Bouma (CSIRO, Aspendale)	
25	Dr. Ir. W. Bouten (Univ. Amsterdam)	
26	Dr. M. Bredemeier (Forschungszentrum Waldökosystemen, Göttingen)	
27	Prof. Dr. Ir. N. van Breemen (Agric. Univ. Wageningen)	
28	J. van de Burg (IBN-DLO)	
29	Dr. T.E. Burk (Dept. Forest Res., Minnesota)	
30	Dr. M.G.R. Cannel (Inst. of Terrestrial Ecol., Penicuik)	
31	Prof. Dr. J. Cermak (Inst. Forest Ecol., Brno)	
32	Dr. J. Cerny (Czech Geol. Serv., Prague)	
33	Ing. M. Cerny (IFER, Prague)	
34	Dr. M.R. Church (US EPA, Env. Res. Lab., Corvallis, OR)	
35	Dr. B.J. Cosby (Dept. Env. Sciences, Virginia Univ., Charlottesville)	
36	Dr. D. van Dam (WAU, Wageningen)	
37	Dr. E. Dambrine (INRA - CRF, Champenoux)	
38	Dr. H.F.G. van Dijk (Univ. Nijmegen)	
39	Dr. N. Dise	
40	Drs. J.C.R. Dopheide (Univ. Amsterdam)	
41	Dr. C.T. Driscoll (Dept. Civil. Env. Eng., Syracuse)	
42	Dr. T. Dueck (IPO-DLO, Wageningen)	
43	Dr. H. Eckersten (Swedish Univ. Agric. Sci., Uppsala)	
44	Dr. L. van der Eerden (IPO-DLO, Wageningen)	
45	Prof. Dr. R. Feddes (Agricultural University, Wageningen).	
46	Dr. R.C. Ferrier (Macaulay Land Use Res. Inst., Aberdeen)	
47	Prof. Dr. H. Flühler (ETH-Zentrum, Schlieren)	
48	Dr. A.D. Friend (ITE, Midlothian)	
49	Dr. T. Frogner (NISK, Ås)	
50	Ir. A. Gärdenäs-Reurslag (Swedish Univ. Agric. Sci., Uppsala)	
51	Dr. Ir. A.J. Gijsman (AB-DLO)	
52	Prof. Dr. C. Gracia (CREAF, Barcelona)	
52	Dr. R. Grote (PIK, Potsdam)	
53	Dr. P. Hari (Inst. Forest Ecol., Helsinki)	
54	Dr. M. Hauhs (BITÖK, Bayreuth)	
55	Dr. Ir. T.J. Heimovaara (UvA, Amsterdam)	
56	Dr. Ir. P. Hofschreuder (Agric. Univ. Wageningen)	
57	Prof. Dr. L. Hordijk (Agric. Univ. Wageningen)	

58 Prof. M. Hornung (Inst. Terrestrial Ecol., Crange-over-Sands)
59 Dr. J. Hýsek (Forestry and Game Res. Inst., Prague)
60 Dr. H. Ilvesniemi (Inst. Forest. Ecol., Helsinki)
61 Prof Dr. P.G. Jarvis (Inst. of Ecol. and Res. Management, Edinburgh)
62 Dr. A. Jenkins (Inst. of Ecol. and Res. Management, Edinburgh)
63 Dr. H. Johnson (Swedish Univ. Agric. Sci., Uppsala)
64 Dr. D.W. Jonhson (Desert Research Inst., Reno, Nevada)
65 Dr. H. Kage (PIK, Potsdam)
66 Dr. J. Kamari
67 Prof. Dr. S. Kellomäki (Faculty Forestry, Joensuu)
68 Prof. Dr. H. van Keulen (AB-DLO, Wageningen)
69 Drs. K. Kramer (IBN-DLO, Wageningen)
70 Dr. H. Krieger (Univ. Kassel)
71 Prof. Dr. S. Linder (Swedish Univ. Agric. Sci., Uppsala)
72 Dr. D. Loustau (INRA, Centre de Recherces de Bordeaux)
73 Dr. R.J. Luxmoore (Oak Ridge National Lab., Oak Ridge)
74 Dr. R.E. McMurtrie (Univ. of New South Wales, Kensington)
75 Ing. W.W.P. Jans (IBN-DLO, Wageningen)
76 Dr. M. Jansen (FG Umweltsystemanalyse, Kassel)
77 Dr. P-E. Jansson (Swedish Univ. Agric. Sci., Uppsala)
78 Dr. A. Jenkins (Inst. Hydrol., Wallingford)
79 Mrs. C. Jonsson (Univ. of Lund)
80 Dr. H. Kage (Inst. Klimatforschung, Berlin)
81 Dr. Ir. W.G. Keltjens (Agric. Univ. Wageningen)
82 Dr. P.J. Kowalik (Techn. Univ. Gdansk)
83 Dr. N. Kräuchi (ETH-Zentrum, Zürich)
84 Mrs. S. Kvindesland (Norw. For. Res. Inst., Ås)
84 Dr. N.P. Lamersdorf (Univ. Göttingen)
85 Ir. M.P. van der Maas (AB-DLO, Wilhelminadorp)
86 Dr. B. Manderscheid (BITÖK, Bayreuth)
87 Dr. A. Lükewille (Umweltbundesamt, Berlin)
88 Dr. E. Mälkönen (Finnish. For. Res. Inst., Vantaa)
89 Dr. E. Matzner (BITÖK, Bayreuth)
90 Dr. H. Meesenberg (Niedersachsische Forstliche Versuchsanstalt, Göttingen)
91 Dr. Ir. J. Mulder (NISK, Norway)
92 Dr. L.-O Nilsson (Swedish Univ. Agric. Sci., Uppsala)
93 Dr. M. van Noordwijk (AB-DLO, Haren)
94 Dr. Ir. H. van Oene (Wageningen)
95 Ir. A.F.M. Olsthoorn (IBN-DLO)
96 Dr. Tönu Oja (Tartu Univ., Tartu)
97 Prof. Dr. T. Paces (Czech. Geol. Survey, Prague)
98 Ing. Th. Pape (Agric. Univ. Wageningen)
99 Prof. F. Penning-de Vries (AB-DLO, Wageningen)
100 Dr. K. Postek (Dept. Civil. Env. Eng., Syracuse)
101 Prof. Dr. H. Pretzsch (Univ. München)
102 Dr. J. Ranger (INRA, Centre de Recherches Forestieres de Nancy)
103 Dr. L. Rasmussen (Danish Forest & Landscape Res. Inst., Lyngby)
104 Ir. G.J. Reinds (Winand Staring Centre, Wageningen)
105 Prof. Dr. J. Reuss (US Forest Service, Fort Collins)
106 Dr. K.S. Richards (Dept. Geography, Cambridge)
107 Dr. J.G.M. Roelofs (Univ. Nijmegen)
108 Dr. W. Robertson (Inst. Terrestrial Ecol., Grange-over-Sands)
109 Dr. R. Røren (Norw. For. Res. Inst., Ås)
110 Prof. Dr. B. Saugier (Lab. Ecologie Vegetale, Paris)
111 Drs. M.P. Schaap (Univ. Amsterdam)
112 Dr. P. Schall (Techn. Univ. München)
113 Dr. J.L. Schnoor (Univ. Iowa)
114 Dr. R. Sievänen (Finnish. For. Res. Inst., Helsinki)
115 Dr. W. Sloan (Inst. Hydrology, Wallingford)
116 Ir. S.M. Smeulders (VROM/LE, The Hague)
117 Dr. E. Steingröver (IBN-DLO, Wageningen)

118 Dr. P. Sollins (Forest Science Dept., Oregon Univ., Corvallis)
119 Dr. T.A. Sogn (Agric. Univ Norway, Ås)
120 Prof. Dr. H. Sverdrup (Univ. of Lund)
121 Dr. A. Tietema (Univ. Amsterdam)
122 Dr. J.A. Tomé (Dept. For., Lisboa)
123 Drs. A.E.G. Tonneijck (IPO-DLO)
124 Dr. H.J.P.A. Verkaar (IBN-DLO, Wageningen)
125 Drs. A. Vermetten (Agric. Univ. Wageningen)
126 Prof. Dr. J.M. Verstraten (Univ. Amsterdam)
127 Dr. Ir. P.H.B. de Visser (Agric. Univ. Wageningen)
128 Dr. P. Warfvinge (Univ. of Lund)
129 Dr. D.A. Weinstein (Boyce Thompson Inst., Ithaca)
130 Dr. P.G. Whitehead (Inst. Hydrology, Wallingford)
131 Dr. P. de Willigen (AB-DLO, Haren)
132 Dr. P.G. Whitehead (Inst. Hydrol., Wallingford)
133 Dr. R.F. Wright (NISK, Ås)
134 Dr. R. Yanaï (Boyce Thompson Inst., Ithaca)
135 Dr. S.E.A.T.M. Van der Zee (Agric. Univ. Wageningen)
136 Bibliotheek IBN-DLO
137 Bibliotheek SC-DLO
138 Depot Nederlandse Publicaties en Nederlandse Bibliografie
139 Directie Rijksinstituut voor Volksgezondheid en Milieuhygiëne
140 Ir. F. Langeweg
141 Ir. R. van den Berg
142 Dr. Ir. C.R. Meinardi
143 Dr. Ir. T. Schneider
144 Ir. G.J. Heij
145 Drs. R.J.M. Maas
146 Ir. A.H.M. Bresser
147 Dr. L.C. Braat
148 Drs. A.H. Bakema
149 Drs. K.F. de Boer
150 Dr. G.P.J. Draaijers
151 Dr. J.W. Erisman
152 Dr. J. Freijer
153 Ing. R.M. Kok
154 Dr. Ir. A. Leijnse
155 Ing. G.B. Makaske
156 Ir. J.G. van Minnen
157 Drs. R. Meijers
158 Dr. J.P. Hettelingh
159 Dr. M. Posch
160 Ir. L.J.M. Boumans
161 Dr. P.S.C. Heuberger
162 Dr. Ir. L.G. Wesselink
163 Drs. F.G. Wortelboer
164 Hoofd Bureau Voorlichting en Public relations
165-166 Bibliotheek RIVM
167 Bureau Projecten- en Rapportenregistratie
168-207 Authors
208-250 Reserve

TABLE OF CONTENTS

MAILING LIST ii

TABLE OF CONTENTS v

PREFACE AND ACKNOWLEDGEMENTS vii

ABSTRACT viii

SAMENVATTING 1

1 INTRODUCTION 3
- 1.1 Background: the 1st and 2nd phases of DPPA 3
- 1.2 The 3rd phase: from regional models to stand-level models 4
- 1.3 Objectives 4
  - 1.3.1 Model validation 5
  - 1.3.2 Stress assessment 5
  - 1.3.3 Critical deposition loads and criteria 5
  - 1.3.4 Scenario analyses 6
  - 1.3.5 Major uncertainties 6
- 1.4 Set-up of this report 7

2 THE MODELS 9
- 2.1 Introduction 9
- 2.2 Hydrology 11
  - 2.2.1 Potential evapotranspiration 12
  - 2.2.2 Canopy interception 13
  - 2.2.3 Potential transpiration and soil evaporation 14
  - 2.2.4 Soil water transport 15
  - 2.2.5 Actual transpiration 15
- 2.3 Nutrient cycling 16
  - 2.3.1 Canopy interactions 16
  - 2.3.2 Litterfall and root decay 17
  - 2.3.3 Mineralization 17
  - 2.3.4 Uptake of nutrients by roots 19
  - 2.3.5 Nitrogen transformations 21
- 2.4 Geochemical process formulations 21
  - 2.4.1 Rate limited reactions 21
  - 2.4.2 Equilibrium reactions 22
- 2.5 Forest growth 23
- 2.6 Forest stress 26

3 THE DATA-SET 29
- 3.1 Introduction: The Speuld site 29
  - 3.1.1 General characteristics of the Speuld site 29
  - 3.1.2 Representability of the Speuld stand 29
- 3.2 Climate, weather and water fluxes in throughfall 30
- 3.3 Air pollution and deposition 32
  - 3.3.1 Throughfall and bulk precipitation measurements 32
  - 3.3.2 Historical deposition data 33
- 3.4 Hydrology 34
  - 3.4.1 Vegetation dependent properties 34
  - 3.4.2 Soil physical characteristics 35
  - 3.4.3 Soil hydrology 35

3.5 Soil chemistry 37
3.5.1 Solid phase characteristics 37
3.5.2 Soil solution composition 39
3.5.3 Model parameters 39
3.6 Forest growth 42
3.6.1 Tree compartments 42
3.6.2 Basic stand data as input to the models 45

4 MODEL CALIBRATION 47
4.1 Strategy 47
4.1.1 The characteristics of the data-set 47
4.1.2 Parameters that need calibration 48
4.1.3 Model performance criteria 49
4.1.4 Solution of the calibration procedure 50
4.2 Hydrology 51
4.2.1 Interception and throughfall 51
4.2.2 Soil water contents 52
4.2.3 Transpiration, soil evaporation and drainage 53
4.2.4 Conclusion 54
4.3 Soil chemistry 54
4.3.1 Soil solution concentrations 54
4.3.2 Element budgets 59
4.4 Forest growth and foliar chemistry 60
4.4.1 Biomass 60
4.4.2 Nutrient contents 61
4.4.3 Nutrient cycling 62
4.5 Simulated manipulation experiments 62

5 SCENARIO ANALYSES 65
5.1 Deposition scenarios 65
5.2 The generic data-set 66
5.2.1 Hydrology 66
5.2.2 Soil chemistry 68
5.2.3 Forest growth and nutrient cycling 70
5.3 Results for region 'Veluwe' 72
5.3.1 Hydrology 72
5.3.2 Soil chemistry 73
5.3.3 Forest growth 79
5.4 Comparison of results for the three deposition scenarios 81
5.5 Comparison of results of ReSAM and NuCSAM 83

6 GENERAL DISCUSSION AND CONCLUSIONS 85
6.1 Model validation 85
6.2 Stress assessment 86
6.3 Critical values 87
6.4 Scenario analyses 87
6.5 Major uncertainties 88
6.6 Recommendations for future research 88
6.7 Major conclusions 89

7 REFERENCES 91

PREFACE AND ACKNOWLEDGEMENTS

This report presents the results of the modelling theme within the Dutch Priority Programme on Acidification (DPPA3; theme II). The following projects were part of this theme:

- Development and application of methods for calibration of DAS models, both on a regional scale as at the site level (P.H.M. Janssen and P.S.C. Heuberger, National Institute of Public Health and Environmental Protection).
- Modification of the integrated forest-soil model SoilVeg (C. van Heerden, A. Tiktak and J.J.M. van Grinsven, National Institute of Public Health and Environmental Protection).
- Extension of the soil acidification model ReSAM towards a soil acidification and nutrient cycling model (NuCSAM) on the stand level (J. Kros, J.E. Groenenberg, C. van der Salm and W. de Vries, DLO-Winand Staring Centre).
- Development and validation of an integrated forest stand model for long-term analysis (G.M.J. Mohren and J.R. van de Veen, DLO-Institute of Forestry and Nature Research).

In 1991, the modellers working in the field of integrated modelling set-up a working group on integrated, stand-level modelling. Besides the participants in the above described four projects, this working group consisted of D. van Dam (Wageningen Agricultural University) and J.G. van Minnen (National Institute of Public Health and Environmental Protection). Two major products of the working group were:

- The organisation of an international Workshop on comparison of integrated Forest-Soil-Atmosphere Models (Van Grinsven *et al.*, 1995). This workshop was held in Leusden between May 10 and 14, 1993. During this workshop, concepts and performance of 18 models were discussed. Model performance was analysed by applying the models to the Solling Norway Spruce site. All Dutch model groups participated in the workshop, thus placing the modelling activities in an international perspective. The workshop was sponsored by the European Communities, DPPA and RIVM.
- The application of the models to the Speuld experimental forest. Results of this application are described in this report.

The working group further organised discussion sessions on subjects relevant to this theme, and coordinated various aspects of the programme (compilation of data-sets for calibration and validation, development of common model modules, etc). For certain discussion sessions, researchers working in other (mostly experimental) fields were invited.

The realization of this report could never have been accomplished without the help of many individuals, and without financial support by the Dutch Priority Programme on Acidification. F. Bianchi (DLO-Institute for Forestry and Nature Research) helped in making the data available. I acknowledge all experimental researchers, in particular those who made the Speuld data-set available. Data were originally collected by M.P. van der Maas, Th. Pape, N. van Breemen, P. de Visser (Wageningen Agricultural University), W. Bouten, J.J.M. Verstraten, (University of Amsterdam), E.G. Steingröver, W.W.P. Jans, A.F.M. Olsthoorn (DLO-Institute for Forestry and Nature Research), J.W. Erisman (National Institute of Public Health and Environmental Protection), and many others whose name cannot be mentioned here.

We hope that this report, together with the proceedings of the Solling workshop, will provide new insights into forest stress relationships. But more than that, we hope that it will stimulate researchers, both in the Netherlands and abroad, to continue research into forest stress relationships. There is still a lot of work to be done!

The Authors

January 3, 1995

ABSTRACT

Large efforts have been dedicated to investigate effects of atmospheric deposition of sulphur and nitrogen on trees and soil at the forest stand level. For this purpose intensive monitoring programs and integrated models of the water, carbon and nutrient cycle have been developed. This report describes an application of the nutrient cycling and soil acidification model NuCSAM and the integrated water, carbon and nutrient cycling models SoilVeg and ForGro to the Speuld site, a Douglas fir stand on a Cambic podzol. This site was monitored between 1987 and 1991. The models were parameterized and calibrated for this site. Simulated soil water contents, soil solution chemistry, foliage biomass and nutrient status and stem growth between 1987 and 1991 were comparable with observations. However, the models showed large differences with respect to quantities that could not be measured, such as transpiration, leaching fluxes, root uptake fluxes and mineralization fluxes. The generality of the integrated models was further tested by an approximate simulation of a site irrigation and fertigation experiment at a nearby Douglas fir stand between 1987 and 1991. The direction and magnitude of simulated effects of irrigation and fertigation on stem growth, litter fall and needle nutrient status were generally right, but the observed enhanced nitrogen mineralization could not be simulated. Simulation of site response to three Dutch deposition scenarios between 1994 and 2050 showed large differences between the three models, particularly for nitrogen cycling and foliage nutrient status. Nevertheless, all models indicate a fast response of soil solution chemistry to changing deposition. Both SoilVeg and ForGro indicate that direct effects of elevated ozone and SOx concentrations in the atmosphere, and effects of pH and the Al concentration in the soil solution are subsidiary to effects of drought and nitrogen. Our understanding of effects of acid atmospheric deposition on forests, which is based on laboratory experiments, short monitoring studies and integrated simulation is inadequate to quantitatively predict the long-term impact of forests on a nationwide scale.

Key words
acidification, nitrogen deposition, forest-growth, forest-stress assessment, monitoring, models, irrigation, fertigation, scenario studies, uncertainties, simulation.

SAMENVATTING

De invloed op bossen van de depositie van zwavel en stikstof, ozon en van 'traditionele' stress factoren (zoals droogte) werd in de afgelopen jaren op grote schaal onderzocht. Hiertoe zijn een aantal intensieve monitoring studies opgezet en werden modellen van de kringloop van water, nutriënten en assimilaten ontwikkeld. Dit rapport beschrijft de toepassing van het bodemverzuringsmodel NuCSAM, en de geïntegreerde modellen SoilVeg en ForGro op het Speulderbos, een Douglas-opstand op een holtpodzol. In dit bos werd van 1987 t/m 1991 een uitgebreide meetcampagne uitgevoerd. De gesimuleerde bodemwatergehalten, concentraties van stoffen in het bodemwater, naaldmassa's, stam-aanwas en nutriëntenstatus kwamen redelijk goed overeen met de metingen. De modellen vertoonden echter aanzienlijke onderlinge verschillen op het gebied van grootheden welke niet gemeten konden worden, zoals bosverdamping, drainage, nutriëntenopname en mineralisatie. Het gedrag van de geïntegreerde modellen werd geverifieerd door toepassing van deze modellen op een irrigatie- en fertigatie experiment op een nabij gelegen Douglas opstand. De modellen konden in het algemeen de effecten van irrigatie en fertigatie op de stam-aanwas redelijk goed voorspellen, maar er waren grote verschillen wat betreft de voorspelde nutriënten status en de stikstof-mineralisatie. De modellen werden vervolgens gebruikt voor scenario analyses voor de periode 1994-2050. Ook hier werden grote verschillen tussen de modellen gevonden voor met name de stikstofkringloop en de nutriënten status (met name het N-gehalte in bladeren). Alle modellen voorspelden dat de concentraties van sulfaat en aluminium in de bodemoplossing snel omlaag gaan na een afname van de verzurende depositie, en dat de concentratie van nitraat een aantal jaren hoog blijft na een afname in de stikstofdepositie. Dit laatste wordt veroorzaakt door opslag van een overmaat aan stikstof in de biomassa en het strooisel. Uit de resultaten van de geïntegreerde modellen blijkt verder dat de directe effecten van verhoogde SOx en ozon concentraties in de atmosfeer, alsmede de indirecte effecten van een lage pH en hoge aluminium concentratie een minder groot probleem opleveren dan de effecten van droogte en de overmaat aan stikstof. Onze kennis van de effecten van luchtverontreining en zure depositie op bossen is in het algemeen gebaseerd op laboratoriumstudies en korte monitoring studies. Tot dusverre is het bijna onmogelijk om effecten die in het laboratorium gevonden werden te vertalen naar de veldsituatie. Zolang dit het geval is, blijft elke voorspelling en extrapolatie die met geïntegreerde modellen gedaan wordt onzeker, zeker als het gaat om de voorspelling van effecten op een landelijke schaal.

Trefwoorden
verzuring, stikstofdepositie, effecten, bossen, monitoring, modellen, irrigatie, fertigatie, scenario-studies, onzekerheden, bosgroei, simulatie.

1 INTRODUCTION

1.1 Background: the 1st and 2nd phases of DPPA

During the first two phases of the Dutch Priority Programme on Acidification (DPPA), the integrated Dutch Acidification Systems (DAS) model has been developed (Heij and Schneider, 1991). This model aims at evaluating the long-term effectiveness of acidification abatement strategies on a number of receptor systems (forests, forest-soils, heathland and aquatic ecosystems). The model describes the complete causality chain from emissions to effects in a regionalized way. Important effect modules within DAS are the forest soil model ReSAM and the forest-growth model SoilVeg-2. The time-step of all DAS modules is one year.

The DAS model was used for scenario analysis at the end of the 2nd phase of DPPA (Heij and Schneider, 1991; Tiktak *et al.*, 1992). The scenarios were based on abatement strategies announced in the National Dutch Environmental Policy Plan Plus ($NEPP^+$). Some conclusions with respect to forest soils and forests, based on results from ReSAM and SoilVeg-2, were:

- deposition reduction leads to a fast (almost instantaneous) improvement in soil solution chemistry, i.e. an increase in pH and a reduction of the Al/Ca and NH_4/K ratio's,
- the exceedance of the critical Al concentration in the soil solution decreased from about 75% of the total forest area now to 40% in 2000, the exceedance of the critical Al/Ca ratio reduced from about 65% to 40%,
- a reduction of the acid deposition to 1200 $mol_c\ ha^{-1}\ a^{-1}$ was needed to stop the exhaustion of the pool of secondary aluminum compounds. These hydroxides provide an important pool for buffering protons,
- the nitrogen content of needles exceeded the critical level of 1.8% between 1970 and 2000 in all areas with high NH_x deposition.
- forest growth was stimulated by high nitrogen deposition during the period 1970-1990 in relatively unpolluted areas. In the polluted areas of the South-Eastern part of the Netherlands, negative aspects of high deposition rates prevailed,
- high levels of SO_2 and O_3 reduced photosynthesis by only 5%, whereas indirect effects, such as the reduction of magnesium uptake by plant roots due to high aluminum concentrations in the soil solution could be as high as 20%.

At the end of the 2nd phase of DPPA, there remained some important shortages in the integrated models:

- it was not possible to distinguish natural stresses[1] from anthropogenic stresses,
- the forest growth module SoilVeg-2 (Berdowski *et al.*, 1991) was only applied to Douglas fir (and not to important species such as Scots pine),
- the modules were not or only partly validated. None of the modules were applied to the stand level, which is the most appropriate level for validating this type of models as most measurements are carried out at this particular level of detail. The forest soil

[1] A stress is defined as a condition that reduces the effectiveness of plant processes (not necessarily causing damage to the plant) or reduces plant structure directly (Van Heerden & Yanaï, 1994). Conditions leading to natural stress are drought, frost and plagues. For this report relevant conditions leading to anthropogenic stresses are air pollution, acid deposition and nitrogen deposition.

module ReSAM (De Vries *et al.*, 1995a) was validated against a regional data-set containing data from 150 forest stands (De Vries *et al.*, 1992). However, as this data-set only represented one point in time, validation of the predicted changes in time could not be carried out.

- Within the forest module SoilVeg-2, forest stress was calculated on the basis of regressions between environmental conditions on the one hand and photosynthesis and uptake on the other. Parameterization of such relationships strongly depends on results from process-oriented models that include the essentials of whole-tree physiology, such as the model ForGro (Mohren, 1987; Mohren *et al.*, 1993). ForGro has been developed within the framework of DPPA to achieve a quantitative estimate of forest growth reduction due to natural stress factors versus the reduction due to air pollution and soil acidification. At the end of the 2nd phase, the results of ForGro and SoilVeg-2 were not compared with each other. Moreover, effects of nutrient limitations on forest growth were not simulated by ForGro.

1.2 The 3rd phase: from regional models to stand-level models

Two of the research questions in §1.1 (distinguishing natural stresses from anthropogenic stresses and model validation) require models with a higher temporal resolution than for regional applications for the following reasons: (i) conditions leading to forest stress (for example drought) cannot be simulated with models that use a yearly time-step (see for example Tiktak and Bouten, 1992) and (ii) yearly average concentrations cannot be compared directly to measurements as these show high temporal dynamics. In order to answer these questions, the DAS modules SoilVeg-2 and ReSAM were extended to stand-level models SoilVeg-3 and NuCSAM by:

- incorporation of a hydrological module to simulate daily soil water contents and soil water fluxes in both upward and downward direction,
- incorporation of a heat transport module to simulate the seasonal and depth variation of soil temperatures,
- incorporation of a solute transport module to simulate upward and downward solute transport.
- incorporation of temperature dependence in the formulations for biogeochemical processes to simulate these processes on a daily basis.

In addition:

- NuCSAM was extended with modules for dissolution of iron and cycling of phosphorous,
- ForGro was coupled to NuCSAM to simulate effects of nutrient limitations on forest growth,
- NuCSAM was extended with a more detailed description of mineralisation, and
- NucSAM was extended with a chemical equilibrium module, EPIDIM (Groenendijk, 1995), to account for ion speciation.

1.3 Objectives and general methodology

The main objectives of the projects within the modelling theme were:

- Validation of the DPPA-2 forest and forest soil models (ReSAM and SoilVeg-2),
- Quantification of forest growth in relation to natural stress factors, air pollution, atmospheric deposition, soil acidification and disturbed nutrient cycling,
- Assessment of the major model uncertainties,
- Verification of critical loads and critical levels,

- Extrapolation of the present state of forest and forest soil into the future for various deposition scenarios.

1.3.1 Model validation

One of the most important reasons for developing the DPPA-3 stand-level models was validation and building scientific justification for the regional (DPPA-2) models. The regional models, which aim at predicting long-term changes, cannot be validated with results from relatively short (3-10 years) monitoring programmes. Therefore, validation of these models was carried out in two steps. First, the results of the three stand-level models (NuCSAM, SoilVeg-3 and ForGro) were directly compared to measurements at two sites. Then, the results of the stand-level model NuCSAM was compared to results of the regional model ReSAM. For validation, the following two intensively monitored sites were chosen:

- a Dutch Douglas fir stand in the Speulderbos (one of the so called experimental AciForN sites). Data on forest hydrology, soil chemistry and tree growth were available for the period 1986-1990 (Heij & Schneider, 1991; Evers *et al.*, 1987).
- a Norway Spruce stand at Solling (Germany). Monitoring data were available for the period 1969-1990. Although the data-set is focused on soil chemistry and nutrient cycling, the data-set is very suitable for validation of the models over a longer time span (Bredemeier *et al.*, 1995; Tiktak *et al.*, 1995). This exercise was carried out as part of an international workshop on comparison of Forest-Soil-Atmosphere Models (Van Grinsven *et al.*, 1995).

1.3.2 Stress assessment

Several hypotheses that link forest growth and forest vitality to air pollution, atmospheric deposition, soil acidification and disturbed nutrient cycling have been developed. Examples are the Al-toxicity hypothesis (Ulrich, 1983) and the nitrogen saturation hypothesis (Skeffington, 1988). Such hypothetical effect relationships can be tested by applying a mechanistic and comprehensive simulation model to an intensively monitored forest stand. It is clear that under prevailing conditions at such a monitoring site, boundary conditions vary slowly, and the variation in the response of tree and soil are small or non-existent. This knowledge was a major motivation to start experimental manipulation studies (Beier *et al.*, 1993; De Visser, 1994). This approach inspired us to perform manipulation experiments with the models. Simulations were carried out for optimal irrigation and fertilization, reduction of sulphate and nitrogen input in throughfall, and elimination of air pollution.

1.3.3 Critical deposition loads and criteria

Information on critical loads for total acidity and nitrogen are a prerequisite for policy decisions on emission reductions. In the Netherlands, critical loads have been derived indirectly from critical values for ion concentrations or ion ratios in the soil solution (De Vries, 1994). Critical values for forests were mostly derived from pot trials and laboratory experiments. Table 1 gives an overview of these critical values. A full discussion of the various criteria is given in De Vries (1994).

TABLE 1
Critical levels to derive critical loads for forests (De Vries, 1994).

Effect	Criterion	Unit	Value
Nutrient imbalances	NH_4/K ratio in soil solution	(mol mol^{-1})	5
Increased susceptibility[a]	N-content in leaves	(%)	1.8
Damage to the root system	(Al^{3+}) in soil solution	(mol_c m^{-3})	0.2
	Al/Ca ratio in soil solution	(mol mol^{-1})	1.0
Depletion of buffering mechanisms	No depletion of the pool of secondary Al-compounds in the soil		

a) Refers to frost, damage, pests and diseases

Verification of these critical levels was carried out by correlative field studies (e.g. Roelofs *et al.*, 1985). In this study, the integrated models were used to assess the validity of present critical values. We did not aim at deriving alternatives, although models could be useful to redefine critical loads (De Vries *et al.*, 1995c).

1.3.4 Scenario analyses

All models were used to assess the long-term development of soil solution chemistry (in particular Al concentration in the soil solution, Al/Ca ratio, content of secondary aluminum compounds and nutrient status) and forest growth. This goal was achieved by performing scenario analyses for the following two generic forest-soil combinations:

- Douglas fir on a Cambic podzol[1],
- Scots pine on a Haplic arenosol[1].

For both combinations, model simulations were carried out with deposition scenarios that are representative for Dutch regions with low, average and high deposition rates, respectively. It was assumed that in a clean region, the target acid deposition load of 1400 mol_c ha^{-1} a^{-1} (NMP+) is reached in 2010, whereas in average and polluted regions these loads are reached in 2050 and 2100, respectively (Keizer, 1994).

1.3.5 Major uncertainties

One of the problems with calibrating a complicated model is that it is difficult, if not impossible, to find a unique set of model parameters. One way to improve the uniqueness of the obtained calibration is using automated and objective calibration procedures. In view of the large number of model parameters that need calibration, such a calibration procedure is very time-consuming. For this reason, automated calibration procedures have not been applied to the models under consideration, but strict (manual) calibration procedures have been postulated. However, if the uniqueness of the calibration remains questionable, results of scenario analyses are also uncertain. Model uncertainty can be assessed by performing thorough and systematic uncertainty analyses. Confidence in predictions from individual models will also increase when other models predict the same magnitude and trends of model outputs. Therefore, in this study the major model

[1] Soil classification according to FAO (1988). According to the American Soil Taxonomy, these soils can be classified as Typic Dystochrepts and Typic Udipsamments, respectively.

uncertainties were assessed by comparing results from the three stand-level models NuCSAM, SoilVeg-3 and ForGro.

1.4 Set-up of this report

In this report, emphasis is given to the application of the models to the Speuld site. However, as the Solling application provided interesting information on the long-term behaviour of the models and placed our modelling activities in an international perspective, a summary and some major conclusions from this exercise are included. A complete description is found in the proceedings of the workshop (Van Grinsven *et al.*, 1995).

After this introduction, the models are described briefly in chapter 2. A full description of all models can be found in publications by the individual research groups.

Chapter 3 describes the Speuld data-set. The first part of this chapter describes the monitoring site and the common data-set. The last section describes some model specific data.

Chapter 4 describes the Speuld application. This chapter starts with an introduction on methodologies. Then, the parameters that need calibration are described. Finally, some results are presented. Chapter 4 is organized along a disciplinary division of model components, viz. hydrology, chemistry and forest growth. The chapter ends with some results from simulated manipulations experiments. These simulations are inspired by experimental simulations. By 'virtually' eliminating individual stress factors in the model calibrations for Speuld, their effect on growth, nutritional status or soil chemical status can be quantified.

Chapter 5 describes the results of the scenario analyses. The first sections describe the common data-set (scenarios, weather, soil data and forest data). Then, the results are discussed.

Chapter 6 summarizes the most important results and gives the conclusions and recommendations. These conclusions are grouped in the same themes as specified in §1.3 (i.e. objectives and generical methodology).

2 THE MODELS

2.1 Introduction

This report presents the results from five different models or model versions (table 2).

TABLE 2
Acronyms, full names and references for the models described in this paper.

Acronym	Full name	Compartments	Reference
ReSAM	Regional Soil Acidification Model	soil	De Vries *et al.*, 1995a
NuCSAM	Nutrient Cycling and Soil Acidification Model	soil	Groenenberg *et al.*, 1995
SoilVeg-2	Soil Vegetation model, version 2	integrated	Berdowski *et al.*, 1991
SoilVeg-3	Soil Vegetation model, version 3	integrated	Van Heerden *et al.*, 1995
ForGro[a]	Forest Growth Model	integrated	Mohren *et al.*, 1993

[a]) The ForGro version discussed here is linked with NuCSAM as the soil chemistry sub-model.

Table 3 summarizes the most important characteristics of the five models. All models are characterized by a process-oriented, deterministic approach. The DPPA-2 models ReSAM and SoilVeg-2 have specifically been developed to evaluate long-term responses of soils and forests, respectively, to deposition scenarios on a regional scale. For this reason, these models do not include seasonal dynamics (temporal resolution or input/output time-step is one year). On the contrary, the DPPA-3 models (ForGro linked with NuCSAM, NuCSAM and SoilVeg-3) were developed for application and validation on the stand-level (see §1.3). These models simulate seasonal dynamics and require daily input of weather data.

Scenario analysis was the primary aim for developing the regional models ReSAM and SoilVeg-2, but was only a secondary reason for developing the stand-level models. The most important reasons for developing the DPPA-3 models NuCSAM and SoilVeg-3 were validation and stress assessment (§1.3). ForGro serves as a reference model to SoilVeg-2 and SoilVeg-3 with respect to quantification of interactions at the stomatal and root level. SoilVeg contains empirical relationships for the description of stress that can only be validated by comparing the model results with results from a physiological model, such as ForGro. Another reason for developing these models was to built scientific justification for the regional models. These models, which aim at predicting long-term changes, cannot be validated with results from relatively short (3-10 years) monitoring programmes. Therefore, validation of these models was carried out in two steps (see §1.3). Note, however, that regional models sometimes can be validated directly by comparing the model outputs with long-term data-sets. See for example Van der Salm *et al.* (1995) who applied the model ReSAM to the Solling data-set which has a length of more than 20 years. Unfortunately, such long-term data-sets are not available for sites in the Netherlands.

NuCSAM and ReSAM are models that focus on soil chemistry (table 3). To account for the effect of nutrient cycling on soil chemistry in the root zone, fluxes of water and nutrients to and from the tree are described by forcing functions (boundary conditions). ForGro and SoilVeg describe the flow of water, carbon and nutrients both in the tree and in the soil. These two models can be classified as integrated and closed-system Forest-Soil-

Atmosphere models (Landsberg *et al.*, 1991; Tiktak and Van Grinsven, 1995). ForGro contains the most comprehensive description of tree processes. The model is a physiologically based carbon-balance model of forest growth. Most process formulations in SoilVeg have an empirical basis. The major presumption is that indirect effects of acid deposition are of major importance, leading to a model concept in which nutrient availability is a key factor for forest growth, while gross photosynthesis is regarded a boundary condition (Berdowski *et al.*, 1991; Van Heerden *et al.*, 1995).

TABLE 3
Summary of general model characteristics and compartments.

Subject	Model				
	ForGro	NuCSAM	SoilVeg-3	SoilVeg-2	ReSAM
Application scale	stand	stand	stand	regional	regional
I/O time step	day	day	day	year	year
Aims [a]					
scenario analysis	○	○	○	●	●
validation	●	●	●	-	-
stress assessment	●	-[e]	●	○	-[e]
'reference model'	●	●	●	-	-
Compartments [b]					
tree	●	-[d]	●	●	-[d]
soil	●	●	●	○	○
Processes [c]					
deposition/can. interaction	●	○	○	○	○
hydrology	●	●●	●	○	○
heat transport	●	●	●	-	-
geochemistry	●●	●●	●	○	○
nutrient cycling	●●	●	●	○	○
forest growth	●	-[d]	●	○	-[d]

a) Major aim of the model (●), secondary aim of the model (○), or not an aim of the model (-).
b) All major compartments included (●), some compartments lumped (○), or not included (-).
c) Process formulations mechanistic (●●), detailed and partly empirical (●), empirical (○), or not included (-).
d) Forest growth and nutrient uptake included as a forcing function.
e) In an indirect way; through the Al concentration and the Al/Ca ratio in the soil solution.

ReSAM and SoilVeg-2 do not simulate hydrological processes but use yearly average soil water fluxes and root uptake fluxes as calculated with an external hydrological model (SWATRE; Belmans *et al.*, 1983). NuCSAM, SoilVeg-3 and ForGro (see table 4) all include hydrological submodels for calculating snow-fall, canopy water dynamics, forest-floor water dynamics and soil water dynamics. The stand-level models simulate heat transport and soil temperatures on a daily basis, the regional models use average yearly soil temperatures as a boundary condition.

NuCSAM and ForGro contain the most extended description of soil processes (table 4). NuCSAM is derived from ReSAM. The process formulations within all soil chemical modules, although rather complex and process-oriented, have an empirical basis (De

Vries, 1994). The most important extensions of NuCSAM compared with ReSAM are: (i) NuCSAM describes both upward and downward transport of water and solutes, (ii) all processes (transport and biogeochemistry) are described within NuCSAM on a daily basis, (iii) NuCSAM describes the behaviour of iron and phosphorous, (iv) NuCSAM accounts for ion speciation using a chemical equilibrium module (EPIDIM) and (v) a more detailed description of mineralization is included. Phosphorous is included, as it is a major limiting nutrient in Dutch forest soils (Mohren *et al.*, 1986). The biogeochemical process formulations in SoilVeg-2 are derived from ReSAM. In SoilVeg-3, the biogeochemical process formulations were adapted in the same way as in NuCSAM, but iron, phosphorous and ion association were not included.

TABLE 4
Major principles of the stand level models NuCSAM, SoilVeg-3 and ForGro. For further explanation: see text.

Compartment	Model		
	NuCSAM	SoilVeg-3	ForGro
Hydrology (§2.2)	Solution of Richard's equation. Potential transpiration from Makkink and an empirical crop factor	Solution of water content from empirical equations with soil water flux and water uptake. Potential transpiration as in NuCSAM	Solution of water content from an empirical relation with soil water flux. Transpiration from Penman-Monteith.
Nutrient uptake (§2.3)	Forced by stem growth and fixed nutrient contents. N-content driven by deposition.	Driven by water uptake, nutrient concentration in soil solution and selectivity coefficients.	Driven by demand and limited by radial diffusion from the bulk soil to the root.
Soil chemistry (§2.4)	Gaines-Thomas cation exchange. 1st order nitrification and silicate weathering. Elovich Al-hydroxide weathering. Ion speciation.	Equations and parameterization as in NuCSAM. Phosphate is not considered.	ForGro uses NuCSAM as submodel.
Forest growth (§2.5)	Logistic stem growth and fixed biomass ratios.	Gross photosynthesis calculated from transpiration. Multiple nutrient productivity concept. Nutrient allocation age dependent.	Photosynthesis is driven by light interception. Gross carbon assimilation is summed per leaf layer. Fixed allocation scheme.
Effect relations (§2.6)	No effect model. Empirical relation between N-deposition and N-content of foliage.	Empirical reduction of photosynthesis with ambient SO_2 and O_3. Al and pH affect root uptake and root growth. Direct canopy uptake of NH_3.	Nutrient shortage, and stomatal uptake of SO_2 and O_3 in foliage reduce photosynthesis. Al affects root growth and nutrient uptake. Direct uptake of NH_3.

2.2 Hydrology

Figure 1 shows the hydrological cycle in a forest stand. A description of the transport of water is necessary to predict the concentration and amount of solutes in the soil. Further, soil water status will affect most biochemical processes like mineralization, nitrification, denitrification and the uptake of water by plant roots. The stand-level models NuCSAM, SoilVeg-3 and ForGro describe the entire hydrological cycle on a daily basis. In SoilVeg-3

Figure 1
The hydrological cycle in a forest stand.

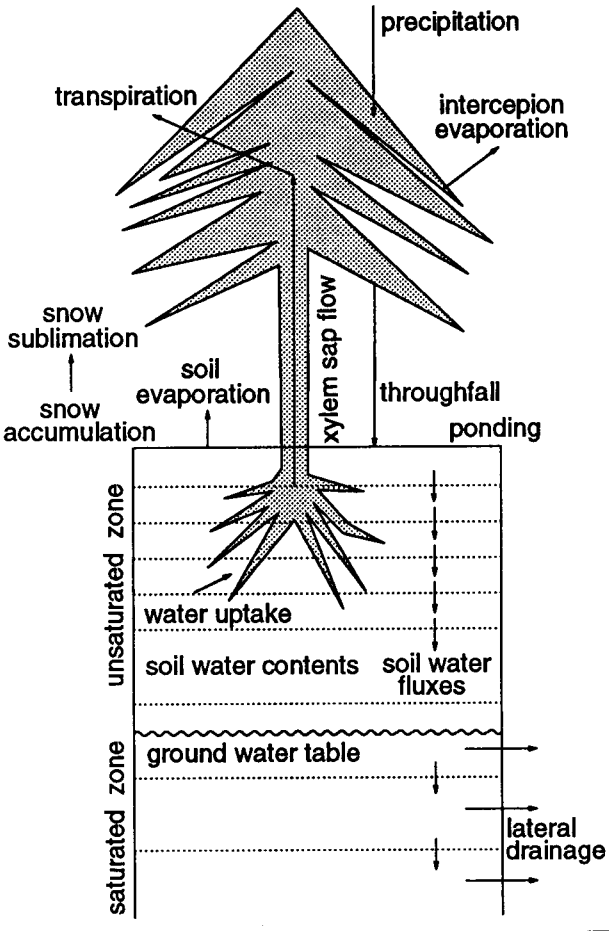

and ForGro, the hydrological submodel is an integral part of the model. In this way, dynamic feed-backs between hydrological processes on the one hand and forest growth and nutrient uptake on the other, can be simulated. NuCSAM uses soil water fluxes, soil water contents, etc. simulated by a stand-alone hydrological model (an adapted version of the SWATRE model (Belmans *et al.*, 1983)). In the regional models ReSAM and SoilVeg-2, average yearly soil water fluxes and soil water contents as calculated with SWATRE (De Visser and De Vries, 1989) were used.

2.2.1 Potential evapotranspiration

The calculation of the maximum or potential evapotranspiration depends on the level of detail and process aggregation of the models. In the most detailed approach, the conductances of the forest canopy for transport of energy and water vapour are explicitly modelled (ForGro). This model uses the Penman-Monteith equation:

$$E_{pm} = \frac{1}{\lambda} \cdot \frac{sR_n + \rho C_p \delta q g_a}{s + \gamma(1 + g_a/g_c)} \cdot f_s \qquad (1)$$

where λ (J g^{-1}) is specific heat of evaporation, E_{pm} (m d^{-1}) the Penman-Monteith potential evapotranspiration, s (g g^{-1} K^{-1}) the derivative of the saturated water vapour curve, R_n (W m^{-2}) energy available at the evaporating surface, ρ (g m^{-3}) density of air, C_p (J g^{-1} K^{-1}) the specific heat capacity of air, δq (g kg^{-1}) specific water vapour deficit at reference level, γ (g g^{-1} K^{-1}) psychrometer constant, g_c and g_a (m s^{-1}) are the canopy and aerodynamic conductances, and f_s (s d^{-1}) is the number of seconds in a day. Equation (1) requires the description of stomatal conductance as a function of time. The stomatal conductance is derived from net-photosynthesis, vapour pressure deficit and foliar water status.

In NuCSAM and SoilVeg-3, the potential transpiration of the stand under consideration is calculated by multiplying the reference evapotranspiration according to Makkink (1957) by an empirical, season dependent crop factor. For conditions in the Netherlands, the Makkink equation is written as:

$$E_r = \frac{\beta}{\lambda} \cdot \frac{s}{s+\gamma} \cdot K\downarrow \cdot f_s \qquad (2)$$

in which E_r (m d^{-1}) is the Makkink reference evapotranspiration, s (g g^{-1} K^{-1}) is derivative of the saturation water vapour pressure temperature curve, γ (g g^{-1} K^{-1}) is psychrometer

constant, $K\downarrow$ (W m^{-2}) is global radiation, λ (J g^{-1}) is specific heat of evaporation and β (-) is empirical constant related to the geographical latitude, which for conditions in the Netherlands is equal to 0.65.

2.2.2 Canopy interception

All models use a relatively simple empirical one-layer canopy-interception submodel. Water is supplied to the canopy by precipitation and lost by throughfall and evaporation of intercepted water:

$$A_{wc} = A_{wc} + \Delta t \cdot (P - TF - E_i) \tag{3}$$

where A_{wc} (m) is amount of water intercepted by the canopy, P (m d^{-1}) is daily precipitation, TF (m d^{-1}) is daily throughfall, E_i (m d^{-1}) is evaporation of intercepted water and Δt (d) is time-step (which is one day).

In all models, the amount of water intercepted is calculated by using a coefficient of free throughfall in combination with a threshold value.

The evaporation of intercepted water, however, is threaded rather differently. In NuCSAM, the calculation of the interception evaporation is based on Gash (1979). The Gash model uses an analytical approximation for the calculation of daily interception. However, unlike the original Gash model, NuCSAM uses daily evaporation rates instead of yearly average evaporation rates. As evaporation rates are lower during rainfall, empirical correction factors have been introduced for the dry and wet part of the day. The simulations start with the calculation of the amount of rainfall required to saturate the canopy, P_s (m):

$$P_s = -\frac{A_{wc,\max}}{E_r \cdot fE_{wet}} \cdot \ln\left(1 - \frac{E_r \cdot fE_{wet}}{\bar{R}} \cdot \frac{1}{sc}\right) \cdot \bar{R} \tag{4}$$

where sc (-) the soil cover fraction, $A_{wc,max}$ (m) the maximum amount of water stored in the canopy, E_r (m d^{-1}) the reference evapotranspiration, fE_{wet} (-) a correction factor for the evaporation rate during rainfall, $\bar{R}$ (m d^{-1}) the average rainfall intensity and P (m) the precipitation. The interception evaporation is now calculated as:

$$\begin{aligned} &\text{if } P < P_s: && E_i = P \cdot sc \\ &\text{if } P \geq P_s: && E_i = P_s \cdot sc + \left(\frac{E_r \cdot fE_{wet}}{\bar{R}}\right) \cdot (P - P_s) \end{aligned} \tag{5}$$

The canopy water storage at the end of the day is calculated as:

$$A_{wc} = A_{wc,o} \cdot \exp\left(-\frac{E_r \cdot fE_{dry}}{A_{wc,\max}} \cdot t_d\right) \tag{6}$$

where A_{wc} (m) is the water storage at the end of the day, $A_{wc,o}$ (m) the water storage at the start of the dry part of the day, fE_{dry} (-) a correction factor for the evaporation rate during

the dry part of the day, and t_d (d) the length of the dry part of the day, which is calculated from the precipitation and average rainfall intensity:

$$t_d = 1 - (P / \bar{R}) \tag{7}$$

In SoilVeg-3, the evaporation of intercepted water is calculated based on estimating the energy contributions from direct radiation, E_r (m d^{-1}) and local advection, E_a (m d^{-1}):

$$E_r = sd \cdot E_o \cdot f(LAI)$$
$$E_a = \frac{\delta T_{max} \cdot T_{air} \cdot (h + h_{sup})\, \rho_{air} \cdot c_{air}}{\rho_w \cdot (c_w \cdot (100 - T_{air}) + \lambda)} \tag{8}$$

where sd (d) is storm duration, f(LAI) (-) is leaf area index dependent correction factor, δT_{max} (d^{-1}) maximum relative temperature change of plant environment, T_{air} (°C) is air temperature, h (m) is vegetation height, h_{sup} (m) is supplemental height representing the air volume above the vegetation from which energy is extracted by advection, c_{air} (J g^{-1} K^{-1}) is heat capacity of air, c_w (J g^{-1} K^{-1}) is heat capacity of water and λ (J g^{-1} K^{-1}) is heat of evaporation of water, ρ_w (kg m^{-3}) is the density of water and ρ_{air} (kg m^{-3}) is the density of air.

2.2.3 Potential transpiration and soil evaporation

In all models, the potential transpiration and potential soil evaporation are calculated by partitioning the potential evapotranspiration on the basis of the available energy by a method equivalent to Van Grinsven *et al.*, 1987 and Tiktak and Bouten, 1992):

$$E^*_{pl} = \max\left[0, \{f_c \,.\, sc \,.\, E_r - f_i \,.\, E_i\}\right]$$
$$E^*_s = (1 - sc) \cdot E_r \tag{9}$$

in which E^*_{pl} (m d^{-1}) is the potential transpiration, E^*_s (m d^{-1}) is the potential soil evaporation, f_c (-) is an empirical factor that accounts for crop characteristics, sc (-) is the soil cover fraction, E_i (m d^{-1}) is evaporation of intercepted water, and f_i (-) is the fraction of the daily interception that reduces the potential transpiration. The gap factor is calculated on the basis of the leaf area index.

In NuCSAM, the actual soil evaporation rate is calculated as a function of time since the last rainfall event according to Black *et al.* (1969):

$$E_s = \varepsilon \,.\, \left(\sqrt{t_d + 1} - \sqrt{t_d}\right) E^*_s \tag{10}$$

where E_s (m d^{-1}) is actual soil evaporation, t_d (d) is time from the start of a drying cycle and ε ($d^{-1/2}$) is an empirical parameter.

In SoilVeg-3, the actual soil evaporation rate is calculated as a function of the water content of the uppermost soil layer:

$$E_s = \min\left(\frac{\theta - \theta_{air}}{\theta_{fc} - \theta_{air}} \cdot E_s^*, E_s^*\right) \quad (11)$$

where θ ($m^3\ m^{-3}$) is volumetric water content, θ_{fc} ($m^3\ m^{-3}$) is water content at field capacity and θ_{air} ($m^3\ m^{-3}$) is air-dry water content.

2.2.4 Soil water transport

The transport of water through the soil is simulated according to a deterministic approach based on Richard's equation (NuCSAM) or an empirical field-capacity model (SoilVeg and ForGro). NuCSAM calculates a numerical solution to the Richard's equation:

$$\frac{\partial\theta}{\partial t} = \frac{\partial}{\partial z}\left[K(h)\cdot\left(\frac{\partial h}{\partial z} + 1\right)\right] - S(h) \quad (12)$$

where θ ($m^3\ m^{-3}$) is volumetric water content, t (d) time, z (m) vertical position in the soil, h (m) soil water pressure head, K (m d^{-1}) hydraulic conductivity and S (d^{-1}) sink term accounting for root water uptake. The model allows for upward water transport. ForGro contains a field-capacity submodel that does not allow for soil water transport at water contents below field-capacity:

$$\begin{aligned} \frac{\partial\theta}{\partial t} &= \frac{\partial(J(\theta))}{\partial z} - S(\theta) \qquad (\theta > \theta_{fc}) \\ \frac{\partial\theta}{\partial t} &= -S(\theta) \qquad\qquad (\theta \le \theta_{fc}) \end{aligned} \quad (13)$$

with J (m d^{-1}) as soil water flux, θ_s ($m^3\ m^{-3}$) saturated volumetric water content, and θ_{fc} ($m^3\ m^{-3}$) volumetric water content at field capacity. The relationship between soil water flux and soil water content in ForGro is derived from the output files of more comprehensive soil water transport models. For the Speuld simulations, the output of the model SWIF (Tiktak and Bouten, 1992) was used, for the Solling case NuCSAM simulations were used. The closed-form relationship between soil water content and soil water flux in SoilVeg-3 allows for upward water transport:

$$J(\theta) = J_{cr} \cdot \left(\frac{\theta^{(a\cdot\theta)} - b}{b - 1}\right) \quad (14)$$

with

$$b = e^{(a\cdot\theta_{fc})}$$

where J_{cr} (mm d^{-1}) is maximum upward flux, and a (-) is a constant. The parameters in this $J(\theta)$ function are estimated from soil physical properties (retention and conductivity characteristics), using a procedure described by Van Grinsven and Makaske (1993).

2.2.5 Actual transpiration

The potential transpiration is distributed among soil layers on the basis of the root length distribution in all models. In NuCSAM and SoilVeg-3, reduction of water uptake occurs when soil water pressure heads (NuCSAM; see Figure 2) or soil water contents (SoilVeg-3) drop below a threshold value. The root water uptake fluxes are summed to get the actual transpiration. SoilVeg-3 allows for compensatory uptake from relatively wet soil layers. In ForGro, the root water uptake flux is simulated using the root resistance and the hydraulic

Figure 2
The water uptake reduction function in NuCSAM.

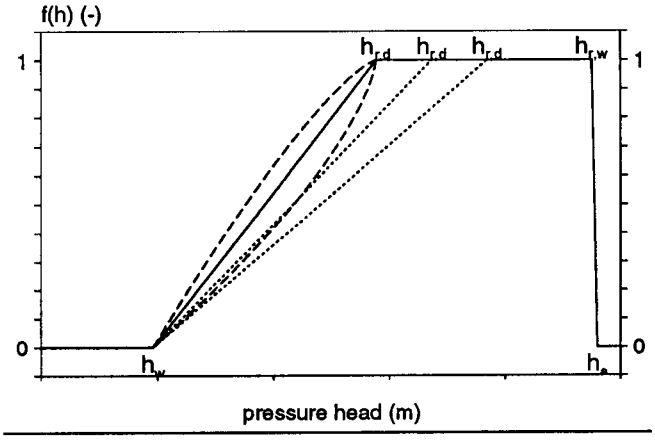

gradient from the bulk soil to the plant. Root resistance depends mainly on rooting density, root radius, and hydraulic conductivity within the rooted zone. In the model semi-empirical expressions are used to quantify these resistances under different circumstances (Gijsman, 1990). In case of restricted soil moisture availability, soil water potential decreases, leading to a decrease in foliage water potential (in MPa), which causes stomatal closure, reducing both transpiration and canopy assimilation. By incorporating this kind of feed-back mechanisms in the model, the effect of drought on growth and exchange of pollutants through the stomata can be studied.

2.3 Nutrient cycling

2.3.1 Canopy interactions

The solute fluxes to the soil surface by throughfall are calculated in NuCSAM, SoilVeg-3 and ForGro from the total deposition corrected for canopy interactions, i.e. foliar uptake and foliar exudation. In all models, foliar uptake of NH_4^+, NO_3^-, SO_4^{2} and H^+ is described as a linear function of the dry deposition of these elements:

$$FX_{fu} = frX_{fu} \cdot FX_{dd} \qquad (15)$$

where FX ($mol_c\ ha^{-1}\ a^{-1}$) refers to the flux of element X, frX_{fu} (-) is the uptake fraction of element X and where the subscript *fu* refers to foliar uptake and *dd* to dry deposition.

In NuCSAM and ForGro, foliar exudation of the base cations NH_4^+ and H^+ is counterbalanced by exchange with Ca^{2+}, Mg^{2+} and K^+ (Draaijers, 1993):

$$FCa_{fe} + FMg_{fe} + FK_{fe} = FNH_{4,fu} + FH_{fu} \qquad (16)$$

where the subscript *fe* refers to foliar exudation and *fu* refers to foliar uptake. The foliar exudation flux of each individual cation, FX_{fe} ($mol_c\ ha^{-1}\ a^{-1}$) is calculated as:

$$FX_{fe} = frX_{fe} \cdot (FNH_{4,fu} + FH_{fu}) \qquad (17)$$

where frX_{fe} (-) is the foliar exudation fraction of Ca^{2+}, Mg^{2+} and K^+. The sum of these fractions equals 1.

In SoilVeg-3, the foliar exudation flux of Ca^{2+}, Mg^{2+} and K^+ is described as a linear function of the amount in the leaves:

$$FX_{fe} = kX_{fe} \cdot A_{lv} \cdot ctX_{lv} \qquad (18)$$

where kX_{fe} (a^{-1}) is the foliar exudation rate constant, A_{lv} ($kg\ ha^{-1}$) is the amount of leaves or needles and ctX_{lv} ($mol_c\ kg^{-1}$) is content of element X in leaves.

2.3.2 *Litterfall and root decay*

Litterfall and root decay are the input to the organic pools of N, P, Ca, Mg, K and S. In NuCSAM, litterfall and root decay are described by first-order rate reactions:

$$FX_{lf} = (1 - frX_{re,lv}) \cdot kX_{lf} \cdot A_{lv} \cdot ctX_{lv} \quad (19)$$

$$FX_{rd} = (1 - frX_{re,rt}) \cdot kX_{rd} \cdot A_{rt} \cdot ctX_{rt} \quad (20)$$

where k_{lf} and k_{rd} (a^{-1}) are the rate constants for litterfall and root decay, A_{lv} *and* A_{rt} (kg ha^{-1}) are the amounts of leaves and fine roots, ctX_{lv} and ctX_{rt} (mol_c kg^{-1}) are the contents of element X in leaves and roots, and $frX_{re,lv}$ and $frX_{re,rt}$ (-) are the reallocation fractions for element X in leaves and fine roots, respectively. The contents of P, Ca, Mg, K and S in leaves and fine roots are assumed to be constant in time. As high contents of nitrogen are caused by high nitrogen deposition rates, the nitrogen content in stems, branches, leaves and fine roots is calculated as a function of nitrogen deposition by ($FN_{td,min} < FN_{td} < FN_{td,max}$):

$$ctN = ctN_{min} + (ctN_{max} - ctN_{min}) \cdot \left(\frac{FN_{td} - FN_{td,min}}{FN_{td,max} - FN_{td,min}} \right) \quad (21)$$

where ctN_{min} and ctN_{max} (mol_c kg^{-1}) are the minimum and the maximum nitrogen content in stems, branches, leaves or fine roots, respectively and $FN_{td,min}$ and $FN_{td,max}$ (mol_c ha^{-1} a^{-1}) are the minimum and the maximum deposition levels between which the nitrogen content in biomass is affected.

SoilVeg and ForGro use the same rate equations, but distinguish between more biomass compartments, i.e. a maximum number of 8 needle age classes, branches, stems, coarse roots and fine roots. For each biomass compartment, a different reallocation fraction is used, but the element content in all needle fractions is assumed equal. The calculation of needle contents in described in the section on forest growth.

2.3.3 *Mineralization*

In SoilVeg-3, for the decomposition of exogenous organic matter (litter) a distinction is made between a rapidly decomposing pool of fresh litter (less than 1 year old) and a slowly decomposing pool of old litter (more than 1 year) (Janssen, 1984). Mineralization of endogenous organic matter is not considered in SoilVeg-3, except for the mineralization from the root necromass. The mineralization flux of N, P, Ca, Mg, K, S and C (mol_c ha^{-1} a^{-1}) from fresh litter is described by a zero order equation:

$$FX_{mi,fl} = \{fr_{le} + fr_{mi} \cdot (1 - fr_{le})\} \cdot FX_{lf} \quad (22)$$

where fr_{mi} (-) is mineralization fraction and fr_{mi} (-) is leaching fraction of element X. Leaching refers to the release of cations directly after litterfall, a process which is especially important for base cations. In SoilVeg, the leaching fraction is set to 1 for all base cations and set to 0 for the other elements. The mineralization flux of N, P, S and C from fresh litter is described by first order kinetics (Van Veen, 1977):

$$FX_{mi,lt} = k_{mi,lt} \cdot A_{lt} \cdot ctX_{lt} \quad (23)$$

where $k_{mi,lt}$ (a^{-1}) is the mineralization rate constant from old litter, A_{lt} (kg ha^{-1}) is the amount of old litter and ctX_{lt} (mol_c kg^{-1}) is the content of element X in old litter. The mineralization of N, P, Ca, Mg, K, S and C from the root necromass is described as:

$$FX_{mi,rn} = k_{mi,rn} \cdot A_{rn} \cdot ctX_{rn} \quad (24)$$

with $k_{mi,rn}$ (a^{-1}) as the mineralization constant of root necromass, A_{rn} (kg ha^{-1}) as the amount of root necromass and ctX_{rn} (mol_c kg^{-1}) as the content of element X in root necromass.

In NuCSAM, both exogenous and endogenous organic matter are distinguished. For the exogenous organic matter, a distinction is made between a litter layer and a fermentation layer. The organic matter in the humus layer is lumped with endogenous organic matter. All equations, except for litter fall fluxes, are first-order rate equations. The mass balances for the litter and fermentation layers (mol_c ha^{-1} a^{-1}) are described by:

$$\frac{d(A_{lt} \cdot ctX_{lt})}{dt} = (1 - fr_{le}) \cdot FX_{lf} - (k_{mi,lt} + k_{hu,lt}) \cdot A_{lt} \cdot ctX_{lt} \quad (25)$$

$$\frac{d(A_{fe} \cdot ctX_{fe})}{dt} = k_{hu,lt} \cdot A_{lt} \cdot ctX_{lt} - (k_{mi,fe} + k_{hu,fe}) \cdot A_{fe} \cdot ctX_{fe} \quad (26)$$

where fr_{le} (-) is the leaching fraction (see also equation (22)), $k_{mi,lt}$ (a^{-1}) is the mineralization constant for the litter layer, $k_{hu,lt}$ (a^{-1}) is the humification constant for the litter layer, $k_{mi,fe}$ (a^{-1}) is the mineralization constant for the fermentation layer and $k_{hu,fe}$ (a^{-1}) is the humification constant for the fermentation layer, ctX_{lt} and ctX_{fe} (mol_c kg^{-1}) are the contents of N, P, K, Ca, Mg and S in the litter and fermentation layers, and A_{lt} and A_{fe} (kg ha^{-1}) are the amounts of litter and fermentation, respectively. For each soil layer within NuCSAM, a mass balance (mol_c ha^{-1} a^{-1}) can be written for the endogenous organic matter:

$$\frac{d(A_{hum,i} \cdot ctX_{hum,i})}{dt} = fr_{hum,i} \cdot (k_{hu,fe} \cdot A_{fe} \cdot ctX_{fe} + k_{mi,rn} \cdot A_{rn} \cdot ctX_{rn} - k_{mi,hum} \cdot A_{hum,i} \cdot ctX_{hum,i}) \quad (27)$$

where $fr_{hum,i}$ (-) is fraction of endogenous organic matter in soil layer i, $k_{hu,fe}$ (a^{-1}) is humification constant for the fermentation layer, $k_{mi,rn}$ (a^{-1}) is mineralization constant for the root necromass, and $k_{mi,hum}$ (a^{-1}) is mineralization constant for the humus layer. The amount of produced organic anions by mineralization is calculated from the charge balance including all other ions.

In all models, the rate constants described above are maximum values which are reduced under non-optimal water contents and soil temperatures. The mineralization constants for nitrogen are also reduced at low N contents (or high C/N ratio's) to account for immobilization by microbes according to Janssen (1983) and De Vries (1994).

2.3.4 Uptake of nutrients by roots

Total uptake of NH_4^+, NO_3^-, Ca^{2+}, Mg^{2+}, K^+, PO_4^{3-} and SO_4^{2-} ($mol_c\ ha^{-1}\ a^{-1}$) is described in NuCSAM by a demand function, which consists of maintenance uptake and growth uptake in stems and branches according to:

$$FX_{ru} = FX_{gu} + FX_{lf} + FX_{fe} + FX_{rd} + FX_{fu} \tag{28}$$

where the subscript *ru* refers to root uptake, *lf* to litter fall, *rd* to root decay, *fe* to foliar exudation, *fu* to foliar uptake and *gu* to growth uptake. The growth uptake is directly related to stem growth, which is described by a logistic growth curve:

$$dAm_{st} = \frac{Am_{st,mx}}{1.0 + e^{-krgrl \cdot (age + t - t_{50})}} \tag{29}$$

and

$$FX_{gu} = dAm_{st} \cdot (ctX_{st} + fr_{gu,br} \cdot ctX_{br}) \tag{30}$$

where $fr_{gu,br}$ (-) is the fraction of the growth uptake for branches, kr_{gl} ($kg\ ha^{-1}\ a^{-1}$) is a logistic rate constant, dAm_{st} ($kg\ ha^{-1}\ a^{-1}$) is the stem growth, $Am_{st,max}$ ($kg\ ha^{-1}$) is the maximum amount of stemwood, ctX_{st} ($mol_c\ kg^{-1}$) is content of element X in stemwood, ctX_{br} ($mol_c\ kg^{-1}$) is content of element X in branches, t (a) is time, t_{50} (a) is time at which the amount of stemwood is 0,5 x $Am_{st,max}$ and *age* (a) is the stand age at the start of the simulation. The contents of Ca, Mg, K and S in stemwood are assumed to be constant in time. The concentration of nitrogen in stems is described as a function of the nitrogen deposition according to Equation (21). The nutrient uptake from a given soil layer i is determined by the given root distribution:

$$FX_{ru,i} = FX_{ru} \cdot fr_{rti} \tag{31}$$

where $FX_{ru,i}$ ($mol_c\ ha^{-1}\ a^{-1}$) is uptake of element X from soil layer i, FX_{ru} ($mol_c\ ha^{-1}\ a^{-1}$) is total uptake of element X, fr_{rti} is the root fraction in soil layer i. NuCSAM includes the possibility for preferent uptake of NH_4^+ over NO_3^- according to (Gijsman, 1990):

$$FNH_{4\,ru} = \left(\frac{1}{1 + 1/f_p NH_{4,ru}} \right) \cdot FN_{ru} \tag{32}$$

where $f_pNH_{4,ru}$ (-) is a preference factor for the uptake of NH_4^+ over NO_3^-. NO_3^- uptake is calculated as the difference between total nitrogen uptake and NH_4^+ uptake:

$$FNO_{3\,ru} = FN_{ru} - FNH_{4\,ru} \tag{33}$$

In SoilVeg, the uptake of nutrients by roots is proportional to the actual water uptake, to the soil solution concentration, to a nutrient-specific selectivity factor, and to the sum of the nutrient allocation fractions to the plant compartments:

$$FX_{ru} = f_c \cdot \left(\sum_{i=1}^{n} frX_{all,i} \right) \cdot fX_{ru} \cdot cX \cdot FW_{ru} \tag{34}$$

with FX_{ru} ($mol_c\ ha^{-1}\ a^{-1}$) as the root uptake flux of element X, fX_{ru} (-) as ion selectivity factor, cX ($mol_c\text{-}m^{-3}$) as the concentration of ion X in the soil solution, $frX_{all,i}$ (-) as the allocation fraction of nutrient X to biomass compartment i (see §2.5), n (-) as the number

of biomass compartments, and f_c (m^2 ha^{-1}) as conversion factor. The ion selectivity factor is a lumped empirical factor accounting for root density, diffusion, active uptake, ion selectivity and soil physical properties. In SoilVeg, the ion selectivity factor is a function of stand development and soil temperature:

$$fX_{ru} = f_T \cdot fX_{ru,ini} + \gamma\left(1.0 + \alpha \cdot e^{-\beta(age-m)}\right)^{\frac{-1.0}{\alpha}-1.0} e^{-\beta(age-m)} \quad (35)$$

with

$$f_t = 2^{(T-T_{avg})/10}$$

with $fX_{ru,ini}$ (-) as the selectivity factor at the start of the simulation, f_t (-) as the temperature correction factor, α (-), β (a^{-1}), γ (-) and m (a) as curve parameters, *age* (a) as the stand age, T as the soil temperature, T_{avg} as the long-term average soil temperature.

In ForGro, nutrient transport through the soil towards the roots is described by a radial diffusion and mass flow model. Nutrient uptake is considered to be determined principally by the plant's demand, independent of the concentration in the soil (Gijsman, 1990). This implies that roots take up nutrients at the required rate (i.e. in accordance with the plant's demand) as long as the supply of nutrients at the root surface is sufficient to meet this demand. This situation is called an 'unconstrained uptake pattern'. When the nutrient demand is higher than the rate of nutrient supply at the root surface, the roots will take up all nutrients reaching the root surface, thus acting as a zero sink ('constrained uptake pattern'). The transport rate towards a root due to mass flow and the nutrient uptake rate by a root have upper bounds, which are determined by the maximum fluxes across the root surface of respectively water and nutrients. The nutrient demand is defined as the amount needed to be taken up by the trees for obtaining maximum growth rate under given external conditions. It is based on maximum tissue contents of nutrients. The demand divided by the total root length per unit soil surface area gives the required uptake rate per unit root length. The roots are considered as regularly distributed, parallel vertical cylinders, each surrounded by a hexagonal block of soil, which can be approximated by a soil cylinder with radius R (m):

$$R = \frac{1}{\sqrt{\pi L_{rv}}} \quad (36)$$

in which L_{rv} (m^3 m^{-3}) is the root length density. The radial diffusion and mass flow model uses the soil water contents and nutrient contents of the bulk soil of each soil layer as a forcing function. The development of gradients around a root is implicitly included in the mathematical transport equations (De Willigen and Van Noordwijk, 1987). Given a certain required uptake rate per unit root length, it is calculated whether roots in a certain layer are able to take up according to an unconstrained uptake pattern. If not, the maximum uptake rate from that layer is calculated as it is determined by the potential transport from the bulk soil towards the root surface (constrained uptake). If roots in a certain layer cannot meet the uptake requirement, it is tested whether roots in other layer (not yet taking up at their maximum rate) can increase their uptake rate.

2.3.5 *Nitrogen transformations*

Nitrification ($mol_c\ ha^{-1}\ a^{-1}$) in a given soil layer are described in NuCSAM, SoilVeg-3 and ForGro as first-order reactions by:

$$F\mathrm{NH}_{4\,ni} = -f_c\,\theta \cdot TL \cdot k_{ni} \cdot c\mathrm{NH}_4 \tag{37}$$

where θ ($m^3\ m^{-3}$) is the volumetric water content, TL (m) is thickness of the soil layer, k_{ni} (a^{-1}) is the nitrification rate constant. As with mineralization, the nitrification rate constant is adjusted on the basis of soil temperature, water content and pH (De Vries, 1988). The nitrification rate constant is reduced at high water contents.

2.4 Geochemical process formulations

2.4.1 *Rate limited reactions*

In all models, protonation and weathering are described by rate-limited first-order reactions. Protonation (the association of organic anions with H^+) is described according to:

$$F\mathrm{RCOO}_{pr} = -f_c \cdot \theta \cdot TL \cdot k_{pr} \cdot c\mathrm{RCOO} \tag{38}$$

where k_{pr} (a^{-1}) is a pH dependent protonation rate constant.

In the case of under-saturation, the weathering (dissolution) fluxes of Al and base cations from carbonates, silicates (primary minerals) and aluminum hydroxides ($mol_c\ ha^{-1}\ a^{-1}$) are described by first-order rate and Elovich reactions. The flux of calcium from dissolution of carbonates is described by:

$$F\mathrm{Ca}_{we\,cb} = f_c \cdot \rho \cdot TL \cdot k\mathrm{Ca}_{we,cb} \cdot ct\mathrm{Ca}_{cb} \cdot (c\mathrm{Ca}_e - c\mathrm{Ca}) \tag{39}$$

where ρ ($kg\ m^{-3}$) is the bulk density, $k\mathrm{Ca}_{we,cb}$ ($m^3\ mol_c^{-1} a^{-1}$) is a weathering rate constant, $ct\mathrm{Ca}_{cb}$ ($mol_c\ kg^{-1}$) is the content of Ca in carbonates, and $c\mathrm{Ca}$ and $c\mathrm{Ca}_e$ ($mol_c\ m^{-3}$) are the concentration and equilibrium concentration of calcium (cf. Eqn. (44)), respectively. The flux of base cations from silicates (primary minerals) is described by (Van Grinsven, 1988):

$$FX_{we,pm} = f_c \cdot \rho \cdot TL \cdot kX_{we\,pm} \cdot ctX_{pm} \cdot c\mathrm{H}^{\alpha(X)} \tag{40}$$

where $kX_{we,pm}$ ($m^3\ mol_c^{-1} a^{-1}$) is a weathering rate constant, ctX_{pm} ($mol_c\ kg^{-1}$) is the content of base cation X in primary minerals, $c\mathrm{H}$ ($mol_c\ m^{-3}$) is the H^+ concentration and α (-) is a parameter. The weathering of aluminum from primary minerals is described by:

$$F\mathrm{Al}_{we\,pm} = 3\,F\mathrm{Ca}_{we\,pm} + 0.6\,F\mathrm{Mg}_{we\,pm} + 3\,F\mathrm{K}_{we\,pm} + 3\,F\mathrm{Na}_{we\,pm} \tag{41}$$

This equation comes down to congruent weathering of equal amounts of Anorthite (Ca), Chlorite (Mg), Microcline (K) and Albite (Na). When the solution is undersaturated with respect to natural gibbsite, the release of aluminum from hydroxides is described by an Elovich equation:

$$F\mathrm{Al}_{we\,ox} = f_c \cdot \rho \cdot TL \cdot k\mathrm{El}_1 \cdot e^{(k\mathrm{El}_2 \cdot ct\mathrm{Al}_{ox})} \cdot (c\mathrm{Al}_e - c\mathrm{Al}) \tag{42}$$

with $c\mathrm{Al}$ and $c\mathrm{Al}_e$ ($mol_c\ m^{-3}$) as actual and equilibrium concentration of aluminum in the soil solution, and *kEl1* ($m^3\ mol_c^{-1} a^{-1}$) and *kEl2* ($kg\ mol_c^{-1}$) as Elovich constants.

The weathering of P is described by the rate-limited equation:

$$FP_{we} = f_c \cdot \rho \cdot TL \cdot kP_{we} \cdot ctP_t \cdot (cP_e - cP) \quad (43)$$

where ρ (kg m^{-3}) is the bulk density, kP_{we} (m^3 mol_c^{-1} a^{-1}) is the weathering rate constant for P, ctP_t (mol_c kg^{-1}) is the total phosphate content, cP (mol_c m^{-3}) is the actual phosphate concentration in the soil solution, and cP_e (mol_c m^{-3}) is the equilibrium concentration of phosphate with apatite, variscite or strengite.

2.4.2 Equilibrium reactions

Equilibrium reactions in NuCSAM, SoilVeg-3 and ForGro include the dissociation of CO_2, the calculation of the concentration of Ca^{2+} in equilibrium with Ca carbonate, the concentration of Al^{3+} in equilibrium with Al hydroxide, adsorption/desorption of SO_4^- and cation exchange. The concentration of Ca^{2+} in equilibrium with Ca carbonate is calculated as:

$$cCa_e = KCa_{cb} \cdot \frac{pCO_2}{(cHCO_3^-)^2} \quad (44)$$

where KCa_{cb} (mol^3 L^{-3} bar^{-1}) is the equilibrium constant for Ca carbonate dissolution and pCO_2 (bar) is the partial CO_2 pressure in the soil. The bicarbonate concentration in the soil solution (mol_c m^{-3}) is calculated from:

$$cHCO_3^- = \frac{(KCO_2 \cdot pCO_2)}{cH^+} \quad (45)$$

where KCO_2 (mol^2 L^{-2} bar^{-1}) is the product of Henry's law constant for the equilibrium between CO_2 in soil water and soil air, and the dissociation constant of H_2CO_3. The concentration of Al^{3+} in equilibrium with natural gibbsite is calculated by:

$$cAl_e = KAl_{ox} \cdot cH^3 \quad (46)$$

where KAl_{ox} (mol^{-2} L^2) is the equilibrium constant for aluminum hydroxide dissolution.

Cation exchange is described by Gaines-Thomas equations with Ca^{2+} as reference ion according to:

$$\frac{frX_{ac}^2}{frCa_{ac}^{z_x}} = KX_{ex} \cdot \frac{cX^2}{cCa^{z_x}} \quad (47)$$

with z_x (-) as valence of cation X, KX_{ex} ($(mol\ L^{-1})^z x^{-2}$) as the Gaines-Thomas selectivity constant for exchange of cation X against Ca, frX_{ac} (-) is fraction of cation X on the adsorption complex. X equals H^+, Al^{3+}, Mg^{2+}, K^+, Na^+, NH_4^+ in all models. In NuCSAM and ForGro, Fe^{3+} is included as well. frX_{ac} is calculated by:

$$frX_{ac} = \frac{ctX_{ac}}{CEC} \quad (48)$$

where CEC (mol_c kg^{-1}) is the cation exchange capacity. The sum of all fractions is equal to 1.

SO_4^{2-} and $H_2PO_4^-$ adsorption in each soil layer is described with a Langmuir equilibrium equation according to:

$$ctX_{ad} = \frac{XSC \cdot KX_{ad} \cdot cX}{1 + (KX_{ad} \cdot cX)} \quad (49)$$

where ctX_{ad} ($mol_c\ kg^{-1}$) is the sorbed amount of anion X, XSC ($mol_c\ kg^{-1}$) is the sorption capacity for X (cf. Eqn. (64)), and KX_{ad} ($m^3\ mol_c^{-1}$) is the equilibrium constant for sorption of anion X.

NuCSAM also includes ion speciation, such as the hydrolysis of Al^{3+} and complexation of aluminum with organic anions. All equilibrium reactions are calculated with the chemical equilibrium program EPIDIM (Groenendijk, 1995).

2.5 Forest growth

Forest growth is simulated by the models with different degrees of detail. In NuCSAM, forest growth is represented by a logistic growth function (§2.3.4) and a nutrient cycling process, in which nutrients are taken up daily by a growing stand, and later returned by means of litter fall and root decay (§2.3.2). The vegetation together with the litter layer merely act as a steady state nutrient cycle, with a small part of the nutrients taken up and stored in the accumulating forest biomass. This vegetation cycle is parameterized by root uptake, storage, litter fall and root decay, which are given as time-independent constants for a particular forest type. There is no feedback of nutrient cycling on growth rate. Growth constants are taken from available field and literature data. Stem growth (kg ha^{-1} a^{-1}) is described with a logistic growth function (see equation (29)). Branch growth (kg ha^{-1} a^{-1}) is derived from the stem growth using a fixed stem/branch ratio fr_{brst} (-):

$$dAm_{br} = fr_{brst} \cdot dAm_{st} \quad (50)$$

The amounts of leaves and roots (kg ha^{-1}) are described as:

$$Am_{lv} = \frac{Am_{st}}{Am_{st,mx}} \cdot Am_{lv,mx} \quad (51)$$

where Am_{lv} (kg ha^{-1}) is the actual amount of foliage (or roots) and $Am_{lv,mx}$ (kg ha^{-1} a^{-1}) is the given maximum amounts of foliage (or roots). The nutrient contents of base cations and sulphur remain constant in all biomass compartments, whereas the nitrogen contents are calculated as a function of the atmospheric deposition.

In SoilVeg-3, gross photosynthesis is linearly related to the actual water uptake by the roots. Gross photosynthesis may be reduced by a low Leaf Area Index or by high SO_2 concentrations (Jeffree, 1981; Van der Eerden *et al.*, 1988) and/or by high ozone concentrations (Linzon *et al.*, 1984; Van der Eerden *et al.*, 1988). Net photosynthesis is calculated by subtracting a temperature dependent maintenance respiration and nutrient fraction dependent growth respiration.

$$R_{m,i} = Q_{10}^{((T_a-25)/10)} \cdot (\alpha . C_i . N_i + \beta . C_i . M_i) \quad (52)$$

where Rm_i (kg m^{-2} d^{-1}) is maintenance respiration for biomass component i, T_a (°C) air temperature, Q_{10} rate of increase of respiration with 10°C temperature increase, C_i (kg m^{-2})

carbon weight, N_j (kg kg^{-1}) nitrogen content and M_j (kg kg^{-1}) mineral content. α and β are constants. Growth respiration, which is the cost of conversion of glucose into structural biomass, is calculated from the biochemical composition of structural biomass:

$$R_g = 0.35.(P_g - R_m) \tag{53}$$

where R_g (kg m^{-2} d^{-1}) is growth respiration. The allocation of assimilates and nutrients is based on an age dependent functional balance between tissues. The age dependence of allocation is described by S-curves, which are calibrated to observed biomass increments:

$$a_j = \alpha + \frac{\gamma}{1 + \exp(-\beta(age - m))} \tag{54}$$

where a_j (-) is fraction of assimilate allocated to compartment j, and α (-), β (a^{-1}), γ (-), and m (a) are constants. The sum of all allocation fractions is equal to one. The allocation fractions are affected by environmental conditions in such a way that the root/shoot ratio increases at low nutrient availability; allocation also increases in cases of needle or root damage. The actual forest growth may be limited by one of the nutrients or by carbon, depending on which of these components allows for the smallest biomass increment. First the potential growth, $G_{pot,X,j}$ (kg) for every nutrient in compartment j is calculated:

$$G_{pot,X,j} = \frac{(C_{X,j} \cdot M_j + A_{X,j})}{C_{grw,X,j}} - M_j \tag{55}$$

with $C_{X,j}$ (kg kg^{-1}) as the concentration of nutrient X in plant compartment j, M_j (kg) as the mass of plant compartment j, $A_{X,j}$ (kg) the allocated amount of nutrient X to plant compartment j, and $C_{grw,X,j}$ (kg kg^{-1}) as the 'growth concentration' of nutrient X in compartment j. The actual growth equals the potential growth for the limiting nutrient which may be carbon. The actual concentration of the limiting nutrient equals the growth concentration (somewhere between an average and a minimum concentration). Actual concentrations for the *non-limiting* nutrients are higher than the growth concentration. When the actual concentration of a (non-limiting) nutrient exceeds a predefined concentration (somewhere between an average and a maximum concentration), the growth concentrations of the other nutrients decrease. If the growth concentration decreases, and the availability of the nutrients remains unchanged, the potential growth increases. The growth of fine roots may also be reduced by high Al^{3+} concentrations in the soil solution according to Göransson (1985) and Thornton (1987).

In ForGro, growth is the main outcome of the model, calculated from underlying physiological and biochemical principles. The model is based on a carbon-balance approach. Light interception drives photosynthesis and canopy assimilation of carbon dioxide. In case water and nutrients impose no restrictions, the photosynthetic performance of a leaf surface depends on the amount of photosynthetic radiation absorbed, on foliage temperature and on the photosynthetic characteristics of the leaf itself. For a given temperature, the relationship between photosynthesis rate per unit of leaf surface and the

amount of adsorbed photosynthetically active radiation is described by a light response curve:

$$P_i = P_{max} \cdot \left\{ 1 - \exp\left(-\varepsilon \cdot \frac{I_{abs,i}}{P_{max}} \right) \right\} - R_i \qquad (56)$$

with P_i (kg ha^{-1} d^{-1}) as the net photosynthesis rate for layer i, P_{max} (kg ha^{-1} d^{-1}) as the gross photosynthesis rate at light saturation, ε (kg ha^{-1} d^{-1} W^{-1} m^2) as the initial light use efficiency at low light, $I_{abs,i}$ (W m^{-2}) as the photosynthetic active radiation absorbed per unit of leaf surface, and R_i (W m^{-2}) the carbon dioxide production due to maintenance respiration. In ForGro, the above equation is used to calculate photosynthesis rates for different leaf layers in the canopy, in relation to light climate and absorption of photosynthetically active radiation. From the actual photosynthesis rate P_i, the stomatal conductance is derived assuming a constant C_i / C_a ratio. For Douglas fir, a C_i / C_a ratio of 0.6 was used, derived from experimental work by Smeets *et al.* (1990). Accounting for differences in molar weight between gases diffusing into or out of the stomata, stomatal diffusion resistances can be derived from net photosynthesis rate together with the C_i / C_a ratio. As a result, CO_2 assimilation, transpiration, and uptake of gaseous air pollutants are closely coupled in the model. The maximum photosynthesis at light saturation, P_{max}, can be modified by air pollutants such as SO_2 and O_3, and also depends on the nutrient status of the foliage, on temperature and foliage age.

To arrive at an estimate of gross canopy assimilation (P_g), the assimilation rates per leaf layer in the canopy are summed over the Leaf Area Index. Next, growth and maintenance respiration is accounted for, in order to arrive at dry weight increment:

$$G_i = c_j \cdot a_j \cdot \left(\sum P_{g,i} - \sum R_j \right) - L_i \qquad (57)$$

with G_j (kg ha^{-1} d^{-1}) as net dry weight increment of biomass component j, c_j (kg kg^{-1}) as the dry weight conversion efficiency of component j, a_j (-) as a distribution coefficient for the assimilates available for growth, $\Sigma P_{g,i}$ (kg ha^{-1} d^{-1}) as gross photosynthesis, summed over the foliage layers i, ΣR_j (kg ha^{-1} d^{-1}) as maintenance requirements (see Eqn. (52)) for all living tissue, and L_j (kg ha^{-1} d^{-1}) as the rate of litter loss or biomass turnover for component j. The dry weight of the stem component is converted into total stem volume, using an average measure of basic wood density, and diameter increment is calculated from height and volume increment using a genuine volume function or taper curve.

Thus, forest growth is directly related to weather conditions at the site through the ecophysiology of the tree species. Weather conditions such as temperature and radiation act on photosynthesis rate through modification of P_{max}, just as gaseous air pollutants when they occur in high concentrations. Associated with carbon dioxide assimilation, the tree loses water through the stomata, and a foliage water deficit induced stomatal closure may develop if soil water is short in supply. As a result, gross canopy photosynthesis and net increment is decreased. Nutrient limitations are described in relation to P_{max} as well, decreasing the value for P_{max} when concentrations of N, P, K, Ca or Mg are below a critical level such as deduced from fertilization experiments. Nutrients can either be short in

supply, or nutrient uptake can be reduced due to either low root density, or to increased Al concentrations in the soil solution.

2.6 Forest stress

Tree growth is the outcome of a range of physical, biochemical and physiological processes which are dependent on species characteristics and site conditions. Only seldom (if at all) do these processes act in a completely optimal way. Hence stress, if defined as some non-optimal condition, is ever present. When evaluating the impact of air pollution and soil acidification, interest usually focuses on 'added' stress, as a result anthropogenic influence. However, since such added stress may consist of an enhancement of a traditional stress, e.g. such as through limited availability of base cations in a poor, sandy soil, the distinction cannot be made rigorously.

When a distinction in production situations and growth-influencing factors is made (Mohren and Rabbinge, 1990), 'stress' can be separated into traditional growth limiting factors, such as water and nutrient shortage that determine an attainable production level at a given site, and growth reducing factors that are superimposed on traditional growth limiting factors. Growth reducing factors may act directly at particular physiological processes (e.g. O_3 influence on photosynthesis), or they may act indirectly, thereby enhancing traditional growth limiting factors. The latter is the case when increased leaching of base cations occurs due to soil acidification, and thus nutrient availability is decreased.

As part of the modelling exercise reported here, no explicit distinction is made between growth limiting factors and growth reducing factors, and a precise separation of 'traditional' and 'added' stress is not attempted. Rather, soil acidification and forest growth are related to selected deposition scenario's, where the different ecosystem response to these scenario's is evaluated with the help of presumed causal mechanisms explaining the result.

The main causal mechanisms included in the models involve direct short-term effects of SO_2 and O_3 on photosynthesis and growth (ForGro and SoilVeg), effects of soil acidification on base cation availability in the soil solution (NucSam and SoilVeg), effects of soil acidification on soil indicator variables such as pH, Al/Ca, NH_4/K, NH_4/Ca, NH_4/Mg ratio's, CEC occupation, etc. (NucSam and SoilVeg), effects of soil conditions on root functioning (ForGro and SoilVeg), effects of tree nutrient concentrations on photosynthesis, respiration, assimilate allocation, etc. These effects are partly independent of one another (e.g. impact of gaseous air pollutants vs. impact of soil conditions on root growth), but are to some extent related also. This implies that multiple-stress conditions are taken into account, either as combinations of multipliers or as limiting factors, at the same time allowing for compensatory action between combinations of stress (Van Heerden and Yanaï, 1995). Figure 3 illustrates this for an elementary model of plant growth including photosynthesis, respiration and nutrient uptake.

Basically, the models used here are based on a state-rate variable approach, implying that for a given time step, all rates are completely defined by the states at the beginning of the time step together with the input variables pertaining to this time step. As a result, all rates

Figure 3
Simple model for stress inter-relations in a forest ecosystem (Van Heerden and Yanaï, 1995).

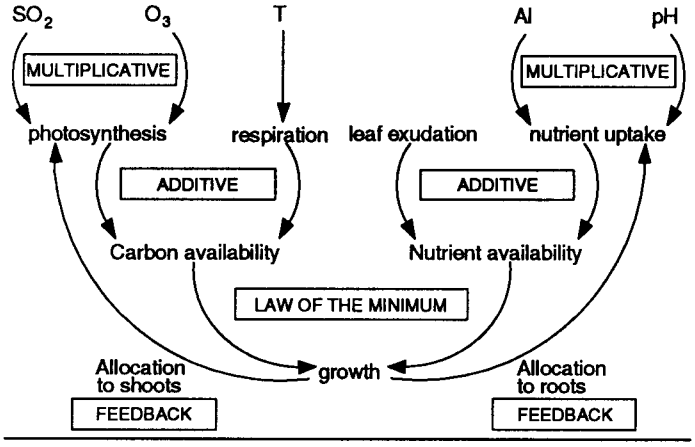

during anyone time step are independent of one another. Thus, individual growth reducing mechanisms can be considered mutually independent. As a result of feedback mechanisms reacting to previous growth reductions however, or due to the growth reduction itself, separate influences at the process level lead to different states that in turn may influence the action of other growth reductions. As an example, although effects of water shortage and ozone on dry matter increment may be considered independent, there is an effect of water availability on plant water status, and thus on stomatal opening, through which stomatal uptake and hence the exposure of ozone in the interior of the leaf, is influenced as well. Thus, although no interrelationships between various growth reducing processes due to air pollution and soil acidification exist for any one time step, the result of the dynamic simulation during which the determining state variables change, can be seen as the combined effect of multiple stress.

For a number of closely related growth reducing phenomena for which the actual mechanism at the process level is not sufficiently clear to be modelled explicitly, sometimes rigorous assumptions have been made to deal with the issue of interdependence. Typically, direct effects of e.g. air pollutants, CO_2 and temperature on photosynthesis sometimes are considered to be multiplicative (SoilVeg), whereas in case of effects of nutrient shortage on growth is usually considered exclusive, implying that the strongest effect of the element that is relatively lowest, is taken and the lesser impacts of the other elements that are short in supply are ignored (ForGro). For this, ForGro assumes a direct effect of nutrient concentration on maximum photosynthesis, and hence on growth.

Concerning the issue of multiple stress vs. single stress, the models used in this study all deal with multiple stress by including a range of separate growth limiting and growth reducing factors. This implies that the impact of a single stress always is quantified against the background of the other growth determining, growth limiting, and growth reducing factors for a particular site and ecosystem.

3 THE DATA-SET

Figure 4
Position of the 10 intensively monitored forest sites.

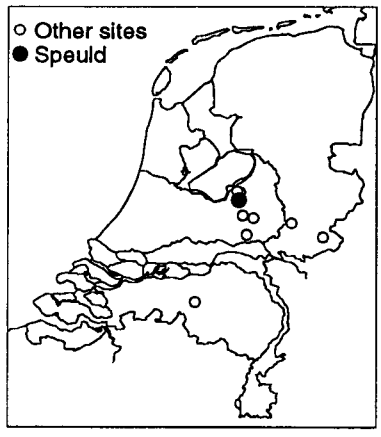

3.1 Introduction: The Speuld site

Since 1980, a total number of 10 Dutch forest sites have been monitored intensively (Figure 4; see also Heij and Schneider, 1991 and Tiktak and Van Grinsven, 1992). At these sites boundary fluxes and states for hydrology, chemistry, forest growth and nutrient status have been measured at various times for at least three years. The most complete monitoring study was carried out in a Douglas fir stand at Speuld (Evers *et al*, 1987). For this reason, the Speuld dataset was chosen for validation of the models NuCSAM, SoilVeg-3 and ForGro.

3.1.1 General characteristics of the Speuld site

The Speuld site is located in a 2.5 ha Douglas fir stand. The geographical location is 52.1°N and 5.4°E. Altitude is 50 m. The stand is surrounded by a large forest of approximately 50 km^2; the nearest edge is at a distance of about 1.5 km. The soil is a well-drained Typic Dystochrept (USDA) or Cambic podzol (FAO, 1988) on heterogeneous sandy loam and loamy sand textured ice-pushed river sediments. A full soil profile description is included in Tiktak *et al.* (1988). The water table is at a depth greater than 40 m throughout the year. The stand was 29 years old at the beginning of 1988. Stem density was 765-812 trees ha^{-1}, with a basal area of 30.7-31.1 m^2 ha^{-1}. Average tree height was 19.5 m. The canopy was well closed, and the one-sided Leaf Area Index (LAI) ranges from about 8 m^2 m^{-2} in spring to about 13 m^2 m^{-2} in early summer. The last thinning was carried out five years before the start of the measurements. The average fine root-length amounted to 19.10^6 m ha^{-1}, of which almost 90% is situated in the top soil to a depth of 0.4 m. There is no understorey vegetation.

3.1.2 Representability of the Speuld stand

An important question to be asked is how representative is the Speuld site compared to other Douglas fir stands and to other forest stands in the Netherlands. When compared with a poor slowly growing and a rich fast growing stand (Table 5), Speuld has a high foliage mass and an extremely high ratio of foliage to fine root mass. Further, Speuld is deficient with respect to phosphate and has high nitrogen concentrations in the foliage.

Element inputs and outputs at Speuld are comparable to those of the other intensively monitored stands (table 6), but S-inputs and N-outputs (and by result also S and Al-outputs) are high compared to fluxes inferred from a nation wide forest survey in 1990 (De Vries *et al.*, 1992).

TABLE 5

Comparison of biomass of Speuld with low and high productive stands (Keyes and Grier, 1981) and with nutrient poor and nutrient rich stands (Berdowski *et al.*, 1991).

Parameter	Unit	Low, poor stand	High, rich stand	Speuld
Age	(a)	22	40	32
Tree density	(ha^{-1})	690	1030	886
Basal area	(m^2 ha^{-1})	30	45	33
Needle mass	(Mg ha^{-1})	10	16	18
Fine root mass	(Mg ha^{-1})	5	11	3
N content in needles	(%)	0.8	2.4	1.8
Mg content in needles	(%)	0.05	0.18	0.10
P content in needles	(%)	0.14	0.22	0.10

TABLE 6

Comparison of element budgets for Speuld with those for other Dutch intensively monitored sites (Heij and Schneider, 1991) and a nation wide forest survey (De Vries *et al.*, 1992).

Parameter	Unit	Speuld	Intensive monitored sites (n=10)	Forest survey (n=147)
S-input	($kmol_c$ ha^{-1} a^{-1})	2.3	2.8	1.8
N-input	($kmol_c$ ha^{-1} a^{-1})	3.6	3.9	4.2
S-output	($kmol_c$ ha^{-1} a^{-1})	3.1	2.7	1.8
NO_3-output	($kmol_c$ ha^{-1} a^{-1})	2.2	1.8	0.7
NH_4-output	($kmol_c$ ha^{-1} a^{-1})	0.0	0.1	0.1
Al-output	($kmol_c$ ha^{-1} a^{-1})	4.6	3.3[a]	1.0
S-out/S-in	(-)	1.3	1.0	1.0
N-out/N-in	(-)	0.6	0.5	0.2

a) Ignoring the Al-output from two calcareous subsoils.

The lower input of S in Speuld can partly be attributed to a substantial decrease of S-deposition in the past decade (Erisman, 1994). The discrepancy for N between the intensive and extensive monitored sites can be explained in part by the absence of wet oak stands in the intensive monitoring studies. These stands have a high potential for N-immobilization. Nevertheless, the representativeness of Speuld with respect to the N-cycle is doubtful.

3.2 Climate, weather and water fluxes in throughfall

General meteorological data were taken from the weather station 'De Bilt', which is situated about 50 km from the Speulderbos site. The data include daily measurements of the average air temperature, precipitation, global radiation, air humidity and wind speed. The climate can be classified as temperate, humid with a 30-year average annual temperature of 9.3 °C (2.0 °C in January and 16.7 °C in July). Annual precipitation amounts to 804 mm a^{-1}, with precipitation distributed quite evenly throughout the year (Figure 5). Annual reference evapotranspiration (Makkink, see eqn. (2)) is 534 mm a^{-1}.

For the period 1988-1990, precipitation was measured continuously at a clearing at 1.3 km from the monitoring site (station 'Drie'; see table 7 for data sources). These data were

Figure 5
Long-term (1960-1990) climatological data measured at De Bilt.

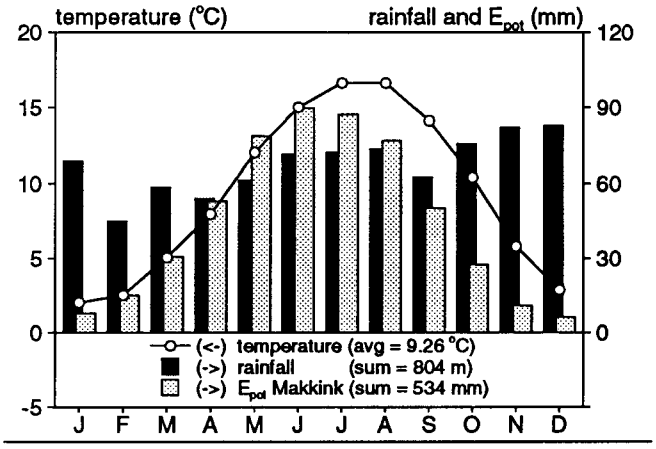

used for the period 1988-1990. Figure 5 shows some long-term characteristics of the data-set. For 1988 the annual precipitation is somewhat higher (865 mm) than the long-term average precipitation, whereas 1989 is normal with respect to precipitation amount (810 mm).

The data-set was extrapolated for scenario analyses using a stochastic weather generator (Richardson and Wright, 1984). The weather generator was calibrated using the weather data from the De Bilt for the period 1960-1990. By using a calibrated weather generator, year to year variations of future weather conditions can be described realistically. Figure 6 shows the frequency distribution of annual precipitation for the period 1960-1990 ('real weather') and 1991-2050 ('generated weather'). The average weather conditions are described quite realistically, but the coefficient of variation is smaller for the generated weather than for the real weather, implying that extreme weather conditions are not simulated. This fact should be kept in mind when discussing the occurrence of conditions leading to stress (e.g. drought stress). Results for global radiation, air temperature and reference evapotranspiration are comparable.

Throughfall was measured fortnightly using 12 funnels (orifice 400 cm^2) for the period 1987-1990. The throughfall funnels were situated in fixed positions and the distance to the nearest tree was chosen randomly according to the method described by Duysings *et al.*, 1986. In 1989, throughfall was also measured using a larger number (36) of funnels. Figure 7 shows the accumulated average throughfall for both data-sets. Despite of the large spatial variability of throughfall (see Bouten *et al.*, 1992), the agreement between both data-sets is good. For the period 1987-1989, the average throughfall fraction over these years is 63% (interception loss is 37%). Stem flow was never observed.

TABLE 7
Sources of the meteorological data-sets.

	Precipitation	Temperature	Global radiation
1950-1987	De Bilt	De Bilt	De Bilt
1988-1990	Drie	De Bilt	De Bilt
1991-1992	De Bilt	De Bilt	De Bilt
1993-2050	WGEN	WGEN	WGEN

Figure 6.
Frequency distribution of rainfall for De Bilt (1960-1990) and WGEN (1991-2050).

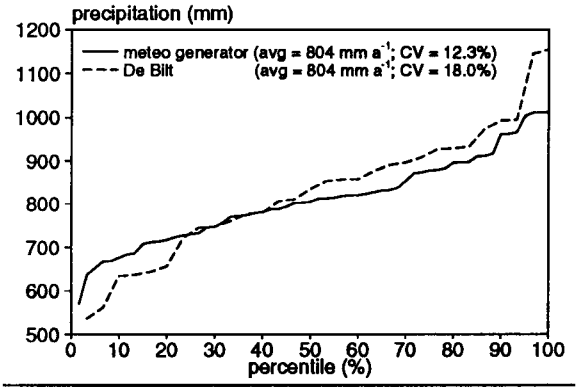

Figure 7.
Average throughfall amount for a data-series using 36 funnels and 12 funnels.

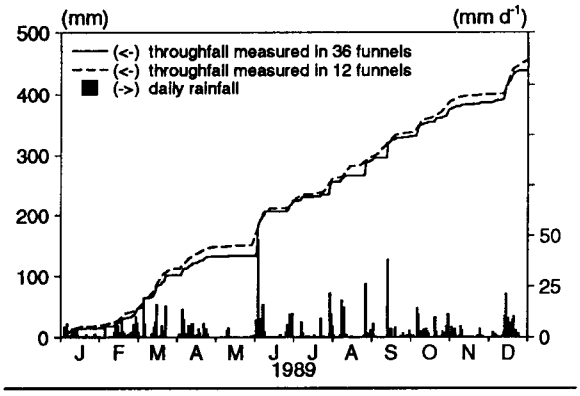

3.3 Air pollution and deposition

3.3.1 Throughfall and bulk precipitation measurements

Total deposition, dry deposition and canopy exchange fluxes were calculated on the basis of throughfall and bulk precipitation measurements by the sodium-filtering approach (Ulrich, 1983; Van der Maas and Pape, 1990; Draaijers, 1993). The measurements were performed on a weekly basis in samplers with a volume of about 5000 cm^3 and a surface area of 400 cm^2. The rim of the throughfall collectors was at a height of 75 cm above ground, and the collectors were arranged evenly throughout the soil monitoring plot. The distance to the nearest tree was chosen randomly, following the approach by Duijsings *et al.*, 1986. Throughfall was pooled to one volume weight sample before analysis. Bulk precipitation was collected from two different sheltered open areas at a distances of 200 m and 1300 m, respectively. The rim of the bulk-precipitation collectors was at a height of 150 cm. The samples were analyzed separately.

All water samples were stored in 100 or 250 ml bottles and stored cool. E_c and pH were determined within 24 hours after sampling. Electric conductivity ($\mu S\ cm^{-1}$) was measured with a Philips conductivity meter (type PW 9501) and conductivity cells (type PW 9513). Calibration was carried out with a 0.05 M KCl solution. pH was measured with an Orion Research pH/mV meter (model 801A) and an Orion combination pH electrode (no. 91-55), using buffer solutions of pH 4 and pH 7. A few drops of KCl were added to weakly buffered samples before pH measurement. Inorganic carbon was determined with a TOC analyzer (Beckman type 915B). Cl^-, SO_4^- and NO_3^- were determined by ion chromatography. HCO_3^- was calculated from pH and inorganic carbon content. Phosphate, silicate and all major cations (K^+, Na^+, NH_4^+, Ca^{2+}, Mg^{2+}, Al_t, Fe_t and Mn) were determined by spectrophotometry.

Table 8 show the fluxes of all major components for the period 1987-1989. Throughfall fluxes of base cations show year to year variations. Erisman *et al.* (1994) compared these deposition figures with atmospheric deposition fluxes calculated from continuous gradient and eddy correlation measurements, which were also performed in Speuld. Their most important conclusion is that total deposition from eddy correlation and gradient

measurements agrees well with total deposition from throughfall measurements for SO_x and NH_x, but that considerable differences are found for NO_y.

TABLE 8

Annual fluxes of major components in wet deposition (WD), dry deposition (DD), total deposition (TD) and canopy exchange (CE) calculated from throughfall and bulk-precipitation measurements. Data source: Van der Maas and Pape, 1990.

	Fluxes ($mol_c\ ha^{-1}\ a^{-1}$)									
	Na^+	K^+	Ca^{2+}	Mg^{2+}	Cl^-	H^+	NH_4^+	NO_3^-	SO_4^{2-}	WA[b]
1987										
WD	464	23	152	132	508	488	725	476	810	198
DD	398	44	228	110	523	-317	2146	346	1150	169
TD	862	67	380	242	1031	171	2872	822	1960	368
CE[a]	0	446	50	68	0	-104	-512	-4	-18	22
1988										
WD	608	20	137	158	804	240	629	274	648	76
DD	556	23	148	152	834	-33	2113	444	1593	112
TD	1164	43	284	310	1638	207	2742	718	2241	188
CE[a]	0	486	173	66	0	-108	-676	-47	-174	219
1989										
WD	339	11	84	91	456	245	631	332	613	10
DD	432	24	168	124	632	-114	2001	487	1425	116
TD	771	35	252	215	1088	131	2633	818	2038	126
CE[a]	0	366	106	66	0	-79	-522	-28	-80	107

a) If CE is positive, than CE refers to canopy leaching, otherwise CE refers to canopy uptake.
b) WA refers to weak acids.

3.3.2 Historical deposition data

Measurements of atmospheric loads, either by the gradient method or by the sodium-filtering approach, are not available for the years before 1987. For this reason, deposition was derived from inference for these years. These figures were published by Erisman (1991) for the period 1980-1986. For the Speuld site, Erisman *et al.* (1994) found a reasonable agreement between total deposition from inference and the measured deposition. For the period 1950-1980, the deposition figures were estimated by scaling the deposition calculated with the DAS-Source Receptor Matrix (SRM) model for region 'Veluwe' (Heij and Schneider, 1991) according to:

$$Dep_{Speuld} = Dep_{DAS} \cdot \frac{AvgDep_{Speuld}}{AvgDep_{DAS}} \qquad (58)$$

where Dep_{Speuld} ($mol_c\ ha^{-1}\ a^{-1}$) is deposition at Speuld, Dep_{DAS} ($mol_c\ ha^{-1}\ a^{-1}$) is deposition calculated with the DAS model, $AvgDep_{Speuld}$ ($mol_c\ ha^{-1}\ a^{-1}$) is average deposition at Speuld for the period 1980-1990 and $AvgDep_{DAS}$ ($mol_c\ ha^{-1}\ a^{-1}$) is average deposition calculated with the DAS model.

Figure 8
Estimates of the deposition of acidifying components (1950-1990) for Speuld and for an average forest in DAS area 'Veluwe'.

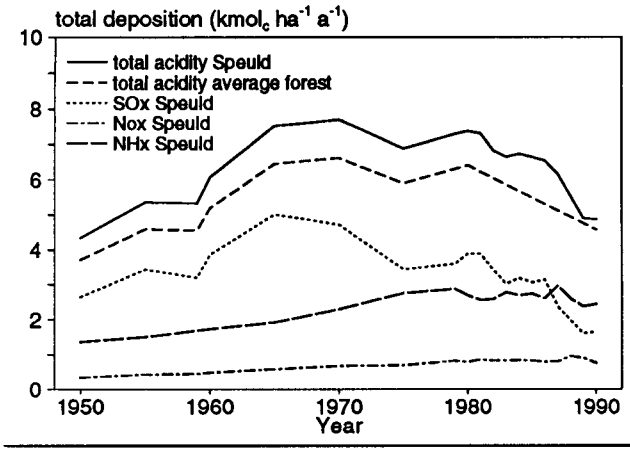

Figure 8 presents the results of the calculations. This figure also shows the total acid deposition calculated with the DAS model. From the figure two major conclusions can be drawn:

- the acid deposition in Speuld is higher than the acid deposition calculated with the DAS model.
- the deposition at Speuld declines after 1987, mainly because of reduced sulphur deposition.

3.4 Hydrology

3.4.1 Vegetation dependent properties

The most important vegetation dependent hydrologic parameters are presented in Table 9. The soil cover fraction, interception efficiency and the depth distribution of water uptake by roots were directly taken from measurements (see references in table). The crop factor, and the reduction and wilting points were taken from Tiktak and Bouten (1994). They calibrated the model SWIF (Tiktak and Bouten, 1992) to the Speuld site. The other parameters are derived from the calibration of NuCSAM to Speuld.

TABLE 9
Vegetation dependent hydrologic parameter values for the Speulderbos site.

Parameter	Symbol	Value	Unit	Eqn.
Soil cover fraction [a]	sc	0.9	(-)	(4), (5)
Average precipitation intensity [d]	R	10.0	(mm)	(4)
Interception efficiency [b]	f_i	0.141	(-)	(9)
Interception capacity [b]	$A_{wc,max}$	2.1	(mm)	(4)
Factor for evaporation [d]				
during dry part of day:	fE_{dry}	1.5	(-)	(6)
during wet part of day:	fE_{wet}	0.5 - 9.0	(-)	(5)
Reduction point [a]	$h_{r,d}$	-600	(cm)	Figure 2
Wilting point [a]	$h_{r,w}$	-6000	(cm)	Figure 2
Crop factor [a]	f_c	0.85	(-)	(9)
Root density [c]:				
litter	R_l	0.05	(-)	(12)
00-20 cm	R_l	0.30	(-)	(12)
20-40 cm	R_l	0.34	(-)	(12)
40-60 cm	R_l	0.15	(-)	(12)
60-80 cm	R_l	0.08	(-)	(12)
> 80 cm	R_l	0.08	(-)	(12)

a) Based on Tiktak and Bouten (1990; 1994).
b) Measured by Bouten (1992).
c) Based on root length distribution measurements by Olsthoorn (1991).
d) Based on the calibration of NucSAM to Speuld.

3.4.2 *Soil physical characteristics*

Water retention characteristics were obtained from simultaneously measured average water contents and pressure heads at a plot of 30 × 30 m^2 (see §3.4.3). This means that the physical characteristics are valid for the same plot as the monitoring data. To extrapolate the retention characteristics outside the range of pressure heads that can be measured with tensiometers, and to obtain conductivity characteristics, the measured data were fitted to the Mualem-Van Genuchten functions (Van Genuchten, 1980):

$$\theta(h) = \theta_r + \frac{(\theta_s - \theta_r)}{[1+(\alpha|h|)^n]^m} \qquad (59)$$

and:

$$K(h) = K_s \cdot \frac{\{1-(\alpha|h|)^{n-1}.[1+(\alpha|h|)^n]^{-m}\}^2}{[1+(\alpha|h|)^n]^{m/2}} \qquad (60)$$

where θ_s ($m^3\ m^{-3}$) is saturated volumetric water content, θ_r ($m^3\ m^{-3}$) residual water content, h (m) pressure head, α (m^{-1}) reciprocal of the air entry value, K (m d^{-1}) hydraulic conductivity, n (-) a fitting parameter and m = 1-1/n. Table 10 summarizes the results of the fitting. For completeness, the results of the fitting for the laboratory water retention characteristics are also included. Notice that both the saturated water content and the n parameter are lower for the field characteristics. The major reason for this is that in the field situation, drying and wetting cycles occur (hysteresis). Using laboratory characteristics in field applications, therefore, leads to a gross overestimation of water contents in the field.

The saturated hydraulic conductivity, K_s, was optimized by Tiktak and Bouten (1992). They performed simulation experiments with the model SWIF for a two-weeks winter period without precipitation. Under such conditions, the hydraulic conductivity can be derived, as evapotranspiration is negligible compared to vertical drainage.

TABLE 10

Parameters of the Mualem-Van Genuchten functions to describe the soil physical properties. Source: Tiktak and Bouten (1992).

Depth	θ_s ($m^3\ m^{-3}$)	θ_r ($m^3\ m^{-3}$)	α (cm^{-1})	n (-)	K_s (cm d^{-1})
Field characteristics (used in the models)					
litter	0.500	0.00	0.10	1.25	800
0-60 cm	0.330	0.00	0.10	1.25	800
> 60 cm	0.210	0.00	0.04	1.40	100
Laboratory characteristics					
0-60 cm	0.429	0.00	0.05	1.37	n.d.[a]
> 60 cm	0.350	0.00	0.04	1.48	n.d.[a]

a) n.d. is 'not determined'.

3.4.3 *Soil hydrology*

Is the soil monitoring plot representative?

The soil hydrological monitoring programme includes measurements of soil water pressure heads, soil water contents, litter water contents and evapotranspiration. Most hydrological measurements were carried out on a plot in the Eastern half of the stand. This plot has a

surface area of 30x30 m, and is situated close to the sampling points for soil solution composition. For the position of the plot within the monitoring site, see Figure 9. Bouten *et al.* (1992) studied wether these plots are representative for the stand by using the water holding capacity (i.e. the water content at field capacity minus the minimum water content). The water holding capacity could be derived from measurements of soil water contents directly after a dry week in early spring (= water content at field capacity) by the regression equation (Tiktak and Bouten, 1990):

$$WC = 0.531 \cdot \theta_{fc} - 0.00012 \qquad (r^2 = 0.85;\ n = 98) \qquad (61)$$

where WC ($m^3\ m^{-3}$) is water holding capacity and θ_{fc} ($m^3\ m^{-3}$) is water content at field capacity.

Figure 9
Map of the soil water content ($m^3\ m^{-3}$) of the upper 50 cm. Source: Bouten *et al.* (1992).

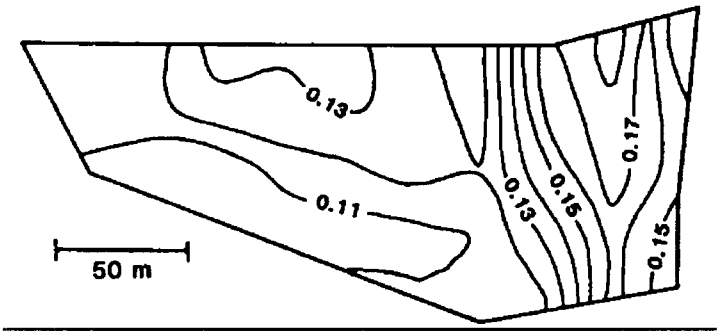

Bouten *et al.*, 1992 present a kriged map of soil water contents at field capacity, based on measurements in a regular grid of 25 x 25 m. Using this map and equation (61), the water holding capacity ranges from 0.0583 $m^3\ m^{-3}$ to 0.0902 $m^3\ m^{-3}$. The soil physical monitoring plot and the soil chemical sampling plots are situated in the area with the highest water holding capacity.

Methods

Soil water pressure heads were measured twice daily with 22 tensiometers at depths ranging from 5 to 200 cm. The tensiometers were connected to a 24-port fluid switch, which was stepped up every 3 min to connect one of the tensiometers with a pressure transducer. All tensiometers were installed at the above mentioned plot.

Soil water contents were measured using three different methods, each method having specific preliminaries and disadvantages. The longest time-series is available for soil water contents measured by the neutron scattering method. There were three access tubes, and readings were made at depths ranging from 50-200 cm at 10 cm intervals. The neutron access tubes were installed at the soil physical monitoring plot. Soil water contents were also measured with Time Domain Reflectometry in the top soil (0-50 cm depth) by 144 vertically installed sensors of 50 cm in length. 108 TDR sensors were distributed over the rooting area of three trees, the other sensors were randomly distributed over eight other sites. Major advantage of the TDR measurements is that water contents could be determined at a large number of positions, major disadvantage is that only one figure is available for the rooting zone as a whole. The third method of measuring water contents was the capacitive method. Disadvantage of this method is that the sensors are very small and not representative for the stand as a whole. Moreover, the measurements did not give reliable figures.

Four samples, with a surface area of 20 x 20 cm, were taken weekly from the top 7 cm of the forest-floor at random positions for gravimetric determination of volumetric water content.

During the last year of the monitoring programme, measurements also included eddy-correlation evapotranspiration, sap flux density and leaf-wetness. These data were used to obtain the average evapotranspiration of the stand. These data were not used in this modelling exercise, as soil hydrological monitoring plot and soil solution sampling points are not representative for the stand as a whole.

3.5 Soil chemistry

3.5.1 Solid phase characteristics

At Speuld, chemical characteristics were derived for three soil pits (Tiktak *et al.*, 1988). The texture of the soil in Speuld shows a strong variability, that is related to the elongated, parallel outcrops of layers of different textures typical of an ice-pushed ridge. Consequently, the results from the three pits show to be different for both soil properties (Figure 10) and the soil solution measurements (Figure 11; see further Van Breemen and Verstraten, 1991). Taking the mean would not lead to representative values, especially for the soil solution measurements which show different temporal dynamics. For this reason, we used the soil chemical properties of one soil pit. We decided to take plot B, as this plot is situated close to the soil physical monitoring plot.

Figure 10
The content of secondary Al compounds and the CEC for the three soil pits.

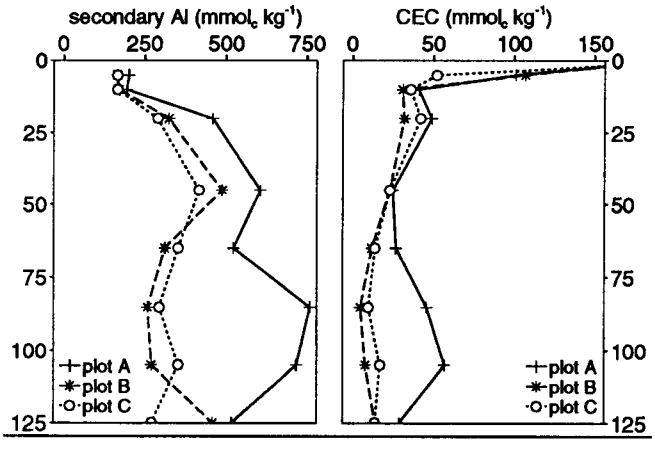

Soil chemical properties were determined once in mineral soil samples taken in 1986. Particle size distribution is presented in Table 11. Most relevant soil chemical data have been summarized in Table 12 and Table 13. The forest floor is 9 cm thick (4 cm litter layer, 2 cm fermentation layer and 3 cm humus layer), with a C/N ratio of 29. The mineral soil has a sandy loam textured top layer of 4 cm, grading through loamy fine sand between 4 and 55 cm depth to fine sand below 55 cm depth. Organic carbon decreases regularly with depth (Table 11) from about 10% at 0 cm depth to 0.5% below 50 cm depth. The cation exchange capacity is high (>100 mmol$_c$ kg^{-1}, cf. Table 12) in the litter layer and top 4 cm of the mineral soil, and decreases to low values (< 30 mmol$_c$ kg^{-1}). The exchange complex is dominated by Al and H. In the top 20 cm, however, the Fe occupation is relatively high (> 10 mmol$_c$ kg^{-1}). Base saturation (measured as an unbuffered Bascomb) is negligible throughout the profile. The profile shows elevated values of secondary Fe and Al compounds at 15 - 35 cm depth. In general, contents of secondary Al compounds are high. Mineralogical analysis of the clay

fraction shows the presence of vermiculite in the top 20 cm, and chlorite between 20 and 70 cm depth. In addition, traces of kaolinite, mica, smectite, quartz and feldspar are found.

TABLE 11

Soil textural and chemical properties of the Speuld-B plot (source: Tiktak *et al.*, 1988).

Horizon	Depth (cm)	Textural analysis (%) < 2	2-16	16-50	50-105	> 150 µm	OM-C (%)	C/N (-)	rho (kg m^{-3})	pH-H_2O	pH-KCl
O	-9-0	-	-	-	-	-	-	29.0	110	-	-
Ah	0-3	<0.5	4.5	33.5	7.0	55.0	9.5	29.0	1115	3.6	2.8
E/Ah	5-10	<0.5	2.0	16.0	11.0	70.5	2.4	34.0	1115	3.7	3.1
Bh2	15-20	<0.5	3.0	21.0	9.5	64.0	1.7	33.2	1315	4.0	3.9
Bw1	30-35	<0.5	3.0	18.5	9.5	64.0	0.6	20.7	1402	4.2	4.4
Bw2	50-55	<0.5	<0.5	14.5	11.0	74.0	0.2	18.0	1585	4.2	4.5
Bw2	70-75	<0.5	<0.5	8.5	11.0	80.0	0.1	13.0	1589	4.4	4.6
C1	90-95	<0.5	<0.5	9.5	10.5	79.5	0.2	15.0	1590	4.4	4.6
C2	110-120	<0.5	0.5	12.0	8.0	79.5	0.2	15.0	1610	4.3	4.4

TABLE 12

CEC, composition of the adsorption complex and content of oxalate extractable aluminum of the Speuld-B plot (source: Tiktak *et al.*, 1988).

Horizon	Depth (cm)	Exchangeable amounts ($mmol_c$ kg^{-1}) [a] H	Al	NH_4	Fe	CEC	secondary Al-compounds [b] ($mmol_c$ kg^{-1})	secondary [c] Fe-compounds ($mmol_c$ kg^{-1})
O	-9-0	191.3	39.2	5.4	0.0	246	-	-
Ah	0-3	56.2	29.8	3.5	11.0	105	165	130
E/Ah	5-10	16.8	23.7	1.0	14.5	58	171	130
Bh2	15-20	5.5	37.7	0.7	10.5	57	324	210
Bw1	30-35	16.0	10.8	0.2	0.8	29	488	210
Bw2	50-55	15.6	7.8	0.1	1.1	26	312	210
Bw2	70-75	13.0	13.0	0.2	1.5	29	259	210
C1	90-95	17.2	19.8	0.1	0.9	40	271	210
C2	110-120	13.7	12.5	0.1	0.9	28	459	60

a) Amounts of exchangeable base cations (Ca^{2+}, Mg^{2+}, Na^+, K^+) always below detection limit

b) Oxalate extractable Al

c) Oxalate extractable Fe; generic data for Cambic Podzol (see text)

TABLE 13

Total elemental analysis (%) of the Speuld-B plot (source: Tiktak *et al.*, 1988).

Horizon	Depth (cm)	SiO_2	Al_2O_3	Fe_2O_3 (%)	FeO	MgO
O	-9-0	0.012	0.198	-	-	-
Ah	0-3	1.501	0.030	0.025	0.148	0.174
E/Ah	5-10	1.683	0.035	0.029	0.168	0.195
Bh2	15-20	2.001	0.050	0.029	0.168	0.212
Bw1	30-35	2.224	0.055	0.036	0.181	0.212
Bw2	50-55	1.977	0.055	0.039	0.203	0.212
Bw2	70-75	1.795	0.055	0.032	0.181	0.214
C1	90-95	2.183	0.089	0.032	0.207	0.261
C2	110-120	2.583	0.114	0.029	0.213	0.284

3.5.2 *Soil solution composition*

Soil solution samples were collected weekly, from porous ceramic cups at depths of 10, 20, 40, 60 and 90 cm into evacuated 250 ml glass bottles. Soil solution was also collected quantitatively every fortnight by an automated continuous sampling procedure, using filter plates and a suction which equals the pressure head in the soil (cf. Tiktak *et al.* 1988). The latter procedure is used to collect flux-weighted average soil solution samples from underneath the litter layer and at depths of 10 and 120 cm. Installation of the cups and plates was carried out in December 1986. Soil chemical monitoring was carried out between January 1987 and March 1991. Analytical procedures are described in §3.3.1. Results of the monitoring for SO_4^{2-} are shown in Figure 11.

Figure 11
The soil water SO_4^{2-} concentration ($mol_c\ m^{-3}$) for three sub-plots at the Speulderbos site.

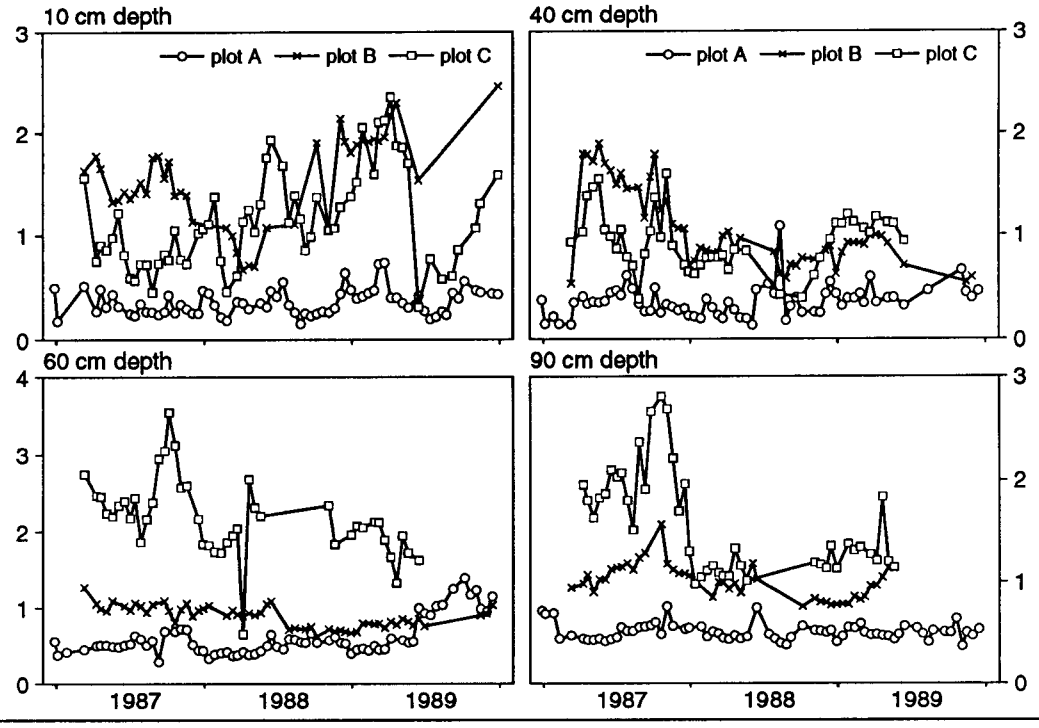

3.5.3 *Model parameters*

For the derivation of the geo-chemical input parameters of the models, the data-set for plot B was used (see §3.5.1). However, parameters were often available for different depths in the soil profile. In order to obtain a coherent set of input parameters, all state variables used in the derivation of input parameters were estimated for the same depths according to:

$$\hat{X}_z = \frac{\Delta z_2 X_1 + \Delta z_1 X_2}{\Delta z_1 + \Delta z_2} \qquad (62)$$

with X_z as the estimated value of state variable X at depth z, $X_{1/2}$ as the measured value of state variable X at depth $z_{1/2}$, and $z_{1/2}$ as the nearest depth with measurement $z_1 < z < z_2$. For state variables related to a soil layer with thickness Δz, z is the depth in the middle of that layer.

Exchange constants

Gaines-Thomas exchange coefficients were calculated from the long-term average soil solution concentrations extracted with cups (plot B; §3.5.2) and the amount of exchangeable cations as measured with Bascomb (Table 12) and Li-EDTA. Fractions of exchangeable cations and total CEC were calculated as the mean of both methods. From the concentrations, activities were calculated with the chemical equilibrium program EPIDIM (Groenendijk, 1995). Coefficients were calculated with equation (47) using Ca^{2+} as the reference ion. As the content of exchangeable base cations was below the detection limit, the exchangeable fractions (fraction of total CEC) of all base cations were set to 0.01 to calculate Gaines-Thomas exchange coefficients and to initialize the models. Results are shown in table 14.

Weathering rate parameters

Parameters for weathering of silicates (equation (40)) were calculated from results of batch experiments (De Vries *et al.*, 1995b) for a generic Cambic Podzol. They estimated the total weathering flux for a 70 cm profile by dividing the fluxes derived from the batch experiments by 50. This factor was introduced to account for differences between field and laboratory conditions. The fluxes presented by De Vries *et al.* (1995b) were multiplied by a factor 10/7 to calculate the weathering fluxes for a 1 m profile. The weathering rate constant for the Speuld profile, $kX_{we,pm}$, is calculated as follows. The coefficients α and $kX_{we,pm}$ are assumed to be layer independent. Parameter α was taken directly from De Vries *et al.* (1995b). The average pH value as measured for plot B by Van der Maas and Pape (1990) was substituted. Total contents of primary minerals and the bulk density were taken from Tiktak *et al.* (1988). Equation (40) can be written down for each soil layer. By substituting all parameters into equation (40), and by assuming that the total weathering fluxes calculated by this equation equals the weathering flux by De Vries *et al.* (1995b), the weathering rate constant can be calculated. The results of the calculations are presented in Table 15.

TABLE 14

Gaines Thomas exchange coefficients $(mol\ l^{-1})^{z-2}$ and cation exchange capacity $(mmol_c\ kg^{-1})$.

Depth	Gaines Thomas exchange coefficient relative to Ca^{2+} $(mol\ L^{-1})^{z-2}$						CEC
(cm)	H^+	Na^+	K^+	NH_4^+	Mg^{2+}	$Al^{3+} + Fe^{3+}$	$(mmol_c\ kg^{-1})$
-9-0	4.00×10^4	42.9	151.9	1890.9	3.4	561.7	245.67
0-5	1.70×10^4	22.3	128.3	289.1	2.5	813.7	96.94
5-10	0.57×10^4	6.7	80.6	13.6	1.2	127.5	58.33
10-20	0.13×10^4	6.0	120.8	6.7	1.1	73.0	57.08
20-30	0.87×10^4	8.6	267.0	11085.1	1.4	32.2	42.83
30-40	6.66×10^4	5.1	162.5	2136.4	0.9	1.8	29.00
40-50	2.50×10^5	3.3	93.7	1624.7	0.7	0.4	26.92
50-60	2.95×10^5	3.1	69.6	10526.7	0.7	0.4	25.67
60-70	2.43×10^5	3.5	59.2	19454.1	0.8	0.7	27.65
70-80	2.33×10^5	4.5	56.5	3625.4	1.0	1.4	28.83
80-100	2.83×10^5	6.6	52.5	0.0	1.2	2.5	39.67

Parameters for weathering of secondary Al compounds (table 16) were taken from batch experiments as described by De Vries *et al.* (1995b). They investigated a total number of

15 sites throughout the Netherlands. For the model applications, we selected the soil horizons that showed most resemblance to Speuld site. These included the Ah, Bhs, BCs and C horizons. The rate constant, *kEl1*, as determined by De Vries *et al.* (1995b) was divided by an arbitrary 100 to account for differences between field and laboratory conditions (Van Grinsven, 1987; Wesselink, 1994).

TABLE 15
Parameters for weathering of silicates (equation (40)).

Cation	total weathering flux[a]	pH dependent $kX_{we,pm}$	α	pH independent $kX_{we,pm}$
	($mol_c\ ha^{-1}\ a^{-1}$)	(a^{-1})	(-)	(a^{-1})
Na^+	80	8.43×10^{-2}	0.87	4.19×10^{-5}
K^+	75	2.33×10^{-1}	1.02	4.87×10^{-2}
Ca^{2+}	45	2.26×10^{-1}	0.85	7.11×10^{-3}
Mg^{2+}	20	1.92×10^{-1}	1.54	8.81×10^{-1}

a) source: De Vries *et al*, 1995b.

TABLE 16
Parameters for the calculation of weathering of oxalate extractable Al (De Vries *et al.*, 1995b)

Depth (cm)	*kEl1* ($kg^{-1}\ a^{-1}$)	*kEl2* ($m^3\ mol_c^{-1}$)	Horizon in De Vries *et al.*
0-10	1.13×10^{-6}	11.4	Ah
10-40	2.04×10^{-4}	9.1	Bhs
40-80	7.49×10^{-4}	7.3	Bcs
80-100	1.67×10^{-4}	9.8	C

Sulphate and phosphate sorption parameters

The sulphate sorption capacity, *SSC* ($mmol_c\ kg^{-1}$), was calculated from the oxalate extractable amount of secondary Al according to (Johnson and Todd, 1983):

$$SSC = 0.02 \cdot ct\,Al_{ox} \tag{63}$$

The phosphate sorption capacity, *PSC* ($mol_c\ kg^{-1}$), was calculated from the equation (Van der Zee, 1988):

$$PSC = 0.2 \cdot (ct\,Al_{ox} + ct\,Fe_{ox}) \tag{64}$$

Contents of oxalate extractable Al are from Tiktak *et al.* (1988), contents of oxalate extractable Fe are from measurements on comparable Cambic podzols (De Vries, personal communication). The Langmuir adsorption constant for SO_4, $KeSO_{4\ ad}$, is set to $0.5\ m^{-3}\ mol^{-1}$ and is extracted from the RESAM database (De Vries *et al.*, 1994). The Langmuir adsorption constant for phosphate, $KeH_2PO_{4\ ad}$ is determined from *Pw* (phosphate in water) and *Pox* (oxalate extractable phosphate) as determined in 150 forest stands in the Netherlands. Results are shown in table 17.

TABLE 17
Sulphate and phosphate sorption capacities as a function of depth, calculated according to equations (63) and (64).

Depth (cm)	*SSC* ($mmol_c\ kg^{-1}$)	*PSC* [a] ($mmol_c\ kg^{-1}$)
0-5	3.3	59
5-10	3.4	60
10-20	5.7	99
20-30	8.1	123
30-40	9.8	140
40-50	7.6	118
50-60	6.3	106
60-70	5.6	98
70-80	5.2	94
80-100	5.4	66

a) derived from generic data for a Cambic Podzol

Al dissolution and nutrient cycling

The Al dissolution constant and parameters for nutrient cycling in all models are presented in table 18.

TABLE 18
Values for soil-layer independent model parameters

Process	Parameter	Unit	Value	Eqn.
Foliar uptake[a]	$fr NH_{4,fu}$	(-)	0.21	(15)
	$fr H_{fu}$	(-)	0.58	(15)
Foliar exudation[a]	$fr Ca_{fe}$	(-)	0.18	(17)
	$fr Mg_{fe}$	(-)	0.11	(17)
	$fr K_{fe}$	(-)	0.71	(17)
Nitrification[b]	k_{nl}	(a^{-1})	100.0	(37)
Al dissolution[c]	KAl_{ox}	($L^2\ mol^{-2}$)	5.0×10^8	(46)

[a] Based on throughfall data over the period 1987-1990 (Van der Maas and Pape, 1990).
[b] Obtained by calibration. The generic value for k_{nl} is 40 a^{-1}.
[c] Average *IAP* for $Al(OH)_3$ at 90 cm over the period 1987-1990, activities calculated from measured concentrations (Van der Maas and Pape,1990).

3.6 Forest growth

3.6.1 Tree compartments

The main ecophysiological research and growth analysis was carried out from 1987 until 1989 (Evers *et al.*, 1991) in a plot adjacent to the plot where most of the soil research was done. The soil subplot had a somewhat higher stand density compared to the ecophysiological plot (812 vs. 765 trees ha^{-1}). After 1989, the biomass analysis was moved to the soil research plot, causing a discontinuity in the data series. Table 19 gives an overview of basic stand data for the soil plot and for the tree physiological plot as measured in December 1988.

TABLE 19

Overview of basic stand data for the soil research plot and for the ecophysiological research plot as measured in December 1988. Data for plot 1 were measured by Jans *et al.* (1994), data for the soil plot (except stand density) were measured by Olsthoorn (1991).

Parameter	Unit	Ecophysiological research plot (plot 1)	Soil research plot (plot 2)
Stand age	(a)	30	30
Stand density[a]	(ha^{-1})	765	812
Height	(m)	19.7	19.4
Diameter at Breast Height (DBH)[b]	(m)	0.226	0.221
Basal area	(m^2 ha^{-1})	30.7	31.1
Stem volume	(m^3 ha^{-1})	279	281
Leaf Area Index (LAI)[c]	(m^2 m^{-2})	10.6	
Specific Leaf Area (SLA)[d]	(m^2 kg^{-1})	5.7	
Basic wood density	(kg m^{-3})	451	448
Biomass	(Mg ha^{-1})		
Foliage[e]		18.5	
current year	(Mg ha^{-1})	6.72	
1 year old	(Mg ha^{-1})	5.34	
2 years old	(Mg ha^{-1})	3.78	
3 years old	(Mg ha^{-1})	1.85	
4 years old	(Mg ha^{-1})	0.77	
Branches[f]	(Mg ha^{-1})	14.0	
Stems			
Sap wood	(Mg ha^{-1})	65.0	
Heart wood	(Mg ha^{-1})	60.0	
Total wood	(Mg ha^{-1})	125.0	
Coarse roots[g]	(Mg ha^{-1})	27.9	
Fine roots	(Mg ha^{-1})		3.2
Litter mass[h]	(Mg ha^{-1})		35

a) Stand density measured by Jans *et al.* (1994). Earlier figures of stand density for the soil research plot (886 trees ha^{-1}) were published by Olsthoorn (1991) and refer to a subplot within the soil research plot.

b) Average DBH for the entire plot (210 trees in plot 1 and 368 trees in plot 2). The average DBH of the 75 sampling trees was higher, viz. 0.231 m for plot 1 and 0.235 m for plot 2.

c) Long-term average LAI (1987-1989) for plot 1 is 13.7 m^2 m^{-2}. The long-term average LAI for plot 2 (1990-1992) is 10.9 m^2 m^{-2} (Jans *et al.*, 1994). The LAI presented by Evers *et al.* (1991) was lower, viz. 10.7 for plot 1 (1986-1988).

d) Using the LAI presented by Evers *et al.* (1991), the SLA must have been 5.8 m^2 kg^{-1}.

e) Steingröver *et al*, 1995.

f) Estimated from stem biomass using allometric equations (Steingröver *et al.*, 1995).

g) Calculated from the DBH using the relation (De Kuiper and Van Dijk, 1988): $W_{cr} = 0.01\ DBH^{2.63}$ ($r^2 = 0.96$), with W_{cr} (Mg ha^{-1}) as the dry weight of coarse roots.

h) Measured by Tiktak and Bouten (1992). The litter mass is an average value for 485 samples.

State variables that must be known at the beginning of the simulation include the element contents in needles, stems, branches, roots and litter. Data related to these compartments are given in Table 20. Data are given for the end of the year 1988.

TABLE 20
Data on biomass and element contents of needles, roots and stems of Speuld stand.

Compartment	Biomass (Mg ha^{-1})	Element content (% of dry weight)					
		N	P	K	Ca	Mg	S
Foliage[a]	18.5	1.84	0.15	0.58	0.33	0.09	0.14
Branches[b]	14.0	0.30	0.02	0.10	0.05	0.03	0.05
Sapwood[b]	60.0	0.20	0.02	0.10	0.05	0.01	0.05
Heartwood[b]	65.0	0.05	0.01	0.02	0.05	0.01	0.01
Coarse roots[b]	27.9	0.30	0.02	0.10	0.05	0.01	0.05
Fine roots[c]	3.2	1.00	0.06	0.08	0.16	0.04	0.10

a) measured in the ecophysiological research (Evers *et al.*, 1991).
b) nutrient contents in branches, wood and coarse roots inferred from general data (Berdowski *et al.*, 1991).
c) measured in the soil research plot by Olsthoorn (1991).

Needle fall was measured by three different methods (Table 21). First, needle fall was derived indirectly from observations on needle occupancy (Steingröver *et al.*, 1995). These measurements were also used for deriving needle growth data. Secondly, needle fall was measured directly using 12 litter traps with a surface area of 1 m^2 (Van der Maas and Pape, 1990). Finally, additional measurements were carried out by Steingröver *et al.* (1995). They used a large net with an area of 45 m^2. Unfortunately, they did not replicate these measurements.

TABLE 21
Needle fall and needle growth derived from observations on needle occupancy, litter traps and a large net. For references: see text.

Year	Plot[a]	needle mass (Mg ha^{-1})	needle loss (Mg ha^{-1} a^{-1})			needle growth (Mg ha^{-1} a^{-1})
			needle occupancy	litter traps	litter net	
1988	1	18.5	6.53	2.19		6.53
1989	1	17.5	6.77	3.35	2.83	5.90
1990	2	19.0				
1991	2	19.2	7.77			8.02
1992	2	20.8	6.11			7.52

a) Plot for needle occupancy measurements. Litter trap measurements were carried out in plot 2 (soil plot) and litter net measurements in plot 1 (ecophysiological plot).

From the above table it is obvious that needle fall obtained from direct measurements is much lower than needle fall inferred from needle occupancy. This discrepancy can only partly be attributed to stand heterogeneity. In view of the number of needle age classes observed in Speuld (viz. 4) and the needle fall fractions derived from the needle occupancy measurements, the lower needle fall figures as obtained from direct measurements cannot be used in combination with the high biomass figures measured by Steingröver *et al.* (1995). For this reason, the higher needle fall figures were used. The root length

distribution is presented in §3.4.1, table 9. Turnover rates for fine roots were 1.0 a^{-1} (Olsthoorn and Tiktak, 1991).

Needle mass, and estimated needle increment and needle loss are high compared to data from other sites (§3.1.2). In the same time, root biomass is low. All this has major consequences for nutrient cycling through litter fall, and for assimilate allocation and the whole tree carbon budget.

3.6.2 Basic stand data as input to the models

As the data from the soil research plot were used to calibrate the models, it was chosen to apply all models using basic stand characteristics as in the soil research plot. Table 22 gives a reconstruction of growth data for this plot. These growth data were used for model calibration.

TABLE 22

Stand structure data for the soil research plot (average of 370 trees). Data refer to the condition at the end of the year, with growth rates referring to the previous year (Steingröver *et al.*, 1995).

Year	DBH (m)	Height (m)	Basal Area (m^2 ha^{-1})	increment (m^2 ha^{-1} a^{-1})	Stem Volume (m^3 ha^{-1})	increment (m^3 ha^{-1} a^{-1})	(Mg ha^{-1} a^{-1})[a]
1986	0.206	(18.1)[b]	(27.06)		(232)		
1987	0.213	(18.7)	(28.93)	(1.87)	(254)	(22)	(12.1)
1988	0.221	(19.4)	(31.15)	(2.22)	(281)	(27)	(14.8)
1989	0.226	(19.8)	(32.57)	(1.42)	(298)	(17)	(9.4)
1990	0.235	20.4	35.22	(2.65)	329	(31)	(17.0)
1991	0.240	21.1	36.73	1.51	352	23	12.5
1992	0.249	21.6	39.54	2.81	384	32	17.9
1993	0.254	22.2	41.14	1.60	408	24	13.0

a) Data used for fitting of the growth function in NuCSAM (Eqn. (29)). The following parameters were derived: kr_{grl} = 0.09 a^{-1}, $Am_{st,mx}$ = 540 Mg ha^{-1} and t_{50} = 38.1 a.

b) Data in brackets were reconstructed using the assumption described above.

For monitoring of needle occupancy, a smaller number of trees (75) was used. These trees had a somewhat higher average DBH than the trees in the entire soil monitoring plot. To account for possible bias resulting from sampling a subset of above-average trees, a correction on needle mass, needle loss and needle growth was applied based on tree basal area. The 75 trees used for monitoring of needle occupancy had an average DBH of 0.272 m, or basal area of 0.580 m^2 at the end of 1992. The entire soil research plot had an average DBH of 0.249 m or basal area of 0.487 m^2. All data related to needle turnover were multiplied by 0.487/0.580 = 0.84. Thus, the total needle mass used in the models was 15.5 Mg ha^{-1} and the needle fall was about 5.5 Mg ha^{-1}. We used an LAI of 10.7 m^2 m^{-2} and a SLA of 5.8 m^2 kg^{-1}. These values were taken from Evers *et al.* (1991) as new figures were not available when the simulations were carried out.

4 MODEL CALIBRATION

The applied models render an approximate description of the system under study and contain parameters, initial and boundary conditions, which are incompletely known. More information on these quantities, which are often not measurable, is required to obtain accurate inferences from the model, and for judging its performance adequately. Hence, model calibration is required to determine these values accurately from the available measurements, taking into account the intended model use and available prior knowledge.

Model calibration thus becomes a critical phase in the modelling process. Despite its importance, the required activities for calibration are often given little consideration, and in many cases the model is calibrated using non-reproducible methods. As the models under consideration contain a large number of parameters, a well-structured and systematic calibration approach is needed, supported by useful guidelines.

4.1 Strategy

Janssen and Heuberger (1995a) present a general outline of the calibration[1] process, and distinguish various important steps:

- identify the characteristics of the data-set.
- identify the parameters that need calibration, preferably by performing model analyses (sensitivity and uncertainty analyses).
- specification of model performance criteria, which express the discrepancy between measurements and model results.
- solution of the calibration problem, which often consists of adjusting the model parameters such that the model results match the measurements adequately (e.g. minimal misfit).

The calibration process is usually completed by assessing the accuracy and quality of the obtained model (validation aspects; see Janssen and Heuberger (1995a)).

In the sequel it is briefly addressed how the above mentioned issues apply for the calibration of the various models on the Speuld data-set.

4.1.1 The characteristics of the data-set

Measurements were carried out at different spatial scales and at different positions within the stand. Most soil hydrological measurements were carried out at one plot of 30×30 m^2, although an attempt has been made to scale these measurements to stand average values (Bouten *et al.*, 1992). Soil chemical measurements are 'point' measurements. Samples were taken from three plots and the volume of soil sampled is small. Also the tree physiological measurements were carried out at one point within the forest stand. On the other hand, eddy correlation measurements of deposition and transpiration are representative at a scale which is larger than the stand. Measurements of throughfall amounts, throughfall quality and of forest growth, although point measurements, were

[1] Model calibration is defined as the determination of the model parameters, boundary and initial conditions and/or structure on basis of measurements, and of prior knowledge.

scaled to average values. However, all these measurements were carried out at the Eastern half of the stand, possibly leading to a deviation from stand average values.

Due to these different spatial scales it is almost impossible to combine all measurements within one data-set. Consider the following example: If the hydrological part of the models is calibrated using the average transpiration measured by eddy correlation as a criterion, the hydrological regime will be different from the hydrological regime at the soil chemical sampling points. For this reason, the hydrological part of the models was calibrated using data from the soil monitoring plot only. This calibration is not representative for the stand as a whole, but can be used in combination with the soil chemical data-set.

4.1.2 Parameters that need calibration

Ideally, the selection of parameters to be calibrated is based on systematic sensitivity and uncertainty analyses. Such analyses were carried out for ReSAM (Kros *et al.*, 1993) and for SoilVeg-2 (Van Grinsven *et al.*, 1991). For the site models discussed here, calibration was limited to a small number of parameters, which are briefly addressed per model.

NuCSAM

The choice of the model parameters that need calibration was based on an uncertainty analysis for the model ReSAM (Kros *et al.*, 1993). Table 23 summarizes the parameters for which the solute concentrations were most sensitive. These parameters have been chosen for model calibration. The choice of the hydrological parameters to be calibrated (not shown in table) was based on Tiktak and Bouten (1992).

TABLE 23

NuCSAM model parameters that were calibrated.

#	Parameter	Description	Effect on concentration of:	Eqn.
1	kr_{ni}	nitrification rate constant	NO_3^- and NH_4^+	(37)
2	kEl_1	Elovich constant	Al^{3+} and H^+	(42)
3	$ctNlv_{mx}$	Maximum N-content of leaves	NO_3^- and NH_4^+	(21)
4	$krCa_{we,pm}$	rate constant for Ca-weathering	Ca^{2+}	(40)
5	$krMg_{we,pm}$	rate constant for Mg-weathering	Mg^{2+}	(40)

ForGro

The main parameters used for calibrating the model where the set of parameters describing assimilate allocation and the distribution of dry matter increment over the biomass components (equation (57)). It turned out to be necessary to increase the proportion of assimilates going into foliage growth, in order to simulate the high LAI values measured at the site (§3.6). Increase in allocation to foliage leads to a decrease in stem, root or branch increment. The calibration to LAI was taken at the expense of stem growth, as any decrease in root growth might influence nutrient and water uptake, thereby possibly inducing adverse side effects of the calibration. Fine root growth simulated with the model matched the field data measured by Olsthoorn, 1991.

SoilVeg

The crucial step in calibration of SoilVeg is parameterization of the age-dependent empirical relationships for gross nutrient uptake (Eqn. (35)) and carbon allocation to biomass compartments (Eqn. (54)). These empirical curves can be fitted on site observations or (generic) yield tables to estimate biomass and nutrient content for the wood, foliage and root compartments. Both empirical relationships were fitted for a reference situation which is specific for any combination of forest and soil. In the reference situation, no trends in climatological variables and external nutrient inputs are assumed. Moreover, once the stand has reached the mature phase, the total mass of fine roots and foliage remains constant in time and nutrient contents are constant in all plant compartments.

Extensive data-sets on biomass increment and nutrient content were obtained from literature for Douglas fir (Berdowski *et al*, 1991) to support both empirical relationships. Obviously there is a large scatter in the data due to the fact that they apply to a wide range of Douglas fir genotypes, soil types, air quality and climates. The assumption that air quality and climate for the selected stand data show no trend cannot be validated. This is a serious source of uncertainty for the SoilVeg extrapolations. Using forest yield tables as an alternative to the actual observation data reduces the data scatter but yield tables cannot be linked to data on nutrient contents of foliage and roots.

4.1.3 Model performance criteria

For the evaluation of model performance in relation to observation data in Speuld, statistical indicators as described by Janssen and Heuberger (1995a) have been used. As each of these indicators gives different information about model behaviour, two different performance measurements were use, as described below:

$$\text{NME} = \frac{(\overline{p}-\overline{o})}{\overline{o}}$$

and

$$\text{NMAE} = \frac{\sum_{i=1}^{n}(\,|p_i - o_i|\,)}{n \cdot \overline{o}} \qquad (65)$$

Here, NME (-) is the Normalized Mean Error, NMAE (-) is the Normalized Mean Absolute Error, p_i is the predicted value, o_i is the observed value, $\overline{o}$ and $\overline{p}$ are the averages for the observed and predicted values, and n is the number of observations. The NME compares predictions and observations on an *average* basis (i.e. over the whole time-span). The NME thus expresses the bias in average values of model predictions and observations and gives a rough indication of overestimation (NME > 0) or underestimation (NME < 0). The NMAE is an absolute indicator for the discrepancy between model predictions and observations. The NMAE does not allow for compensation of positive and negative discrepancies. A NMAE of zero is considered optimal.

These criteria can be defined and evaluated for various model quantities, individually as well as jointly. For a fair comparison between model results and observations, their

temporal and spatial scale should be compatible. For model calibration, model results were compared with accumulated throughfall amounts (§3.2), soil water contents (§3.4.3), soil solution composition (§3.5.2), stem growth, needle mass and concentration of nutrient in needles (§3.6).

The presented misfit criteria consider only specific aspects of the system under study, and express the agreement between model data and data in a very condensed form, i.e. in one number. Therefore, the use of these quantitative criteria should be supplemented by qualitative techniques (e.g. visual comparison of measurements and model results).

4.1.4 Solution of the calibration procedure

An automated and objective calibration method has been developed, viz. the Rotated Random Scan method (Janssen and Heuberger, 1995b; Janssen, 1995a; Janssen and Sanders, 1995). This method is a procedure for restricting the uncertainty in the parameters, by efficiently scanning the parameter space for a set of model parameters, which match the data adequately. The procedure is especially suited for situations where data are scarce and inaccurate, or for calibration studies where a substantial reduction of the initial parameter range is desired, in order to increase the effectiveness and efficiency of the subsequent fine-tuning of the parameters. Associated techniques for sensitivity analysis have been developed, to enable an adequate selection of parameters to be calibrated (Janssen, 1995b, 1995c).

These procedures were not applied for the site models under consideration, because of the large number of model parameters that needed calibration, the interaction between the model parameters and the non-linear behaviour of the models. However, an automated method has been applied for calibration of the steady state regional soil acidification model MACAL (Kros *et al.*, 1994). For the Speuld site, the models were provisionally calibrated by visual minimization of the difference between observed and simulated time series of measured data. Visual interpretation is not always unambiguous and robust. Therefore, also performance criteria as described above (§4.1.3) have been evaluated.

In view of the large number of state variables that are relevant for hydrology, soil chemistry and forest growth, it is not meaningful to develop one model performance criterion that considerers all these states. One reason is that there is no guideline to weigh the various state variables in such a criterion. Instead, model parameterization and model calibration followed a sequential procedure, guided by the strength of the interactions between hydrology, chemistry, and tree processes. Hydrology affects soil solution chemistry but not vice versa. The effects of soil hydrology and soil solution chemistry on nutrient uptake and tree growth are stronger than vice versa. The calibration and parameterization procedure is outlined below.

Step 1: Parameterization and calibration of the hydrological submodels.

- Parameterization of the soil water transport modules, water uptake distribution with depth and water uptake reduction functions.
- Calibration and cross-validation using time series of throughfall and water contents.
- Validation using time series of soil solution concentration of Cl^- and SO_4^{2-}.

Step 2: Parameterization and calibration of the soil chemistry submodels.

- Parameterization of cation exchange, bio-chemical transformation and nutrient uptake distribution with depth.
- Calibration and cross-validation using time series of soil solution concentrations.

Step 3: Parameterization and calibration of the forest growth submodels.

- Parameterization of the root uptake module, allocation of carbon and nutrients to various plant components.
- Calibration and cross-validation using biomass increment, nutrient contents in biomass components and time series of soil solution concentrations.

4.2 Hydrology

4.2.1 Interception and throughfall

Figure 12
Accumulated simulated throughfall for the years 1988 and 1989.

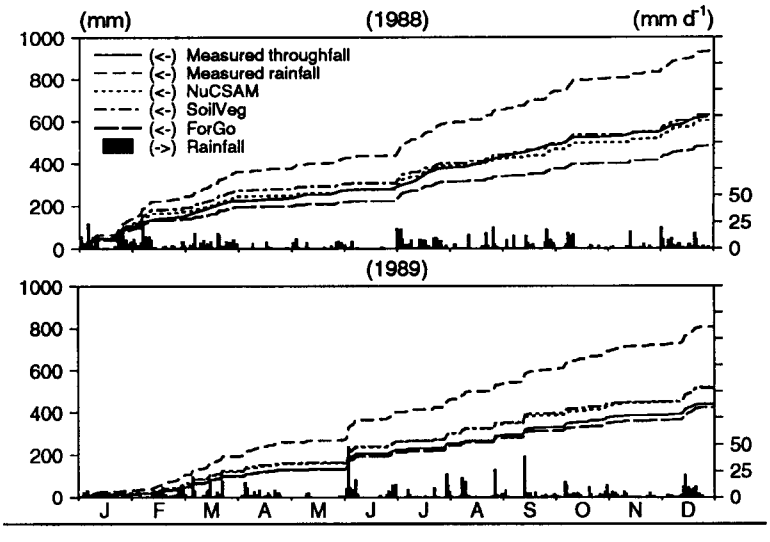

Simulated throughfall amounts are presented in Figure 12. Table 24 presents the annual water balances for the period 1987-1989. ForGro simulates a high annual interception compared to the other models, mainly resulting from different modelling philosophies. ForGro is a 'state of the art' process oriented model, which was not calibrated, but was parameterised using generic data. In view of the high Leaf Area Index at the Speuld site, these generic data do not apply to Speuld. The calibrated models SoilVeg and NuCSAM overestimate the accumulated throughfall amount for 1989 and underestimate the throughfall amount for 1987. For 1988, throughfall amounts are in close agreement with measured throughfall values (maximum deviation < 10% of observed value). The overestimation of throughfall for 1989 is mainly caused by deviations between measured precipitation at Drie and on-site measured precipitation (see footnote in table 24). SoilVeg and NuCSAM simulate almost equal throughfall and interception amounts for 1989, but considerable differences occur for the other years with the largest deviations occurring in 1987. This reflects the uncertainty in both the parameterization and concepts of the evaporation part of the interception modules. In 1989, rainfall mainly occurred as large

storms. After such storms, a large part of the total precipitation drains instantaneously from the canopy and evaporation loss is relatively small. In 1987, however, a large part of the annual precipitation was in the form of small storms and evaporation losses were high.

TABLE 24
Simulated water balance terms for the Speuld experimental forest.

	1987			1988			1989		
Fluxes ($mm\ a^{-1}$)	NuC SAM	Soil Veg	For Gro	NuC SAM	Soil Veg	For Gro	NuC SAM	Soil Veg	For Gro
Precipitation[a]	976	976	976	933	933	933	806	806	806
Interception	357	315	404	331	303	449	285	286	384
Throughfall	619	661	572	602	630	484	521	519	422
Evaporation	55	73	24	56	79	19	66	88	21
Transpiration	365	359	336	323	301	311	371	382	390
Drainage	199	280	222	221	255	177	84	51	58
Transpiration reduction (%)	0.8	3	9	13	22	10	16	22	18
Measured throughfall		660			618			449	

a) Precipitation measured at Drie is input to the models. On-site measured precipitation was 950 mm a^{-1} for 1987, 935 mm a^{-1} for 1988 and 710 mm a^{-1} for 1989. These values were not used, because on-site measurements were not carried out daily.

4.2.2 Soil water contents

Simulated soil water contents for 1989 are shown in Figure 13. Table 25 gives an overview of performance criteria for the discrepancy between the observed and measured soil water contents. For the 0-50 cm soil layer, the average soil water contents are overestimated by ForGro (NME = 0.521). NuCSAM gives the best performance for this soil layer. The overestimation by ForGro results from a different parameterization of the empirical relationship between soil water fluxes and water contents. These relationships were derived for a subplot with a higher water holding capacity. In the 50-100 cm soil layer, soil water contents are underestimated by NuCSAM. However, differences mainly occur in autumn, indicating that rewetting of the soil occurs too late. The same conclusion applies to ForGro, whereas SoilVeg gives an overestimation for this soil layer. None of the models predict the dynamic behaviour of measured soil water contents correctly, probably indicating that fingered flow is a relevant hydrological process for Speuld.

TABLE 25
Performance criteria for the discrepancy between observed and measured soil water contents.

Model	0-50 cm[a]		50-100 cm[b]	
	NME	NMAE	NME	NMAE
NuCSAM	0.097	0.248	-0.130	0.174
SoilVeg	0.293	0.329	-0.012	0.209
ForGro	0.521	0.522	0.021	0.196

a) Model output compared with TDR measurements (n = 88).
b) Model output compared with neutron probe measurements (plot B; n = 43).

Figure 13
Comparison of observed and simulated water contents in the 0-50 and 50-100 cm soil layers for the year 1989.

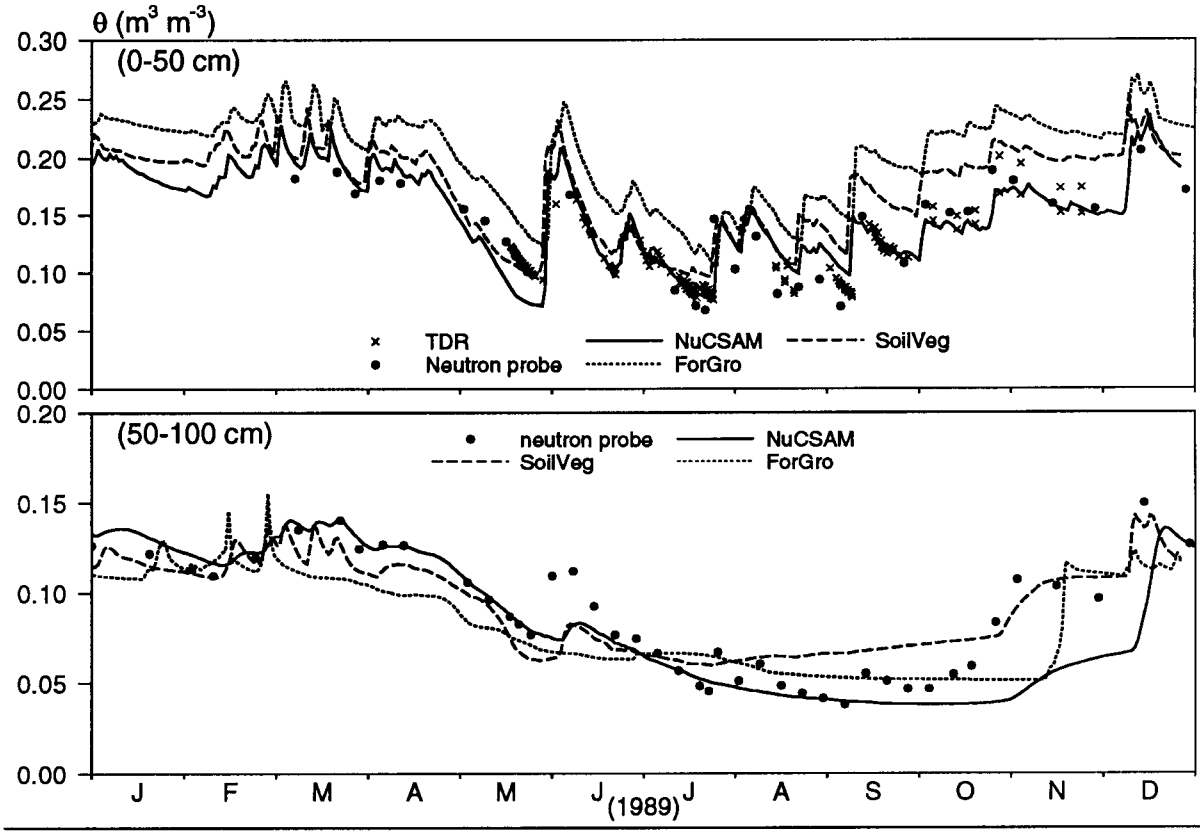

4.2.3 Transpiration, soil evaporation and drainage

The hydrological submodels are mainly intended for calculating vertical drainage fluxes, soil evaporation fluxes and transpiration. These fluxes are important for forest functioning (transpiration) and transport of solutes (drainage).

Simulated transpiration figures are comparable for all models. This is remarkable, as both model concepts and modelling philosophies were different for SoilVeg and NuCSAM on the one hand and ForGro on the other. ForGro uses the Penman-Monteith equation parameterised with general data, whereas SoilVeg and NuCSAM use the Makkink equation in combination with an empirical (calibrated) crop factor. SoilVeg and NuCSAM used the same crop factor, based on Tiktak and Bouten (1994). In a separate hydrological study carried out at Speuld, Tiktak and Bouten (1994) compared simulated transpiration with measured transpiration data. They found comparable transpiration figures. Table 24 also shows the annual reduction of transpiration. ForGro predicts the lowest transpiration reduction. Probably the most important reason is the lower potential evapotranspiration simulated by ForGro. This demonstrates that the actual degree of transpiration reduction is highly uncertain and is dependent on the definition of potential transpiration.

There is a large variation of simulated soil evaporation obtained (Table 24). These differences are mainly caused by differences in the process formulations for soil

evaporation, demonstrating the lack of consensus at this point, due to a common shortage of data for validating the models at this point.

The overall effect of simulated hydrological processes is demonstrated by drainage fluxes. Differences between the models are as high as 50% of the average value for all models, mainly caused by differences in interception and soil evaporation. This clearly demonstrates the uncertainty of these fluxes.

4.2.4 Conclusion

It is difficult to make a fair comparison of model performance with the produced simulation results. Although a common data-set was distributed amongst the modellers, modellers often used different model parameters. Probably, these effects of parameterization overshadowed the differences of model behaviour. Bouten *et al.* (1995) pointed out the same problem for the Solling application. From this exercise and from an earlier hydrological study performed at the same site (Tiktak and Bouten, 1994), it is obvious that more complex models not necessarily give better results than simple models.

4.3 Soil chemistry

4.3.1 Soil solution concentrations

Results of the calibration are shown for 20 cm depth in Figure 14 and 90 cm depth in Figure 15. Table 26 shows the NME and NMAE (Eqn. (65)) for the major components for 10, 20 and 90 cm depth.

pH

Simulated pH values showed to be very different, especially for 20 cm. Simulated pH values are calculated from the charge balance in all models. Thus, pH values are affected by virtually all biogeochemical processes, and interpretation of differences between the models on the basis of pH is difficult. Models showed good agreement at different depths, i.e. NuCSAM at 10 cm (figure not shown), SoilVeg at 20 cm (Figure 14) and ForGro at 90 cm depth (Figure 15). This is also reflected by the performance criteria, i.e. the Normalized Mean Absolute Error (NMAE) for H^+ at these depths (table 26). It must be noted that the relatively high pH simulated by ForGro at 20 cm depth is at least partly induced by the very low NO_3^- concentration simulated by this model for that depth.

Aluminum

The large differences between simulated pH values are not reflected in the Al^{3+} concentration. In general, all models produced comparable results. This is especially true for 20 cm. Focusing on SoilVeg results for 20 cm, it can be concluded that both pH and Al behaviour in Speuld can be described with a combination of the Al-hydroxide equilibrium model (Eqn. (46)) and rate limited dissolution of Al-hydroxides (Eq. 42). This contrasts with the results from the model comparison study for the Solling site in Germany (Kros and Warfvinge, 1995). Results at 20 cm showed higher and smaller peaks for NucSAM, whereas the opposite is true for SoilVeg and ForGro. This may be due to differences in transpiration dynamics, as this phenomenon also occurs for SO_4^{2-} and Cl^-. Although the differences in the topsoil are rather small, at 90 cm the ForGro results are better than the

results from the other two models (the NMAE for ForGro is 0.30, whereas NucSAM and SoilVeg values showed to be higher than 0.50; table 26). In addition it is notable that the ForGro results show a less dynamic behaviour than the other models at 90 cm, whereas the opposite is true for 10 cm. This is a result of the hydrological process formulations used: The process formulations for soil water transport in Forgro do not allow for soil water transport at water contents below field capacity. The opposite is true for SoilVeg and NuCSAM (see also §2.2.4).

Calcium

All models underestimate the Ca^{2+} concentration at 20 cm depth. This is reflected by the NME, which is $\leq$ -0.50 for all three models. At 90 cm depth, NuCSAM gives a slight underestimation, whereas SoilVeg and ForGro overestimate the calcium concentrations. The underestimation of the Ca^{2+} concentration at 20 cm depth is probably due to either an overestimation of the calcium root uptake in the topsoil or an underestimation of the calcium cycling through the vegetation. Changing the internal cycling of base cations within the system will lead to higher calcium concentrations in the topsoil, without affecting the calcium concentrations below the root zone (i.e. > 90 cm). Because of the moderate fit for 90 cm (i.e. below the root zone), it is presumable that the calcium input by weathering and deposition is correct.

Nitrate

NO_3^- concentrations were reasonably reproduced by SoilVeg (NMAE = 0.35-0.62) and NucSAM (NMAE = 0.41-0.54), whereas the performance for ForGro was poor (NMAE = 0.71-0.95). The underestimation by ForGro is caused by a lower N-mineralization (see table 27) for this model (about 3 $kmol_c\ ha^{-1}\ a^{-1}$) as compared to SoilVeg and NuCSAM (about 6 $kmol_c\ ha^{-1}\ a^{-1}$). Comparing these results with the results of a model comparison study for the Solling site (Kros and Warfvinge, 1995), it is notable that the nitrogen behaviour can be simulated reasonably with NucSAM and SoilVeg for Speuld, whereas for Solling this was not possible.

Sulphate and chloride

For 90 cm, the SO_4^{2-} and Cl^- concentrations were predicted rather poor by all models (MNAE = 0.40 - 0.58). This is striking because Cl^- and SO_4^{2-} are rather conservative anions in Dutch forest soils. The rather poor performance for these anions is most likely caused by the strong spatial variability of throughfall fluxes and spatial patterns of water uptake by words. Consequently, the hydrological calibration is not valid for the soil chemical monitoring pit.

Figure 14
Simulations of soil water chemistry by NuCSAM, SoilVeg and ForGro for 20 cm depth.

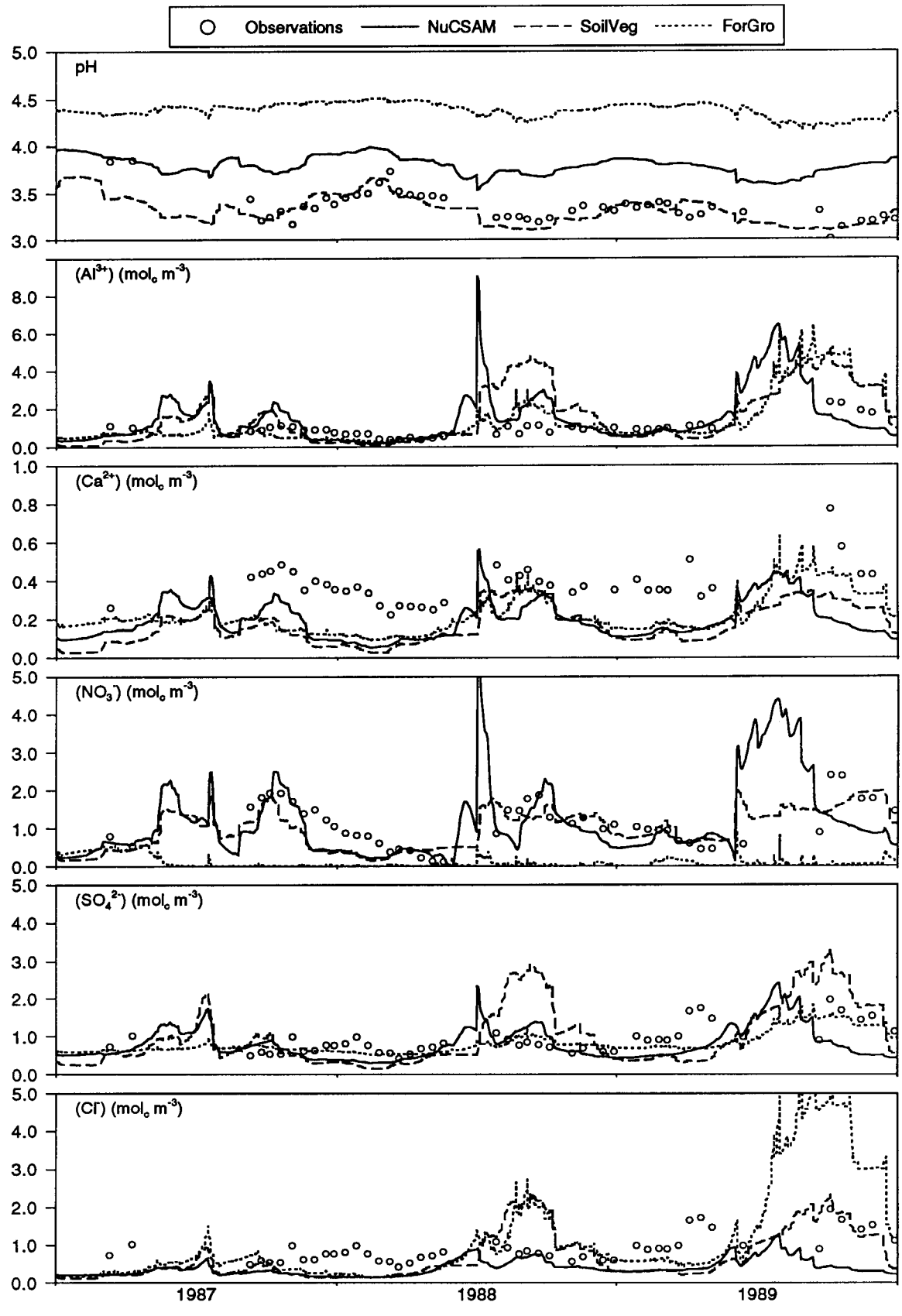

Figure 15
Simulations of soil water chemistry by NuCSAM, SoilVeg and ForGro for 90 cm depth.

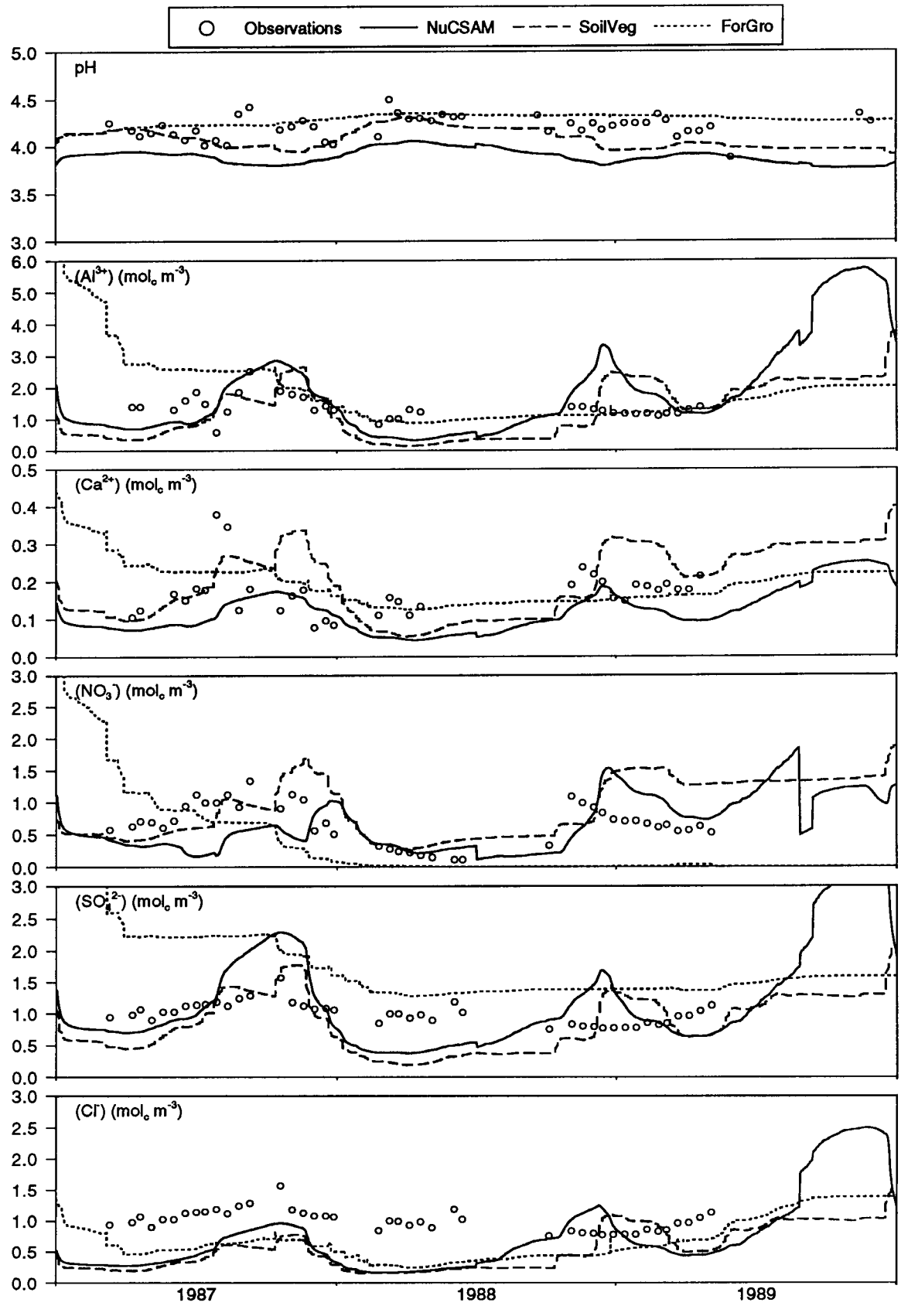

TABLE 26

Performance of NucSAM, ForGro and SoilVeg during the observation period.

Parameter	Performance measurement (-) and number of observations (-)								
	H^+	Al^{3+}	Ca^{2+}	Mg^{2+}	K^+	NO_3^-	NH_4^+	SO_4^{2-}	Cl^-
Depth 10 cm.									
n[a]	48	37	37	37	37	41	44	41	41
NuCSAM									
NMAE[b]	0.39	0.60	0.52	0.86	0.83	0.54	0.84	0.62	0.65
NME[b]	-0.37	-0.30	-0.45	-0.86	0.80	-0.37	-0.82	-0.60	-0.65
ForGro									
NMAE	0.50	0.94	0.66	0.69	0.40	0.71	0.74	0.70	0.70
NME	-0.04	-0.94	-0.17	-0.55	0.05	-0.68	-0.69	-0.68	-0.70
SoilVeg									
NMAE	0.88	0.73	0.55	0.75	0.34	0.53	0.96	0.69	0.59
NME	0.87	-0.47	-0.51	-0.75	0.25	-0.44	-0.96	-0.65	-0.58
Depth 20 cm.									
n	48	41	40	40	40	46	44	46	46
NuCSAM									
NMAE	0.81	0.49	0.63	0.86	2.16	0.41	4.70	0.44	0.47
NME	-0.81	0.10	-0.63	-0.86	2.16	-0.24	3.94	-0.33	-0.40
ForGro									
NMAE	0.91	0.52	0.50	0.38	0.51	0.95	1.07	0.28	1.10
NME	-0.91	0.12	-0.50	-0.27	0.13	-0.95	0.01	-0.15	0.81
SoilVeg									
NMAE	0.21	1.04	0.59	0.48	0.63	0.35	1.68	0.73	0.81
NME	0.07	0.54	-0.59	-0.48	0.38	-0.14	0.71	0.05	0.27
Depth 90 cm.									
n	48	35	35	35	35	43	34	43	43
NuCSAM									
NMAE	0.32	0.57	0.40	0.54	0.84	0.53	0.97	0.40	0.52
NME	0.20	0.28	-0.34	-0.54	-0.84	0.02	-0.90	0.02	0.04
ForGro									
NMAE	0.25	0.30	0.33	0.22	0.47	0.73	1.56	0.68	0.44
NME	-0.20	0.22	0.06	0.18	-0.47	-0.53	-0.04	0.68	0.03
SoilVeg									
NMAE	0.40	0.55	0.51	0.25	0.26	0.62	0.98	0.41	0.50
NME	0.34	-0.40	0.23	-0.10	-0.05	0.34	-0.85	-0.18	-0.24

a) n is number of observations

b) NMAE is Normalized Mean Absolute Error and NME is Normalized Mean Error (see Eqn. (65)).

4.3.2 *Element budgets*

Despite the moderate success of the chemical calibration and the harmonization of parameterization for the soil component, element budgets (table 27) show large differences between the models. Due to preferential uptake of NH_4^+ (Eqn. (32)), the uptake of nitrogen occurs in equal amounts of NH_4^+ and NO_3^- in NuCSAM and ForGro. In SoilVeg, all NH_4^+ is nitrified before it can be taken up. Consequently, nitrogen uptake occurs mainly in the form of NO_3^-. Remarkable is the relatively low total nitrogen uptake for ForGro (5.67 $kmol_c\ ha^{-1}\ a^{-1}$) in comparison with SoilVeg (7.35 $kmol_c\ ha^{-1}\ a^{-1}$) and NuCSAM (7.36 $kmol_c\ ha^{-1}\ a^{-1}$). SoilVeg and NuCSAM simulate a nitrate surplus, whereas nitrate leaching is almost zero for ForGro. These differences are caused by the lower nitrogen mineralization fluxes for ForGro, which in turn explains the low nitrate concentrations simulated by this model. Different element budgets are also calculated for aluminum, although aluminum leaching from the soil profile is in the same order of magnitude. Most striking differences occur for aluminum exchange and aluminum weathering. SoilVeg calculates negative weathering fluxes for aluminum, caused by net-precipitation of secondary aluminum compounds, whereas the other models calculate net-dissolution. At the same time, SoilVeg calculates high exchange fluxes of aluminum, caused by exchange of Al^{3+} versus H^+. Due to the fast response of both Al-exchange and dissolution of secondary Al-oxides to a change in pH, the contribution of both processes to net Al-mobilization remains unpredictable for short time periods (Van Grinsven *et al.*, 1989). The Al transfer from the oxide pool to the adsorption complex or vice versa within specific years can be much higher than the net Al-mobilization. The large differences between the models are also caused by different initialization periods. NuCSAM uses an initialization period of 15 years (1973-1988) to establish an equilibrium between cation exchange and other processes, whereas the initialization period was 5 years for SoilVeg and 1 year for ForGro.

TABLE 27

Comparison of major terms of the simulated element budgets for NO_3^-, NH_4^+, Al^{3+} and Ca^{2+} for the soil component. Element budgets are averages for the period 1988-1991. Positive fluxes indicate an increase in the soil solution concentration.

	Fluxes ($kmol_c\ ha^{-1}\ a^{-1}$)											
	NO_3^-			NH_4^+			Al^{3+}			Ca^{2+}		
Process	SV[a]	FG[a]	NC[a]	SV	FG	NC	SV	FG	NC	SV	FG	NC
throughfall	0.84	0.56	0.76	2.09	2.09	2.21	0.01	0.04	0.00	0.38	0.36	0.38
uptake	-6.96	-2.78	-3.85	-0.40	-2.89	-3.51	0.00	0.00	0.00	-1.38	-1.74	-1.51
mineralization	0.00	0.00	0.00	5.79	3.25	6.18	0.00	0.00	0.00	1.11	1.06	1.05
nitrification	7.40	2.47	5.03	-7.40	-2.47	-5.03	0.00	0.00	0.00	0.00	0.00	0.00
weathering[b]	0.00	0.00	0.00	0.00	0.00	0.00	-5.43	8.50	4.02	0.15	0.06	0.05
exchange	0.00	0.00	0.00	-0.09	1.15	0.10	8.71	-3.68	0.30	0.09	0.39	0.26
leaching	-1.23	-0.03	-1.84	-0.00	-0.01	-0.00	-2.14	-3.20	-3.67	-0.29	-0.11	-0.23

a) SV = SoilVeg, FG = ForGro and NC = NuCSAM.

b) including dissolution/precipitation of secondary aluminum compounds.

4.4 Forest growth and foliar chemistry

4.4.1 Biomass

Figure 16
Simulated stem mass, foliage mass and fine root mass simulated with the three models.

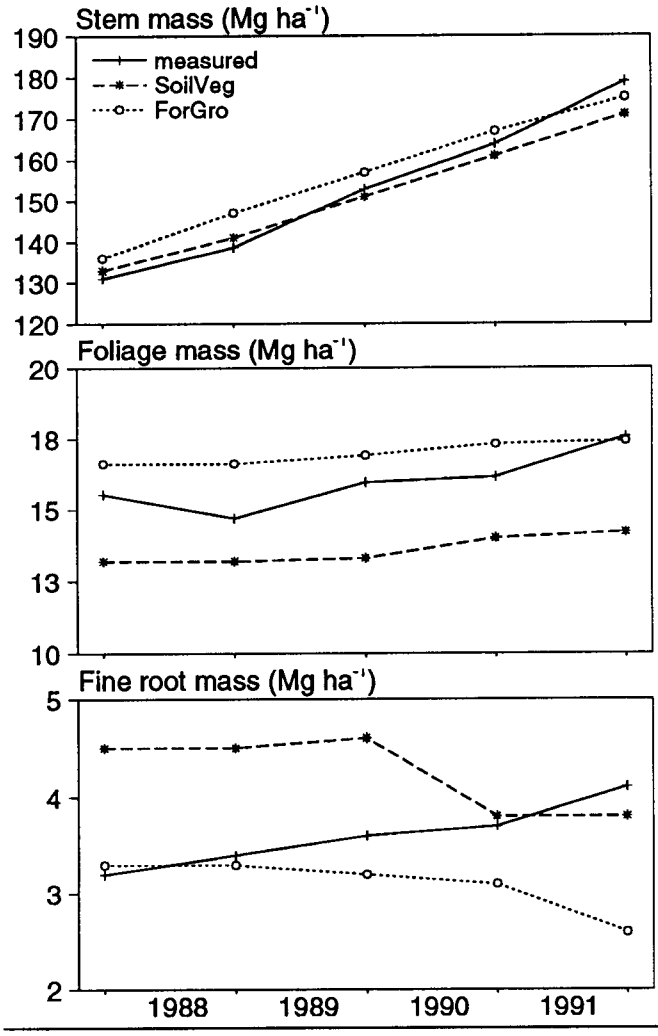

Figure 16 shows the simulated biomasses. The agreement between simulated and measured stem mass is good, but the total increase of stem mass between 1988 and 1992 (47 Mg ha^{-1}) is not reproduced by the models. Moreover, the strong year to year variations in measured stem mass increases are not simulated. It should be noted that the measured DBH is strongly dependent on the time of observation: After a dry period the measured DBH is smaller than directly after a wet period. This variability in the measurements imposes a large uncertainty, both in the DBH measurements, and in the biomass figures. Foliage mass is overestimated by ForGro and underestimated by SoilVeg. These differences are at least partly caused by different interpretations of the biomass measurements. The foliage mass for Speuld should be qualified as very high. Literature data on other highly productive sites report maximum foliage masses of 15-16 Mg ha^{-1} (see Table 5). With respect to results for foliage mass increments one can only conclude that the relation between values for individual years is practically absent, both when comparing models to observations or models amongst themselves. In other words: when combining the system knowledge as presented in the models, and actual observations of climatic parameters and soil water and nutrient status, we cannot analyse differences in stem growth and foliage mass between individual years. Differences between simulated fine root masses are mainly due to different definitions[1], but simulations are close to observations. Foliage mass to fine root mass ratio's are

[1] In SoilVeg, fine-roots are defined as roots smaller than 5 mm diameter, whereas fine-roots are smaller than 2 mm in the other models.

extremely high, which is thought to be typical for forest ecosystems with a high nitrogen input (Kurz and Kimmins, 1987; Walters and Reich, 1989).

4.4.2 Nutrient contents

Figure 17
Simulated nutrient contents in the foliage for Speuld (1987-1992).

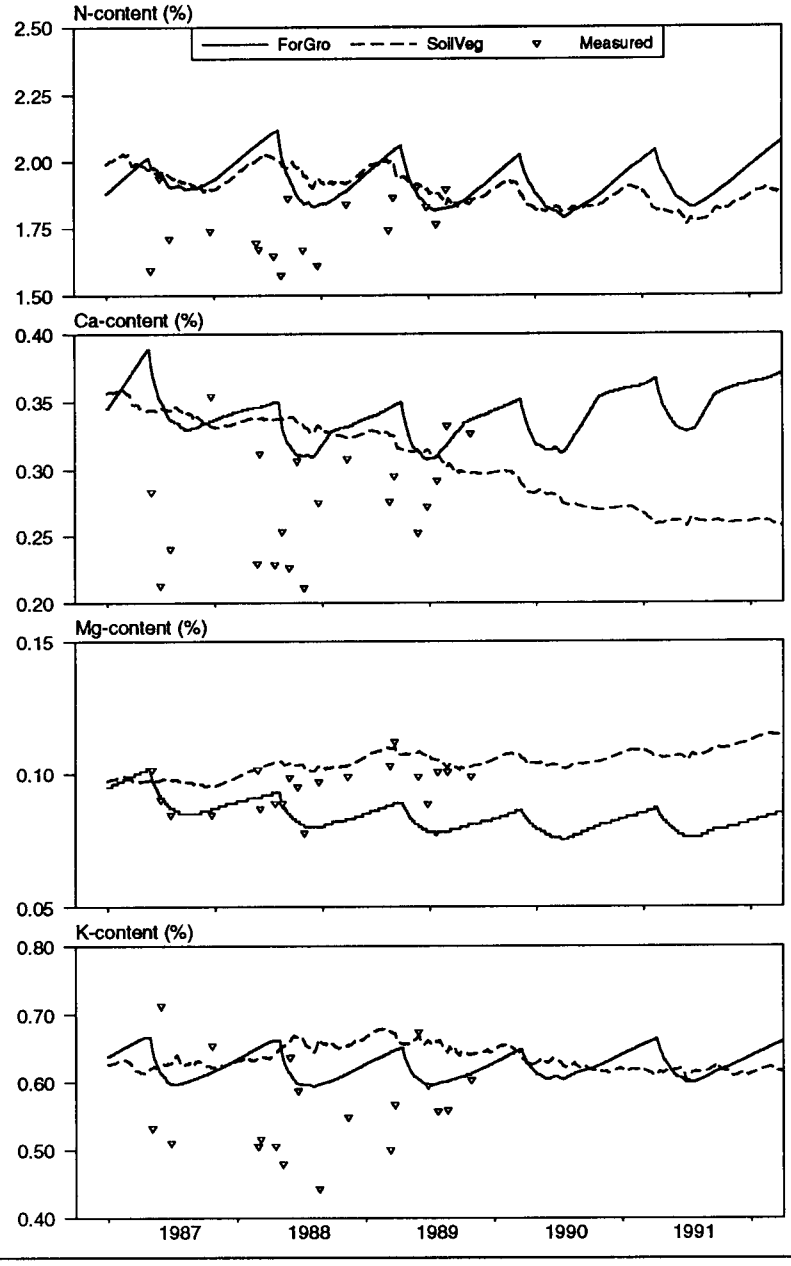

Nutrient contents are generally overestimated, with the exception of Mg. With respect to results for foliar nutrient contents, there is hardly any relation between observed and simulated contents for individual years. Moreover, trends are sometimes completely different. For example: the simulated nitrogen contents show a decreasing trend, whereas the opposite is true for the observed nitrogen contents. In other words: when combining the system knowledge as present in the models, and actual observations of climatic parameters and soil water and nutrient status, we cannot explain differences in foliar nutrient contents between individual years.

Both the observed, and the measured nitrogen contents are high. Again, this is typical for forest ecosystems with a high nitrogen input. The concentration of the other nutrients is in the lower part of measured ranges. For none of the nutrients, there is a deficiency.

4.4.3 Nutrient cycling

Table 28 shows the major terms of the nutrient budgets (1988-1991) for N, Ca, Mg and K for SoilVeg and ForGro in the tree. SoilVeg simulates higher root uptake fluxes, leaf-uptake fluxes and turnover losses for nitrogen, whereas base cation fluxes are slightly lower as compared to ForGro. The higher root uptake fluxes for nitrogen are most striking, and are due to different model concepts. In SoilVeg, nutrient uptake is mainly driven by the nutrient availability in the soil, whereas in ForGro uptake is mainly driven by the plant demand. Although nitrogen uptake simulated by ForGro is lower than the nitrogen uptake simulated by SoilVeg, ForGro simulates very low nitrate concentrations in the soil solution (see Figure 14). This is caused by the lower mineralization (Table 27) of nitrogen calculated by ForGro. Moreover, ForGro calculates a high nitrogen demand, which is larger than the nitrogen availability in the soil solution. Root uptake in ForGro is reduced when concentrations in the soil solution become low. This is mainly caused by a feed-back mechanism between the soil solution concentration and nutrient uptake (diffusion limited uptake; see also Gijsman, 1990). Apparently, the relationship between the diffusion constant and the soil solution concentration is parameterized in such a way that uptake can occur until very low and non-realistic soil solution concentrations.

TABLE 28

Comparison of major terms of the element budgets for N, Ca, Mg and K for the tree component. Data are averages for 1988-1991.

	Fluxes (kg ha^{-1} a^{-1})							
	N		Ca		Mg		K	
Proces	SV[a]	FG[a]	SV	FG	SV	FG	SV	FG
Root uptake	102.28	79.46	27.52	33.16	5.89	5.82	38.47	40.61
Leaf uptake	21.23	8.14	0.00	0.00	0.00	0.00	0.00	0.00
Leaf exudation	0.00	0.00	1.85	1.16	0.94	0.42	17.55	8.93
Turnover losses[b]	112.16	73.13	23.09	27.59	3.47	5.18	18.03	27.45
Storage	11.21	14.47	2.55	4.40	1.48	0.21	2.85	4.22

a) SV = SoilVeg and FG = ForGro

b) Sum of losses by needle fall, root death and branch fall.

4.5 Simulated manipulation experiments

The validity of the model calibrations was qualitatively assessed by evaluating whether the integrated models SoilVeg and ForGro could reproduce the observed effects of experimental manipulations as conducted for the nearby monitoring site 'Kootwijk' (De Visser, 1994). For this purpose, results from these manipulation experiments were compared to a simulation by the models calibrated for Speuld. It should be noted that the simulations are only approximate, as site conditions at Speuld and the manipulation plot are different and model implementations of elimination of water and nutrient stress are not identical to experimental procedures.

The approximation of the experimental manipulation by SoilVeg and ForGro were essentially different. In the SoilVeg application the irrigation and fertigation were dynamically mimicked by daily adding water and nutrients to the soil. In the ForGro application the soil simulation was left untouched while the reduction factors for

photosynthesis due to drought (equal to the ratio of actual to potential transpiration) and due to nutrient deficiency in the needles were switched off. So the response of the soil solution chemistry in the ForGro application is caused by the feedback of soil to the 'manipulated' photosynthesis reduction factors, and will not have a substantial effect on growth and nutrient status of the tree component. For this reason the soil chemistry results are omitted in Table 29.

TABLE 29

Comparison of observed effects of irrigation (I) and irrigation/fertigation (IF) on a Douglas fir stand at Kootwijk (De Visser, 1994) with simulated effects by SoilVeg and ForGro for the Douglas fir stand at Speuld, relative to an untreated control case.

Parameter	Change (%) relative to an untreated control case					
	Observed		SoilVeg		ForGro	
	I	IF	I	IF	I	IF
(Cl^-) at 20 cm	-52	-53	-17	-11		
(NO_3^-) at 20 cm	+46	+82	-6	+46		
(Mg^{2+}) at 20 cm	+37	-10	-16	+60		
(Al^{3+}) at 20 cm	+16	+28	-17	+34		
Stem mass increment	+19	+25	+6	+62	+19	+24
Litter fall	-7	+9	+1	+18	+9	+5
N-content in foliage	-10	+1	-2	+8	-8	-7
Mg-content in foliage	-2	+8	-4	+11	-2	0

In the field experiment, irrigation caused a large increase of nitrate concentrations, which was not simulated by the models. Apparently, the effect of moisture content on nitrogen mineralization process is still inadequately understood. This was also a major conclusion from the application of these models to Solling (Van Grinsven *et al.*, 1995). By combining the observed effects on Cl^- and NO_3^-, an additional nitrogen mineralization equal to the total net N-flux at 20 cm for the control case can be inferred. This enormous, probably temporary, N-push will also have a dominant effect on the observed growth response, which makes further comparison of observations and simulations awkward. It can be further concluded from the Cl^- data that in the SoilVeg reconstruction less water was applied than in the actual experiment. The main reason for this lies in the large drought sensitivity of the experimental manipulation plot (Kootwijk) as compared to the simulation plot (Speuld) (Tiktak and Bouten, 1990). However, it may also be expected that the experimental irrigation is less effective than the simulated irrigation. The smaller decrease of NO_3^- as compared to the Cl^- concentration for SoilVeg indicates a small enhancement of N-mobilization.

Looking at the observed increased stem increment and decreased N-content in foliage, it seems that the additional N-mineralization does not lead to an an increased uptake of N, which is rather remarkable. The needle mass at the experimental plot did increase, not only because of increased needle growth, but also because needle shedding was delayed (De Visser, 1994). The overall effect is a dilution of needle N. The close similarity between these observations and the ForGro simulation, which in fact did not impose an increased nitrogen uptake, are a further indication that (i) the additionally mineralized nitrogen is not

taken up, and (ii) the increased stem growth is predominantly caused by enhanced transpiration. In contrast, the SoilVeg simulation, after elimination of the drought stress, only predicts a small effect of irrigation, and only the addition of additional nutrients leads to a marked growth increase of stem and foliage. The strong response of growth to nutrient additions in SoilVeg is implied by applying the nutrient-productivity concept (§2.5). The fact that this increase is larger than observed may be due to ignoring phosphorus or due to the larger availability of Mg in SoilVeg than in the experimental plot (Table 29). Again it is remarkable that the simulated effect of fertigation on stem growth by ForGro is identical to the observed effect. Apparently the net growth effect in ForGro, implied by the reduction factor concept of photosynthesis due to nutrient shortage in foliage, is about right. However, judging from the poor prediction by ForGro of the effect on the N and Mg content in foliage, which predominantly decrease due to dilution in biomass, the nearly perfect reproduction of the growth effect should be regarded as somewhat accidental.

5 SCENARIO ANALYSES

All models were applied to evaluate a deposition scenario representing the present targets of the Dutch environmental policy (Keizer, 1994). This scenario is a rather optimistic one with respect to the reduction of deposition. Simulations were carried out for Douglas fir on a Cambic podzol and for Scots pine on a Haplic arenosol, and for Dutch regions with low, average and high deposition rates, respectively. Weather data were randomly selected by a statistical model of historically observed weather data (Richardson and Wright, 1984). The results of these scenario analyses were primarily meant as an example of model use for predictive purposes, as only one deposition scenario and one realization of weather data was evaluated.

5.1 Deposition scenarios

Table 30 presents the deposition scenarios for the six combinations evaluated.

TABLE 30
Total acid deposition ($mol_c\ ha^{-1}\ a^{-1}$) for generic Scots pine (SP) and Douglas fir (DF) stands in Drenthe (situated in the Northern Netherlands), Veluwe (Central Netherlands) and North Limburg (Southern Netherlands).

Year	Total acid deposition ($mol_c\ ha^{-1}\ a^{-1}$)					
	Drenthe		Veluwe		North Limburg	
	SP	DF	SP	DF	SP	DF
1980 [a]	5800	6700	8300	8700	8900	10400
1990 [a]	4300	4900	5400	6400	6800	7900
2000 [b]	2400	2800	2600	3000	4000	4600
2010 [b]	1400	1600	2000	2300	3000	3500
2050 [b]	1400	1600	1400	1600	2000	2300

a) inferred from DEADM calculations (see further text).
b) deposition target (Keizer, 1994).

For the period between 1980 and 1991, the deposition of acidifying components was estimated with the DEADM model (Erisman, 1993). The DEADM model was used to generate data for an average stand, based on meteorological measurements and measurements of concentrations in the atmosphere and precipitation. For the period before 1980, concentration measurements were not available and the deposition was inferred from historical deposition data which were based on emissions in those years (De Boer and Thomas, 1991). The historical deposition was scaled to the DEADM deposition, using the following equation:

$$Ac_{td} = Ac_{td,hist} \cdot \left(\frac{\overline{Ac_{td,DEADM}}}{\overline{Ac_{td,hist}}} \right) \qquad (66)$$

where Ac_{td} ($mol_c\ ha^{-1}\ a^{-1}$) is the total deposition of acidity, $Ac_{td,hist}$ ($mol_c\ ha^{-1}\ a^{-1}$) is the deposition based on emissions, $\overline{Ac_{td,DEADM}}$ ($mol_c\ ha^{-1}\ a^{-1}$) is the average deposition of

acidity calculated with DEADM for the period 1980-1991 and $\overline{Ac_{td,hist}}$ (mol_c ha^{-1} a^{-1}) is the average deposition of acidity based on emission data for 1980-1991. Future deposition data of acidity (1992-2050) were inferred from average DEADM results for 1989-1991 and the deposition targets (Table 30) by linear interpolation. Moreover, it was assumed that the relative contributions of SO_x, NO_x and NH_x were constant and equal to the contributions for 1991. The average deposition figures were converted to deposition figures for Douglas fir and Scots pine by applying filter factors (De Vries, 1991). Scots pine was assumed to behave as an average tree with respect to dry deposition, so the calculated deposition figures directly apply to Scots pine. Dry deposition for generic Douglas fir was inferred from the DEADM results using a dry deposition filter factor of 1.2. Finally, the deposition of base cations was calculated using a filter factor of 2.5 for Scots pine, and 3.0 for Douglas fir.

Figure 18
Deposition scenarios for Scots Pine and Douglas fir stands in the Veluwe.

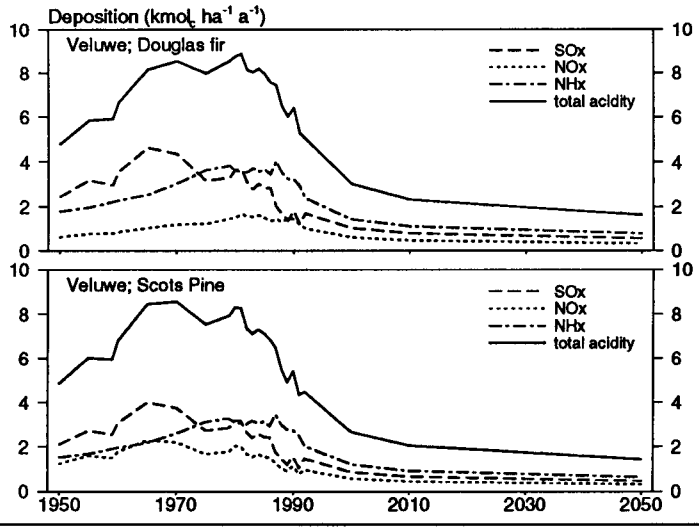

The results for region 'Veluwe' are shown in Figure 18. It is obvious that the DPPA-3 scenario is a rather optimistic one. Deposition targets for 2010 are lower than the deposition calculated on the basis of future emissions. These emission data were based on an evaluation of the current environmental policy (RIVM, 1993). On the other hand, the deposition for a generic Douglas fir stand is higher than the deposition for the Speuld site, due to the large distance of Speuld from forest edges.

5.2 The generic data-set

5.2.1 Hydrology

Soil physical characteristics

The retention and conductivity characteristics were taken from the new 'Staring soil series' (Wösten *et al.*, 1994). For SoilVeg, the data for the old soil series were used (Beuving, 1984) using a procedure described in Van Grinsven and Makaske (1993). These data are an integral part of the SoilVeg database, and have not been updated until now. The empirical relationships between soil water content and flux for ForGro were derived from NuCSAM output. A drawback from using the Staring Soil Series is that they particularly apply to agricultural soils, and not to forest soils. Therefore, the saturated conductivities are underestimated, and retention and conductivity characteristics derived from the Staring

series are steeper (larger values for n; see equations (59) and (60)), particularly for the sub soil. Results are shown in table 31.

TABLE 31
Parameters of the Mualem-Van Genuchten functions to describe the soil physical properties for a Cambic podzol and a Haplic arenosol.

Depth	Code [a]	θ_s ($m^3\ m^{-3}$)	θ_r ($m^3\ m^{-3}$)	α (cm^{-1})	n (-)	K_s [b] ($cm\ d^{-1}$)
Cambic podzol						
litter	(B3)	0.500	0.010	0.0152	1.41	17.8
0-50 cm	(B3)	0.450	0.010	0.0152	1.41	17.8
50-70 cm	(B2)	0.430	0.020	0.0227	1.55	9.7
> 70 cm	(O2)	0.380	0.020	0.0214	2.08	15.6
Haplic arenosol						
litter	(B1)	0.500	0.010	0.0249	1.51	17.4
0-80 cm	(B1)	0.430	0.010	0.0249	1.51	17.4
> 80 cm	(O1)	0.360	0.010	0.0224	2.17	13.2

a) Codes refer to the Staring series.
b) See table 10 for an explanation of symbols.

Crop dependent properties

Parameters for generic Scots pine and Douglas fir are given in table 32.

TABLE 32
Hydrological parameter values for generic Douglas fir on a Cambic podzol and Scots pine on a Haplic arenosol

Parameter	Symbol	Douglas fir	Scots pine	Unit
Canopy gap fraction[a]	G	0.1	0.3	(-)
Average precipitation intensity	R	10.0	10.0	(mm)
Interception efficiency[b]	f_i	0.141	0.141	(-)
Interception capacity[c]	$A_{wc,max}$	2.1	1.6	(mm)
Factor for evaporation				
during dry part of day:	fE_{dry}	1.5	1.5	(-)
during wet part of day:	fE_{wet}	0.5 (summer) - 9.0 (winter	0.5 (summer) - 9.0 (winter)	(-)
Reduction point [d]	h_r	-600	-600	(cm)
Wilting point [d]	h_w	-6000	-6000	(cm)
Crop factor [d]	f_c	0.85	0.70	(-)
Root length distribution [e]:	R_i	cf. table 9	cf. table 9	(-)

a) Based on Tiktak and Bouten (1990; 1994) for Douglas fir and De Visser and De Vries (1989).
b) Measured by Bouten (1992) for Douglas fir.
c) Measured by Mitscherlich and Moll (1970) for Scots pine and Bouten (1992) for Douglas fir.
d) Obtained by Tiktak and Bouten (1990; 1994) for the Speuld site. SoilVeg uses different figures, viz. 1 for Douglas and 0.82 for Scots pine, as this model uses a different definition of evapotranspiration components.
e) Based on root length distribution measurements for Douglas fir by Olsthoorn (1991).

In general, the hydrological parameters used for generic Douglas fir were identical to those used for Speulderbos. Parameters for Scots pine were assumed identical to Douglas fir

when no better alternatives were available. Important differences between Scots pine and Douglas fir are present for the gap factor (larger for Scots pine) and for the interception storage capacity (smaller for Scots pine). Parameters with no source indication were inferred from the NuCSAM calibration.

5.2.2 Soil chemistry

State variables that must be known at the beginning of the simulation include the amount of elements in all soil compartments, i.e. primary minerals, secondary Al-oxides, the adsorption complex and the soil solution.

Data used for the element amounts in primary minerals, secondary Al-oxides and the adsorption complex are given in table 33.

TABLE 33

Element contents in primary minerals, hydroxides and the adsorption complex for the generic Cambic podzol and the Haplic arenosol.

#[f]	Horizon	Depth (cm)	Density[a)] ($kg\ m^{-3}$)	Total contents[b] ($mmol_c\ kg^{-1}$)				$ctAl_{ox}$[c)] ($mmol_c\ kg^{-1}$)	*CEC*[a]	Exchangeable fraction[a] (-)			
				Ca^{2+}	Mg^{2+}	K^+	Na^+			H^+	Al^{3+}	BC[e)]	NH_4^+
Cambic podzol													
0	O	3.5-0[d)]	140						275	0.30	0.08	0.54	0.08
1	Ah	0-10	1345	35	40	230	155	95	42	0.33	0.50	0.12	0.05
2	Ah	10-20	1345	35	40	230	155	95	42	0.33	0.50	0.12	0.05
3	Bhs	20-30	1460	25	45	225	150	185	18	0.10	0.77	0.08	0.05
4	BC	30-50	1535	30	45	240	140	175	18	0.05	0.77	0.08	0.10
5	C	50-70	1535	30	45	240	140	175	18	0.05	0.77	0.08	0.10
6	C	70-110	1555	30	50	240	160	94	4	0.06	0.75	0.07	0.12
Haplic arenosol													
0	O	3.5-0[d)]	140						275	0.30	0.08	0.54	0.08
1	Ah	0-10	1375	75	60	480	430	55	27	0.20	0.63	0.09	0.10
2	C	10-20	1455	40	35	225	175	70	5	0.22	0.49	0.28	0.09
3	C	20-40	1455	40	35	225	175	70	5	0.22	0.49	0.28	0.09
4	C	40-60	1455	40	35	225	175	70	5	0.22	0.49	0.28	0.09
5	C	60-80	1455	40	35	225	175	70	5	0.22	0.49	0.28	0.09
6	C	80-100	1455	40	35	225	175	70	5	0.22	0.49	0.28	0.09

a) Derived from a field survey (Kleijn *et al.*, 1989). The *CEC* was measured in an unbuffered solution of silverthioreum. In a buffered solution, both the *CEC* and the exchangeable H content would have been higher.
b) Derived from laboratory analyses.
c) Derived from a soil information system (Bregt *et al.*, 1986).
d) Thickness calculated for the beginning of the simulation period in 1980.
e) BC is the sum of Ca^{2+}, Mg^{2+}, K^+ and Na^+.
f) Horizon numbers for NuCSAM and ForGro.

The initial content of sorbed sulphate was calculated from the equilibrium with the soil solution SO_4^{2-} concentration, using a sulphate sorption capacity (*SSC*) equal to 2% of the Al-oxalate content (Johnson and Todd, 1983). The initial (i.e. 1980) ion concentrations in each soil layer were derived by running the model during 25 years (1955-1990) using

historical emission-deposition data for the corresponding region. Anion concentrations in 1955 were estimated from the annual atmospheric input at that time and the annual average water flux per layer. Cation concentrations in 1955 were derived by combining the charge balance equation with the various cation exchange equations, using given initial exchangeable cation fractions (cf. table 33), and cation exchange constants (cf. table 35). During the initialization period (1955-1990), the cation contents in primary minerals and hydroxides were kept constant, while the contents of sorbed sulphate and cation contents were continuously updated.

An overview of various overall parameters for Douglas fir on a Cambic podzol and Scots pine on a Haplic arenosol are given in table 34. Most data were derived indirectly from available literature. For example, foliar uptake and foliar exudation fractions were derived from throughfall and bulk deposition data of more than 20 Douglas stands as summarized in Erisman (1990) while using a derivation procedure described in Van der Maas and Pape (1990). Maximum values for the nitrification and protonation rate constants were derived by calibration of model results on measured NH_4^+/NO_3^- ratios and $RCOO^-$ concentrations as given in Van Breemen and Verstraten (1991). An overview of soil-layer dependent parameters is given in table 35.

TABLE 34
Values used for overall model parameters for Douglas fir on a Cambic podzol and Scots pine on a Haplic arenosol.

Process	Parameter	Unit	Value	Derivation
Foliar uptake	$fr NH_{4,fu}$ [a]	-	0.30	Erisman (1990)
	$fr NO_{3,fu}$	-	0.05	Erisman (1990)
	$fr SO_{4,fu}$	-	0.10	Erisman (1990)
Foliar exudation	$fr Ca_{fe}$	-	0.24	Erisman (1990)
	$fr Mg_{fe}$	-	0.13	Erisman (1990)
	$fr K_{fe}$	-	0.63	Erisman (1990)
Litterfall	k_{lf}	a^{-1}	0.28	De Vries et al. (1990)
Root decay	k_{rd}	a^{-1}	1.40	De Vries et al. (1990)
Reallocation	$fr_{re,max}$	-	0.36	Berdowski et al. (1991)
Mineralization	$fr_{mi,lt,max}$	-	0.40	De Vries et al. (1990)
	$k_{mi,lt,max}$	a^{-1}	0.05	De Vries et al. (1990)
	RDA_{mo}	-	1.5	Janssen (1983)
	C/N_{mo}	-	15	Janssen (1983)
Root uptake	$f_p NH_{4,ru}$	-	1.5	Gijsman (1990)
Nitrification	$k_{ni,max}$	a^{-1}	40	ReSAM database.
Denitrification	$k_{de,max}$	a^{-1}	10	Reddy *et al.* (1982)
Protonation	$k_{pr,max}$	a^{-1}	40	ReSAM database.
Al dissolution	KAl_{ox}	$mol^{-2}\ L^2$	$4 \cdot 10^7$	Kleijn *et al.* (1989)
SO_4 adsorption	$KSO_{4,ad}$	$mol^{-1}\ L$	5.10^{-4}	Foster *et al.* (1986)

a) The foliar uptake fractions for H^+ and NH_4^+ were taken equal. This implies that a decrease in NH_4^+ deposition which is compensated by an increase in H^+ deposition does not affect the foliar exudation flux of base cations.

TABLE 35

Elovich constants for Al dissolution, base cation weathering rate constants and Gaines Thomas exchange constants of the Cambic podzol and the Haplic arenosol used in the simulation

Soil horizon	kEL_1 [a] (10^{-7} m^3 kg^{-1} a^{-1})	kEL_2 [a] (10^{-2} kg mol_c^{-1})	Weathering rate constants (10^{-5} a^{-1}) [a]				Exchange constants [b] $(mol\ L^{-1})^z x^{-2}$					
			Ca	Mg	K	Na	H	Al	Mg	K	Na	NH_4
Cambic podzol												
Ah	5.7	9.3	25	11	2.3	2.9	1870	0.62	0.35	0.21	0.77	1.05
Bhs	6.4	6.3	9.1	1.8	5.3	8.5	7830	1.77	0.30	1.31	3.35	6.53
BC	42	4.4	2.9	0.16	3.1	5.9	11470	1.91	0.33	6.14	5.00	30.7
C	87	9.1	17.0	1.5	1.5	2.0	2454	4.41	0.85	8.05	4.04	40.2
Haplic arenosol												
Ah	3.7	9.4	8.3	115	1.0	2.4	6439	1.06	0.30	0.31	0.33	1.53
C	360.0	7.9	16.7	1.6	1.5	2.0	2445	4.41	0.85	8.05	4.04	40.2

a) Derived from batch experiments that were conducted during one year for two Cambic podzols and Haplic arenosols (De Vries, 1994). Base cation weathering rate constants thus derived were divided by 50 to scale results to field weathering rates, that were estimated by the depletion of base cations in these two soil profiles (De Vries and Breeuwsma, 1986). In this model application we assume a negligible pH influence on the weathering rate.

b) Derived from simultaneous measurements of chemical components at the adsorption complex and in the soil solution of two Cambic Podzols at five locations and at four soil depths (Kleijn *et al.*, 1989).

5.2.3 Forest growth and nutrient cycling

Table 36 presents the initial basic stand data for Douglas fir on a Cambic podzol and Scots pine on a Haplic arenosol. Basic stand data were taken from Cannel (1982) and Mälkönen (1970). The initial litter amount was calculated by integrating the various mineralization equations, using a stand age of 30 years. Initial element contents in litter were taken equal to needle contents.

TABLE 36

Initial stand structure conditions for generic Douglas fir and Scots pine.

Parameter	Unit	Douglas fir on Cambic podzol	Scots pine on Haplic arenosol
Stand age	(a)	30	30
Stand density	(ha^{-1})	850	2000
Height	(m)	18.5	9.0
Mean DBH	(m)	0.22	0.11
Basal Area	(m^2 ha^{-1})	32.3	19.0
Stem volume	(m^3 ha^{-1})	286	102
LAI	(m^2 m^{-2})	8.25	2.40
Specific leaf area	(m^2 kg^{-1})	5.5	4.0
Basic wood density	(kg m^{-3})	420	490
Soil organic matter	(Mg ha^{-1})		
L		15	10
F		45	20
H		350	100
Dead roots		15	10

Data related to various tree compartments are given in table 37. Biomass data of needles and fine roots, and element contents in fine roots and stems were based on literature surveys (Janssen and Sevenster, 1995; Scherfose, 1990; De Vries *et al.*, 1990), whereas the element contents in needles were based on a field survey in 1987 in eight Douglas stands (Oterdoom *et al.*, 1987), and 150 stands (Hendriks *et al.*, 1994). For NuCSAM, the biomass of stems was derived from a logistic growth function for Douglas fir (La Bastide and Faber, 1972) using a tree age of 30 years. At this age, the amount of needles and fine roots is assumed at it's maximum.

TABLE 37
Data on biomass and element contents of leaves, fine roots and stems for the generic Douglas fir and Scots pine (see text for data sources).

Compartment	Biomass (kg ha^{-1})	Element content (%)					
		N	Ca	Mg	K	S	P
Douglas fir							
Needles	15000	1.75	0.35	0.12	0.65	0.20	0.15
Fine roots	3500	1.00	0.30	0.05	0.20	0.10	0.06
Coarse roots	15000	0.30	0.05	0.01	0.10	0.05	0.02
Stems	120000	0.20	0.05	0.03	0.06	0.03	0.01
Branches	15000	0.30	0.05	0.03	0.10	0.05	0.02
Scots pine							
Needles	6000	1.85	0.20	0.13	0.50	0.20	0.15
Fine roots	2500	1.00	0.15	0.05	0.15	0.10	0.08
Coarse roots	15000	0.25	0.04	0.03	0.08	0.05	0.02
Stems	50000	0.15	0.04	0.01	0.05	0.03	0.02
Branches	10000	0.40	0.04	0.03	0.08	0.05	0.02

The thinning scheme for generic Douglas fir and generic Scots pine is shown in table 38. These thinning schemes were derived from Janssen and Sevenster (1995). For Douglas fir on a Cambic podzol, site class II was assumed, whereas site class IV was assumed for Scots pine.

TABLE 38
Thinning scheme for generic Douglas fir and generic Scots pine.

Age (a)	Fraction removed (-)			
	Douglas fir		Scots pine	
	FrVol [a]	*FrTree* [a]	*FrVol*	*FrTree*
35	0.12	0.21	0.15	0.23
40	0.11	0.18	0.13	0.20
45	0.10	0.16	0.12	0.18
50	0.08	0.14	0.10	0.16
55	0.07	0.12	0.09	0.13
60	0.06	0.10	0.08	0.12
65	0.05	0.09	0.07	0.10
70	0.05	0.07	0.05	0.09
75	0.04	0.06	0.05	0.07
80	0.04	0.05	0.04	0.06
85	0.03	0.04	0.04	0.06
90	0.03	0.04	0.04	0.06
95	0.03	0.03	0.04	0.06

a) FrVol (-) is fraction of volume removed; FrTree (-) is fraction of trees removed.

5.3 Results for region 'Veluwe'

5.3.1 Hydrology

Table 39 shows the long-term average simulated water balance for Douglas fir on a Cambic podzol and Scots pine on a Haplic arenosol in the 'Veluwe' region. It can be seen that ForGro used lower average precipitation amounts than SoilVeg and NuCSAM (743 mm a^{-1} for ForGro and 804 mm a^{-1} for SoilVeg and NuCSAM). ForGro used an older version of the meteorological data file, with lower precipitation amounts than the long-term average precipitation measured in De Bilt (see Figure 5). This clearly demonstrates the need for central data management when performing a complicated model comparison study as described here. Nevertheless, some general conclusions can be drawn from the table:

- All models simulate a lower average interception evaporation for Scots pine than for Douglas fir, but for NuCSAM the difference is small. NuCSAM simulates the highest interception evaporation, and ForGro simulates lowest interception values.
- Potential transpiration for Douglas fir is higher than for Scots pine, mainly because of the higher crop factor and the lower canopy gap factor for Douglas fir. ForGro simulates the lowest potential transpiration for Scots pine and the highest potential transpiration for Douglas fir. The very low potential transpiration figures for Scots pine as simulated by ForGro are caused by the substantial decrease of the Leaf Area Index and foliage mass as simulated by this model (see Figure 21). This demonstrates that feed-backs between the hydrological submodel and the forest-growth submodel may not be ignored in the long run.
- Actual transpiration for Scots pine is much lower than for Douglas fir due to a lower potential transpiration. For Douglas fir, ForGro simulates the lowest transpiration and the highest transpiration reduction, and the highest drainage fluxes. These high drainage fluxes by ForGro can be explained in part by the lack of a process formulation for capillary rise in ForGro. For Scots pine, ForGro also simulates the lowest actual transpiration, but here the low potential transpiration is the major cause.
- Soil evaporation is lower under Douglas fir than under Scots pine. This is mainly caused by the lower Leaf Area Index and higher canopy gap fraction for Scots pine. The very high soil evaporation under Scots pine as simulated by ForGro is remarkable, and can be attributed to the same effect as described for the potential transpiration.
- Variation in time of potential transpiration, interception evaporation, actual transpiration and soil evaporation is much smaller than variation in time of precipitation.
- The models are not conclusive about the degree of transpiration reduction. This is mainly caused by the uncertainty of the potential transpiration.
- There is hardly any reduction of soil evaporation calculated by NuCSAM. This is the consequence of using the approach by Black *et al.* (1969), which is only sensitive to the length of the period with a daily precipitation less than 0.3 mm. The generated meteorological dataset contains correct drought intervals but apparently underestimates the length of periods without precipitation.
- The average precipitation surplus for Douglas fir is very small.

TABLE 39
Average simulated water balance for Douglas fir on a Cambic podzol and Scots pine on a Haplic arenosol in region 'Veluwe' for the period 1980-2050.

Model	Fluxes and standard deviation (mm a^{-1}) [a]							α (-) [b]
	P	I	E_{pl}	E_s	E_{pl}^*	E_s^*	PS	
Douglas fir on a Cambic podzol								
NuCSAM	804±98	304±35	371±20	59±3	389±17	60±2	74±40	0.96±0.06
SoilVeg	804±98	241±25	363±19	82±15	373±25	94±18	117±75	0.97±0.06
ForGro	743±100	243±47	325±37	38±18	451±32		136±47	0.73±0.10
Scots pine on a Haplic arenosol								
NuCSAM	804±98	288±34	268±11	95±4	272±12	97±5	188±38	0.99±0.03
SoilVeg	804±98	194±19	291±23	116±9	347±24	144±11	202±72	0.84±0.05
ForGro	743±100	100±24	188±30	249±38	237±28		207±74	0.80±0.14

a) P (mm a^{-1}) is precipitation, I (mm a^{-1}) is interception loss, E_{pl} (mm a^{-1}) is transpiration, E_s is soil evaporation, E_{pl}^* (mm a^{-1}) is potential transpiration, E_s^* (mm a^{-1}) is potential soil evaporation, and PS (mm a^{-1}) is precipitation surplus.

b) α (-) is ratio of actual transpiration over potential transpiration (E_{pl} / E_{pl}^*)

Compared to transpiration values given by Roberts (1983) for an average forest in Europe (330 mm a^{-1}), values for Douglas fir are higher and for Scots pine lower. The actual transpiration for Douglas fir is almost similar to that for Speuld. The actual transpiration simulated by NuCSAM for Scots pine (268 mm a^{-1}) compares well with that from previous SWATRE simulations by De Visser and De Vries (1989) (281 mm a^{-1}), but are substantially higher than for Douglas fir (371 mm a^{-1} by NuCSAM and 328 mm a^{-1} by De Visser and De Vries). This should be kept in mind when comparing the new results with regional ReSAM simulations, as the figures by De Visser and De Vries are part of the ReSAM database. For the comparison between ReSAM and NuCSAM, as carried out within this study, the new (higher) figures were used.

5.3.2 Soil chemistry

Figure 19 and Figure 20 show the simulated yearly average soil solution concentrations for the 'Veluwe' region, table 41 gives the major terms of the element budgets for some major components. The figures and table show considerable differences between the models, but some general conclusions can be drawn.

Sulphate, aluminum and pH

Concentrations of sulphate are higher in the soil under Douglas fir than under Scots pine due to higher filtering of air pollutants by Douglas fir, and a lower precipitation surplus. All models simulate a fast response of the sulphate concentration after a reduction in SO_x deposition. For 90 cm, the models simulate comparable sulphate concentrations, which was expected as differences between simulated drainage fluxes are small (see table 39). Remarkable is the high simulated sulphate concentration under Douglas by ForGro for 20 cm, which is caused by differences in the root water uptake distribution with depth compared to the other models. In ForGro, a shallower root water uptake pattern was assumed. Aluminum shows almost the same temporal dynamics as sulphate, although a slight time delay occurs resulting from exchange of sorbed Al^{3+} against Ca^{2+} in the soil

solution. The pH of the soil solution rises for both Douglas fir and Scots pine. Notice, however, that for Scots pine SoilVeg and ForGro simulate a slower increase for the 20 cm soil layer than NuCSAM. SoilVeg simulates lower pH values at 20 cm depth than the other models, with largest deviations occurring for Douglas fir. This is totally in line with the Speuld simulations. For Douglas fir, NuCSAM calculates larger Al-weathering fluxes than SoilVeg (table 41). This may be one of the reasons for the higher pH simulated by NuCSAM. It is remarkable that differences are found for Al-weathering, as both models use the same process formulations. An explanation may be that higher water fluxes in the topsoil simulated by NuCSAM cause lower Al-concentrations (see Figure 19), which in turn stimulates Al-weathering.

Nitrate

All models simulate higher concentrations of NO_3^- under Douglas fir than under Scots pine. As with sulphate, this is caused by higher filtering of NO_x and NH_x by Douglas. All models also simulate a time delay for the decrease of the NO_3^- concentration in the soil solution after a decrease in NH_x and NO_y deposition, caused by the release of nitrogen previously stored in living biomass and litter. The largest delay is simulated by SoilVeg for the topsoil under Douglas fir (Figure 19). The major cause is the high initial litter mass for generic Douglas in SoilVeg (60 Mg ha^{-1}, which is high compared to the 40 Mg ha^{-1} measured for Speuld) in combination with a relatively high mineralization rate (Figure 21 and table 40), resulting in a net decrease of litter mass and an extra supply of nitrogen.

TABLE 40

Annual simulated fluxes of NO_3^- and NH_4^+ for generic Douglas fir on a Cambic Podzol for region 'Veluwe', and for 1990 and 2010. As these results apply to two individual years, conclusions with respect to *time-trends* must be drawn carefully (e.g. with respect to mineralization).

Parameter	Fluxes (mol_c ha^{-1} a^{-1})					
	NuCSAM		SoilVeg		ForGro	
	NH_4^+	NO_3^-	NH_4^+	NO_3^-	NH_4^+	NO_3^-
1990						
throughfall	3.20	1.42	3.06	1.42	3.20	1.42
mineralization	6.57	0.00	7.35	0.00	4.26	0.00
root uptake	3.92	2.61	1.13	10.63	4.48	4.01
leaching[a]	0.15	2.92	0.00	-0.24	0.01	0.14
2010						
throughfall	1.09	0.54	1.03	0.44	1.09	0.45
mineralization	3.05	0.00	9.17	0.00	4.35	0.00
root uptake	1.68	1.12	0.70	5.86	2.26	2.93
leaching[a]	0.49	2.53	0.01	4.87	0.01	0.27

a) Refers to 1 m depth

Table 40 and table 41 also shows that root uptake fluxes for nitrogen in 1990 and the period 1990-2000 are higher for SoilVeg than for the other models. Moreover, root uptake occurs in equal proportions for NH_4^+ and NO_3^- in ForGro and NuCSAM, and mainly as NO_3^- in SoilVeg. These differences were already found for the Speuld application and are discussed in §4.4.3. As with the calibration, the low mineralization in ForGro and the lack

of feedback between uptake and soil solution concentration in this model results in very low nitrate concentrations at 90 cm, and thus almost negligible nitrate leaching fluxes. Figure 20 shows a strong annual variation of these fluxes for the other models. For Douglas fir, SoilVeg even predicts a net negative leaching flux in very dry years. In such years, substantial capillary fluxes into the rootzone are simulated by SoilVeg. Remarkable is the low root uptake rate for NuCSAM in 2010 and during the period 2040-2050. This is caused by a fast decrease of the nitrogen content in needles simulated by this model, which in turn is a result of the assumed, non-realistic, empirical relationship between the nitrogen content in needles and the nitrogen deposition (eqn. (21)). This low needle N-content is also the reason for the low nitrogen mineralization in NuCSAM for the period 2040-2050 (see table 41). Differences between the models again demonstrate that there are many uncertainties with respect to the nitrogen cycle (viz. uptake and mineralization).

Al/Ca ratio

Differences between the models are larger than the differences between Douglas and Scots pine. The very high Al/Ca ratios simulated by ForGro and SoilVeg for Scots pine are striking. The extreme Al/Ca ratios simulated by ForGro are a result of the parameterization of the uptake model. As with nitrogen, ForGro allows for Ca^{2+} uptake until very low soil solution concentrations, resulting in low Ca^{2+} concentrations in the soil solution. Thus, the extreme Al/Ca ratios simulated by ForGro remain questionable and unrealistic. All models simulate a time delay for the Al/Ca ratio, which continues to rise for a short time after deposition reduction. This phenomenon was also observed in an application on a Norway Spruce stand at Solling, Germany (Groenenberg *et al.*, 1995). It can be explained by exchange of Ca^{2+} from the soil solution against sorbed Al^{3+}. This is less pronounced in this study than in Solling, due to the smaller CEC of the soils used in this study. Both the Al/Ca ratio and the time-delay for decrease of this ratio is larger for Douglas compared to Scots pine, which is caused by the higher acid load for a soil under Douglas.

Critical values

Regarding the criteria for indirect effects on forest stress (Al/Ca ratio < 1 and no depletion of the pool of secondary aluminum compounds), the results show that SoilVeg and NuCSAM simulate an Al/Ca ratio < 1 at 20 cm depth for both forest-soil combinations in 2050 in the 'Veluwe' region, whereas ForGro simulates an Al/Ca ratio > 1 for Scots pine (see discussion above). Notice that despite the extreme Al/Ca ratios simulated, stem growth is not hampered (see §5.3.3). All models simulate an initial decrease of the pool of secondary aluminum compounds. However, a faster decrease of this pool is simulated for the soil under Douglas fir, whereas for Scots pine NuCSAM even simulates a slight increase of this pool.

Conclusions

The models are conclusive with respect to general trends and differences between both forest-soil combinations (i.e. fast response of the sulphate and aluminum concentrations after a decrease in SO_x deposition, time-delay for the NO_3^- concentration following a decrease in deposition, and higher soil solution concentrations for Douglas). Nevertheless, some major differences are found. This is surprising, as the models use almost the same process formulations for soil chemistry. This demonstrates that the soil chemical status is

strongly affected by nutrient uptake, nutrient mineralization, hydrology and model initialization, and it is in these parts of the models where the major uncertainties are to be found.

TABLE 41
Comparison of major terms of the simulated element budgets for NO_3^-, NH_4^+, Al^{3+} and Ca^{2+} for the soil component for the models SoilVeg and NuCSAM, and for region 'Veluwe'. Element budgets are averages for the periods 1990-2000 and 2040-2050. Positive fluxes indicate an increase in the soil solution concentration.

Parameter	Fluxes ($mol_c\ ha^{-1}\ a^{-1}$)							
	NO_3^-		NH_4^+		Al^{3+}		Ca^{2+}	
	SV[b]	NC[b]	SV[b]	NC[b]	SV[b]	NC[b]	SV[b]	NC[b]
Douglas fir (1990-2000)								
throughfall	0.82	0.99	1.90	2.34	0.00	0.00	1.05	0.84
root uptake	-7.64	-1.85	-0.96	-2.77	0.00	0.00	-1.76	-1.59
mineralization	0.00	0.00	7.86	5.60	0.00	0.00	1.25	1.17
nitrification	8.75	4.43	-8.75	-4.43	0.00	0.00	0.00	0.00
weathering	0.00	0.00	0.00	0.00	1.62	3.47	0.07	0.07
exchange	0.00	0.00	-0.05	-0.01	0.25	0.62	-0.06	-0.10
leaching[a]	-2.16	-3.59	0.00	-0.33	-2.64	-4.16	-0.69	-0.42
Douglas fir (2040-2050)								
throughfall	0.33	0.33	0.77	0.61	0.00	0.00	1.03	0.76
root uptake	-4.82	-1.14	-0.57	-1.71	0.00	0.00	-1.80	-1.51
mineralization	0.00	0.00	5.51	2.60	0.00	0.00	1.30	1.19
nitrification	5.73	1.38	-5.73	-1.38	0.00	0.00	0.00	0.00
weathering	0.00	0.00	0.00	0.00	0.85	0.38	0.07	0.07
exchange	0.00	0.00	0.03	0.00	0.03	0.19	-0.17	-0.37
leaching[a]	-1.32	-0.68	0.00	-0.17	-0.90	-0.79	-0.43	-0.17
Scots pine (1990-2000)								
throughfall	0.77	0.86	1.66	1.75	0.00	0.00	0.87	0.66
root uptake	-2.89	-1.97	-2.73	-2.96	0.00	0.00	1.66	-1.32
mineralization	0.00	0.00	2.73	5.08	0.00	0.00	1.08	1.03
nitrification	2.61	2.99	-2.61	-2.99	0.00	0.00	0.00	0.00
weathering	0.00	0.00	0.00	0.00	0.92	0.89	0.10	0.10
exchange	0.00	0.00	-0.04	0.00	-0.02	0.80	-0.23	-0.21
leaching[a]	-0.52	-1.93	-0.01	-0.90	-1.04	-1.79	-0.16	-0.26
Scots pine (2040-2050)								
throughfall	0.33	0.33	0.67	0.59	0.00	0.00	0.86	0.62
root uptake	-2.89	-1.24	-2.13	-1.92	0.00	0.00	1.65	-1.32
mineralization	0.00	0.00	4.67	2.40	0.00	0.00	1.24	1.03
nitrification	3.21	1.02	-3.21	-1.02	0.00	0.00	0.00	0.00
weathering	0.00	0.00	0.00	0.00	0.21	-0.68	0.10	0.10
exchange	0.00	0.00	0.02	0.00	0.06	0.82	-0.17	-0.25
leaching[a]	-0.64	-0.15	-0.01	-0.10	-0.25	-0.23	-0.34	-0.30

a) Refers to 1 m depth
b) NC = NuCSAM; SV = SoilVeg

Figure 19
Simulated soil water chemistry at 20 cm depth for Douglas fir on a Cambic podzol (left) and for Scots pine on a Haplic arenosol (right) in the 'Veluwe' region.

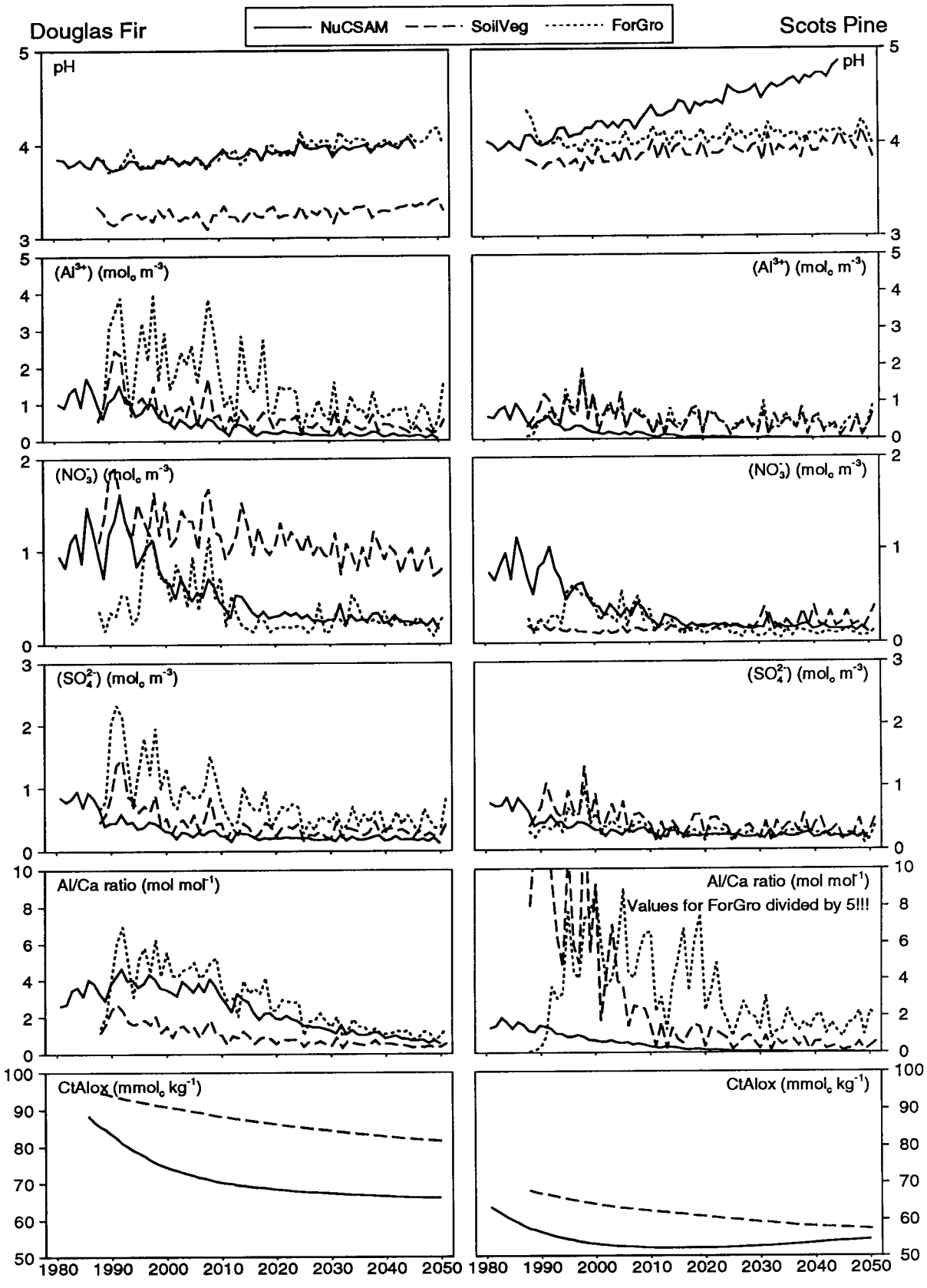

Figure 20
Simulated soil water chemistry at 90 cm depth for Douglas fir on a Cambic podzol (left) and for Scots pine on a Haplic arenosol (right) in the 'Veluwe' region.

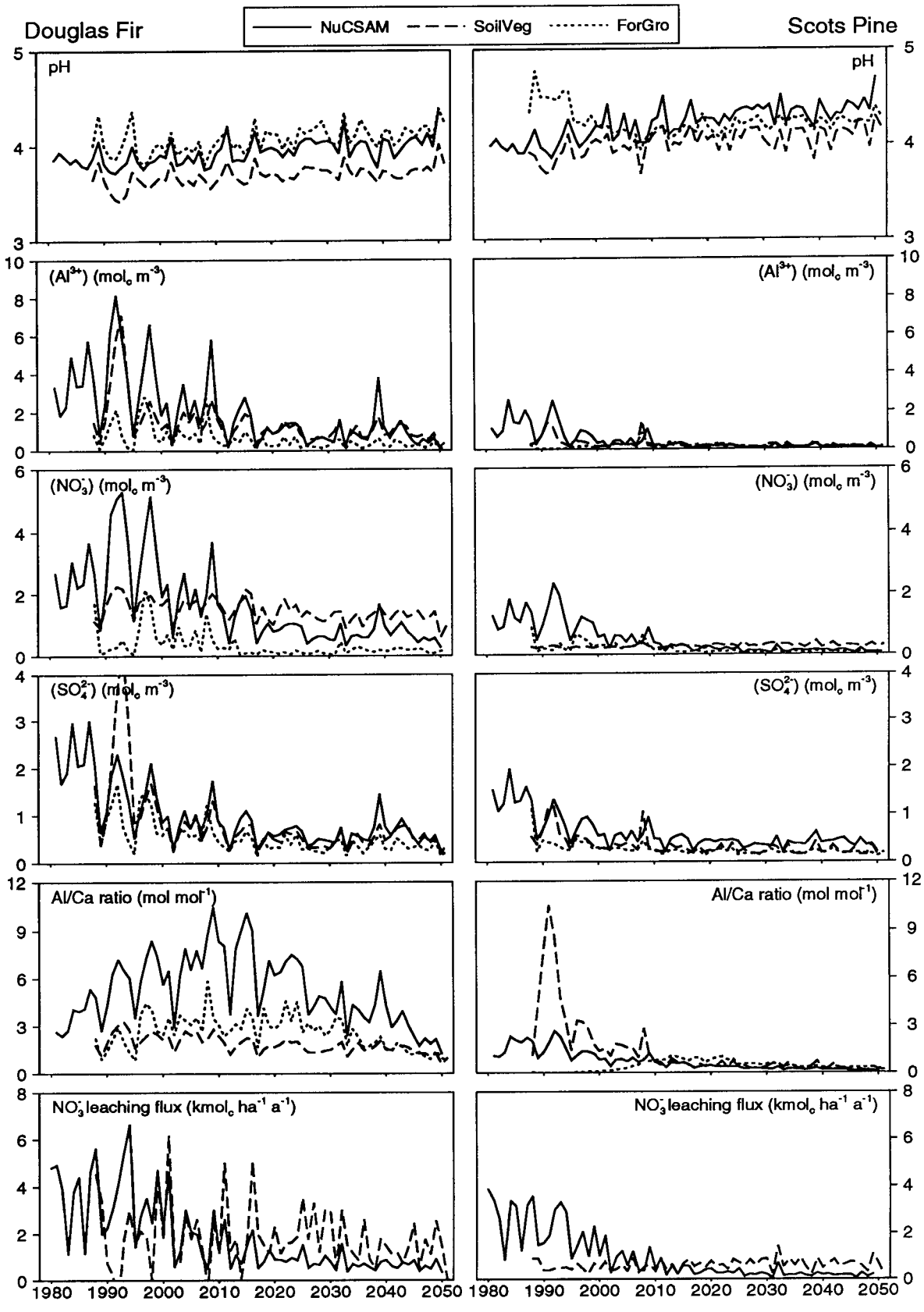

5.3.3 Forest growth and foliar chemistry

Figure 21 shows the simulated stem mass, foliage mass, fine-root mass and litter mass for the 'Veluwe' region by SoilVeg and ForGro. Results show general agreement for simulated stem mass of Scots pine, and considerable differences for Douglas fir after 2010. Both the simulated stem mass and the stem mass increment (growth) are lower for SoilVeg than for ForGro. The lower stem mass increment for Douglas fir as simulated by SoilVeg is caused by reduction of the uptake of magnesium and potassium, which in turn results from a lower pH (long-term average pH is 3.3 for SoilVeg and 3.9 for ForGro; see Figure 19). The decrease of stem mass increment after 2010, which was simulated by SoilVeg for Douglas fir, is caused by the high thinning fraction for Douglas fir (table 38), which applies to the favourable site class II. However, after reduction of the nitrogen deposition, forest growth continues at a rate which is more representative for the less favourable site class IV, and the thinning scheme should have been adjusted accordingly.

Figure 21
Simulated stem mass, foliage mass and fine-root mass of Douglas fir on a Cambic podzol (left) and for Scots pine on a Haplic arenosol (right), and for region 'Veluwe'.

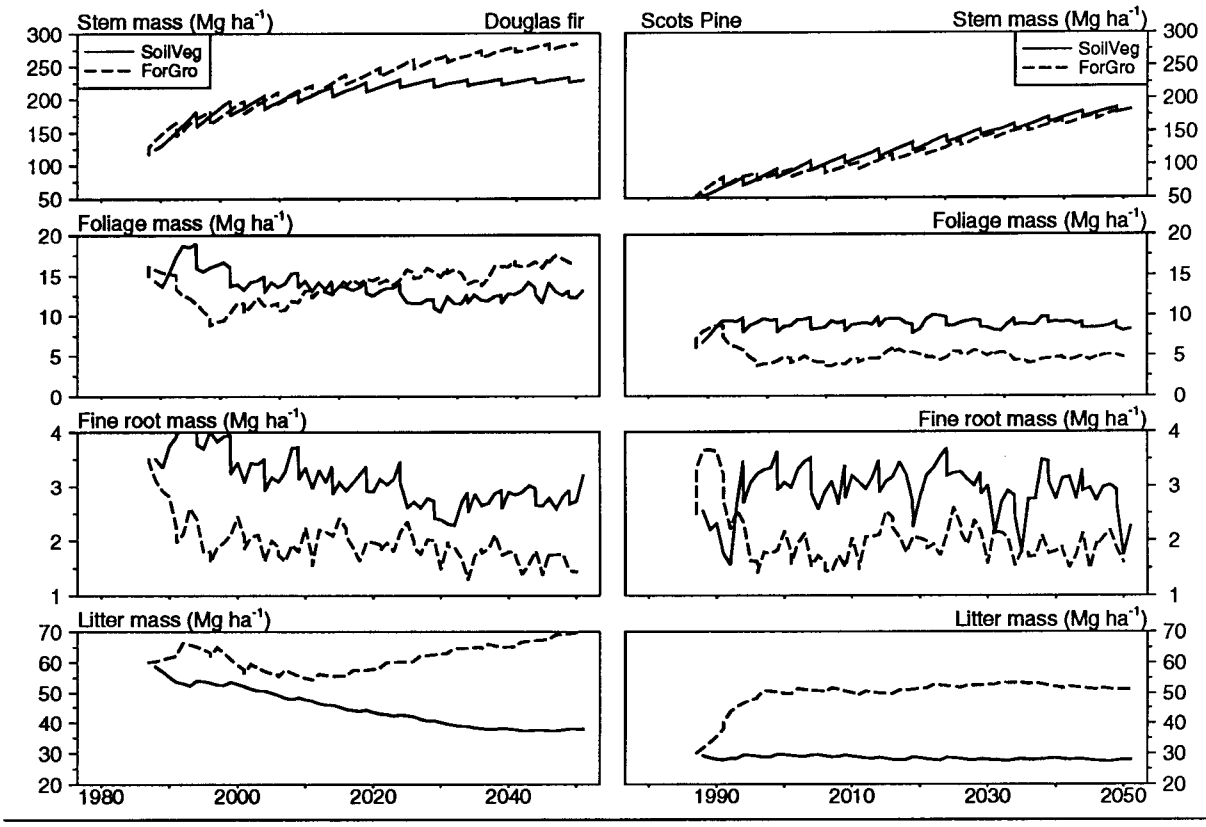

The simulated foliage mass is almost twice as high for Douglas fir than for Scots pine. For Douglas fir, time-trends of foliage biomass are almost opposite for both models. SoilVeg simulates a high initial biomass, showing that adverse effects of high nitrogen deposition, viz. soil acidification and increased plant respiration, are dominant. In ForGro, the normal effects of ageing on assimilate allocation are dominant. The initial decrease of foliage mass of Douglas fir by ForGro is due to the combined effect of the initial conditions of the run, which appear to be not entirely stable, and a growth reduction due to low precipitation

during the growing season in 1992. Figure 21 also shows that SoilVeg simulates a strong decrease of the litter mass below Douglas fir. This subject was already discussed in §5.3.2. The extra supply of nitrogen released from the litter gives an explanation for the slow response of SoilVeg to a reduction of the nitrogen deposition. Differences in fine-root biomass are a result of different definitions of fine-roots (see also §4.4.1).

ForGro simulates low fine-root densities for Douglas fir (not shown in figure). Even with the rather low fine root densities as simulated with the model, soil supply of potassium and calcium was sufficient to prevent severe deficiencies (Figure 22). The ForGro simulations further indicate an initial fast response of the nitrogen content in the foliage, followed by a slower response. The first phase is caused by the decreasing direct nitrogen uptake by the canopy, the second phase is caused by release of nitrogen from the soil. The result is a continuation of the condition with high nitrogen contents, and low contents of phosphorus (not shown) and magnesium (Figure 22). SoilVeg simulates lower nitrogen contents and a stronger increase of the content of cations. The increase of the content of base cations as simulated by SoilVeg is caused by (i) an increase in soil solution pH and decreasing soil solution aluminum concentrations, which in turn stimulates nutrient uptake, and (ii) by reduced dilution of nutrients in the needles, caused by decrease leaf growth.

Figure 22
Simulated nutrient concentrations in needles of Douglas fir on a Cambic Podzol (left) and for Scots pine on a Haplic arenosol (right), and for region 'Veluwe'.

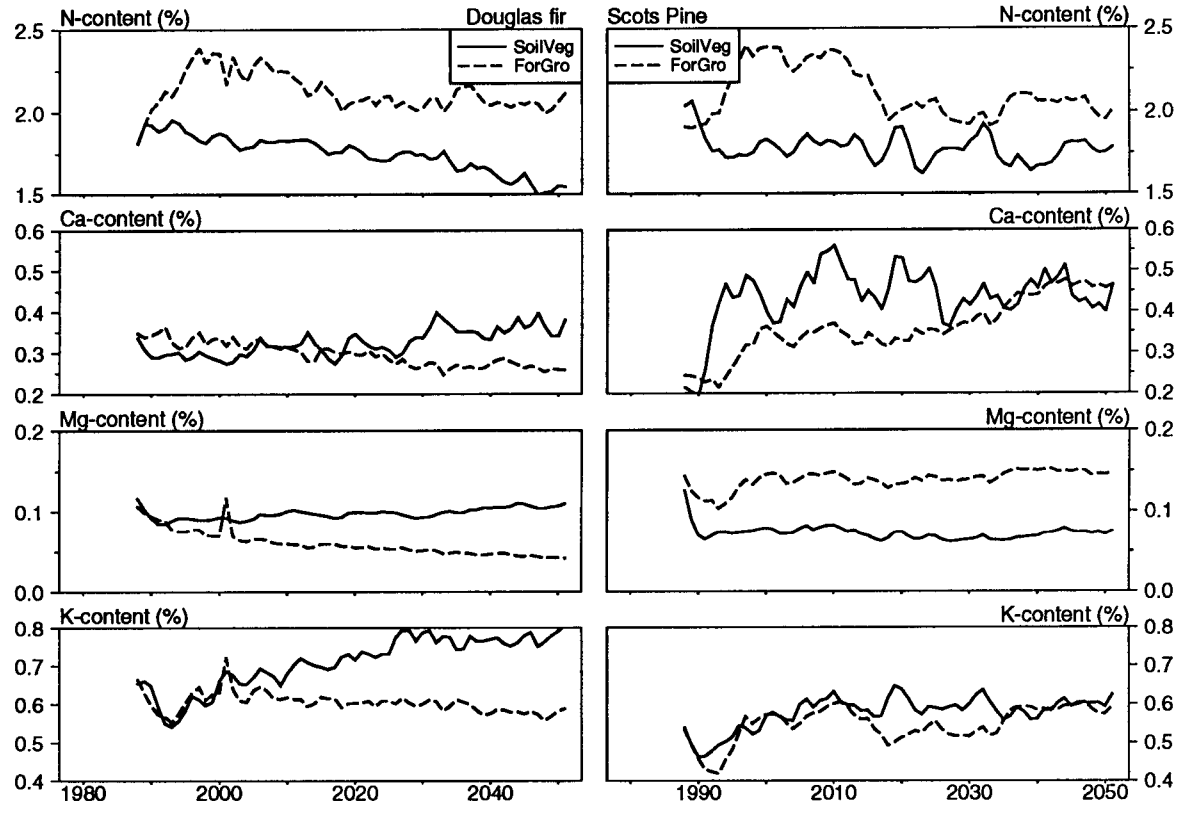

5.4 Comparison of results for the three deposition scenarios

Figure 23 shows the simulated pH at 20 cm depth for all six forest-soil-deposition combinations considered, whereas table 42 shows some important averaged model outputs for the periods 1990-2000 and 2040-2050. All soil parameters in table 42 are shown for 20 cm depth.

Figure 23 shows that the models are not conclusive about the trends in pH-values. However, all models show that for both forest-soil combinations the difference in pH of the topsoil (20 cm) is very small for the regions Drenthe and Veluwe. Only region Northern-Limburg, the region with the highest deposition level, can be distinguished with a lower pH and higher NO_3^-, SO_4^{2-} and Al^{3+} concentrations (table 42; Al^{3+} and pH shown only).

Figure 23
Simulated pH at 20 cm depth by NuCSAM, SoilVeg and ForGro for Douglas fir on a Cambic podzol (left) and Scots pine on a Haplic arenosol (right) for scenario 'Drenthe', 'Veluwe' and 'N-Limburg'.

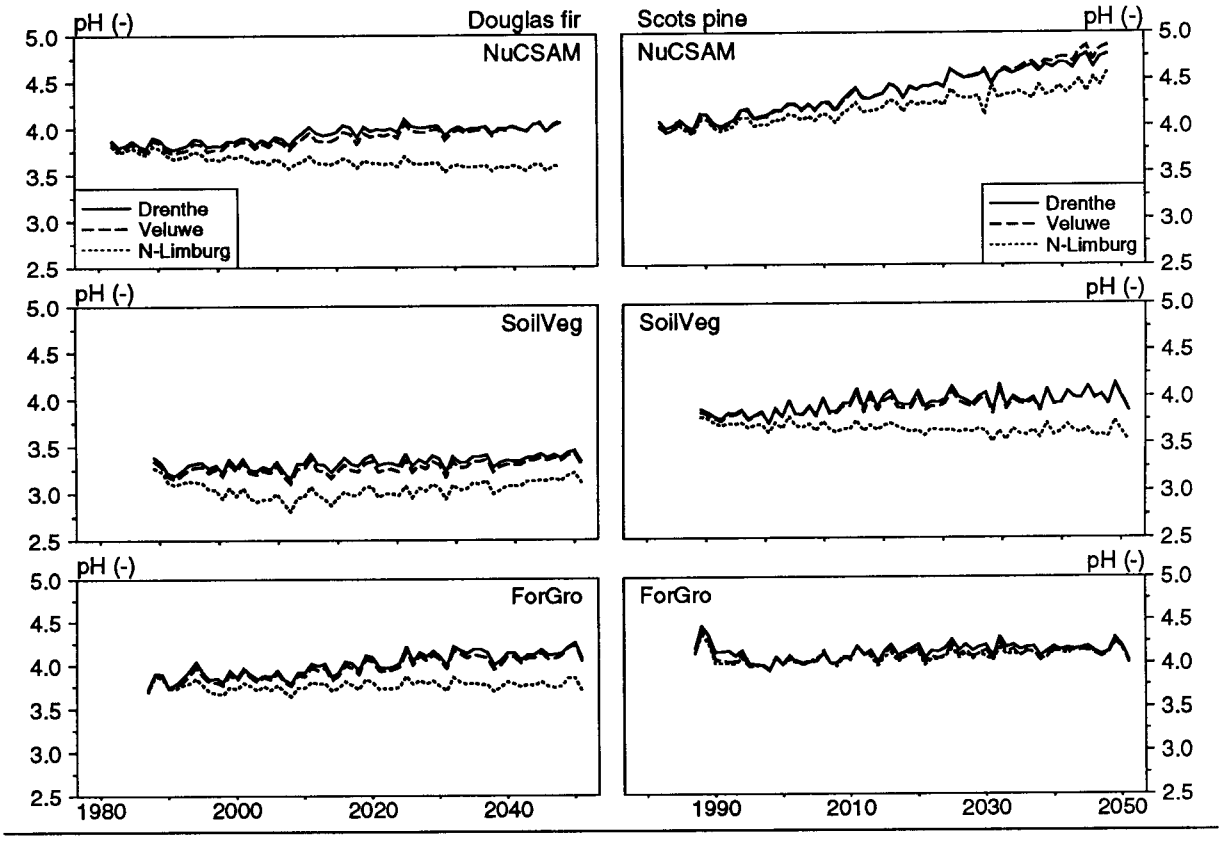

For the subsoil (90 cm), NO_3^- and SO_4^{2-} concentrations differ for the three regions, which is also reflected in the difference in nitrate leaching at 90 cm (table 42). However, effects on the pH and Al concentration at 90 cm are limited. There is quite a large difference in the fate of the pool of secondary aluminum compounds (oxalate extractable Al). For region Drenthe and Veluwe this amounts stabilizes or even increases, as for region Northern-Limburg there is an ongoing decrease of this pool, which can lead to an exhaustion of this pool and pH drop in the long run.

TABLE 42

Mean predicted soil and tree status simulated by NuCSAM, SoilVeg and ForGro between 1990 and 2000, and between 2040 and 2050 for generic Douglas fir on a Cambic podzol and generic Scots pine on a Haplic arenosol. Soil parameters are given for 20 cm depth.

Model variable	Unit	Douglas fir on a Cambic podzol						Scots pine on a Haplic arenosol					
		Period 1990-2000			2040-2050			1990-2000			2040-2050		
		Model [a] NC	SV	FR	NC	SV	FR	NC	SV	FR	NC	SV	FR
Drenthe													
pH [b]	(-)	3.8	3.3	3.8	4.0	3.4	4.1	4.1	3.8	4.0	4.7	4.0	4.1
Al-concentration [b]	(mol_c m^{-3})	0.8	1.2	2.7	0.2	0.3	0.8	0.3	0.9	0.7	0.1	0.4	0.3
ctAlox [c]	($mmol_c$ kg^{-1})	81	93	-	70	83	-	57	71	-	57	65	-
Al/Ca [d]	(mol mol^{-1})	4.4	1.8	5.5	1.0	0.5	1.5	0.9	8.6	24.8	0.0	0.4	16.8
NO_3 leaching	(kg ha^{-1})	16	14	-	3	1	-	8	4	-	0	1	-
Needle mass	(Mg ha^{-1})	7.8	14.8	11.5	7.8	11.3	17.4	3.4	8.3	5.7	3.4	8.3	4.9
Stem mass	(Mg ha^{-1})	-	161	170	-	200	284	-	71	82	-	154	181
N content leaves	(%)	1.5	1.8	2.0	1.0	1.5	1.9	1.2	1.7	1.9	1.0	1.7	1.8
Veluwe													
pH [b]	(-)	3.8	3.2	3.8	4.0	3.4	4.0	4.0	3.8	4.0	4.8	4.0	4.1
Al-concentration [b]	(mol_c m^{-3})	1.0	1.4	2.7	0.1	0.3	0.7	0.4	0.9	0.8	0.0	0.3	0.4
ctAlox [c]	($mmol_c$ kg^{-1})	78	92	-	66	82	-	54	71	-	54	62	-
Al/Ca [d]	(mol mol^{-1})	4.0	1.9	5.7	0.8	0.4	1.2	1.0	9.0	30.2	0.0	0.3	10.4
NO_3 leaching	(kg ha^{-1})	25	20	-	5	13	-	13	5	-	1	6	-
Needle mass	(Mg ha^{-1})	7.8	16.2	13.0	17.6	12.8	17.4	3.4	8.9	5.4	3.4	8.6	4.7
Stem mass	(Mg ha^{-1})	-	168	168	-	227	277	-	75	76	-	177	146
N content leaves	(%)	1.9	1.9	2.2	1.0	1.6	2.0	1.7	1.8	2.2	1.0	1.8	2.0
N-Limburg													
pH [b]	(-)	3.7	3.1	3.7	3.6	3.1	3.8	4.0	3.7	4.0	-	3.6	4.1
Al-concentration [b]	(mol_c m^{-3})	1.5	1.2	2.7	0.5	0.3	0.8	0.6	0.9	0.7	-	0.4	0.3
ctAlox [c]	($mmol_c$ kg^{-1})	81	91	-	70	76	-	57	68	-	-	42	-
Al/Ca [d]	(mol mol^{-1})	4.4	2.4	12.0	1.0	0.5	3.3	0.9	9.6	60.1	-	0.6	26.9
NO_3 leaching	(kg ha^{-1})	36	30	-	10	15	-	20	7	-	-	1.2	-
Needle mass	(Mg ha^{-1})	7.8	13.2	11.1	7.8	13.8	16.4	3.4	9.4	4.8	-	9.2	4.0
Stem mass	(Mg ha^{-1})	-	166	167	-	221	271	-	78	76	-	182	146
N content leaves	(%)	2.5	2.5	2.3	1.8	1.5	2.2	2.2	2.3	2.2	-	2.3	2.3

a) NC = NuCSAM, SV = SoilVeg and FR = ForGro
b) pH and Al-concentration at 20 cm depth.
c) ctAlox refers to content of secondary aluminum compounds at 20 cm depth.
d) Al/Ca at 20 cm depth.

For Scots pine, SoilVeg simulates the highest stem mass and foliage mass for Northern-Limburg. This is clearly a result of the high nitrogen deposition in this region. For Douglas fir, the intermediate scenario Veluwe gives the highest biomass growth. Here, adverse effects of the lower soil solution pH on uptake of Mg^{2+} and K^{+} dominate. The scenario analyses further show that the high nitrogen inputs in Northern-Limburg lead to extreme nitrogen contents in the foliage (tabel 42). SoilVeg predicts nitrogen contents that are very close to the maximum value.

Regarding the criteria for indirect effects on forest stress, results from SoilVeg and NuCSAM show that the scenarios for Drenthe and Veluwe for both Douglas fir and Scots pine will cause a reduction in the Al/Ca ratio down to or even below the defined critical

values in the year 2050. The same is true for Scots pine in region N-Limburg, but for Douglas fir in this region the Al/Ca ratio remains above the critical values up to 2050. The extreme and non-realistic Al/Ca ratios simulated by ForGro are caused by very low Ca^{2+} concentrations simulated by ForGro. This problem was already mentioned in §5.3.2, and again emphasizes the problems with modelling nutrient cycling.

In conclusion it can be stated that for some key model outputs, e.g. the Al-concentration and stem mass the three models give comparable differences between results for both periods. However, for pH, nitrate leaching, nitrogen uptake by trees (not shown), needle mass and N-content in the foliage, differences are dominated by differences between the models.

5.5 Comparison of results of ReSAM and NuCSAM

Figure 24 shows the results of a ReSAM application for generic Douglas fir on a Cambic Podzol in the Veluwe, together with the NuCSAM results and the ReSAM results using a scenario that was described by Heij and Schneider (1991) (referred to as DPPA-2). The DPPA-2 scenario is even more optimistic than the DPPA-3 scenario, as it was assumed that the deposition target of 1400 $mol_c\ ha^{-1}\ a^{-1}$ was already reached in the year 2010, instead of in the year 2050.

The agreement between the soil solution concentrations simulated by NuCSAM and ReSAM was generally good, except for the Al/Ca ratio. The most remarkable difference between the two model results is that the NuCSAM outputs are fickle, while the ReSAM outputs are strongly smoothed. This is, of course, inherent to the nature of the models: daily based (NuCSAM) versus annual average based (ReSAM). Differences in the topsoil are mainly due to a different root uptake pattern, with NuCSAM withdrawing more water from the deeper soil layers. The differences in simulated depletion of the pool of secondary aluminum compounds and NO_3^- leaching are small. The Al/Ca ratio as simulated with NuCSAM shows a time delay compared to the Al/Ca ratio simulated with ReSAM. This phenomenon was also observed for the Solling Norway Spruce stand (Kros *et al.*, 1994). The time delay for the Al/Ca ratio is due to a slower response of the exchange complex in NuCSAM, caused by differences in the temporal and spatial resolution of the models. In ReSAM, thicker soil layer were used. Nonetheless, the agreement between ReSAM and NuCSAM is rather good, and ReSAM can be used instead of NuCSAM for long-term predictions. However, when major emphasis is on stress assessment, short term temporal dynamics cannot be ignored, as both the maximum Al concentration and the maximum Al/Ca ratio are not simulated reasonably by a yearly averaged model (see Figure 24).

Differences between the results for the DPPA-2 and DPPA-3 scenarios as evaluated with ReSAM are small, although relatively large differences occurred during the period 1980-2000. Differences are partly caused to the different initialization periods. For the DPPA-2 scenarios, the model run started in 1955, whereas the model runs started in 1970 for the DPPA-3 scenarios. However, differences in pH increased during the simulation period, and the DPPA-3 scenario predicts a stronger decrease of the pool of secondary aluminum compounds.

Figure 24
Comparison of simulated soil solution chemistry by NuCSAM and ReSAM at 20 cm depth (left) and 90 cm depth (right). Simulations were carried out for generic Douglas fir on a Cambic podzol for two scenarios.

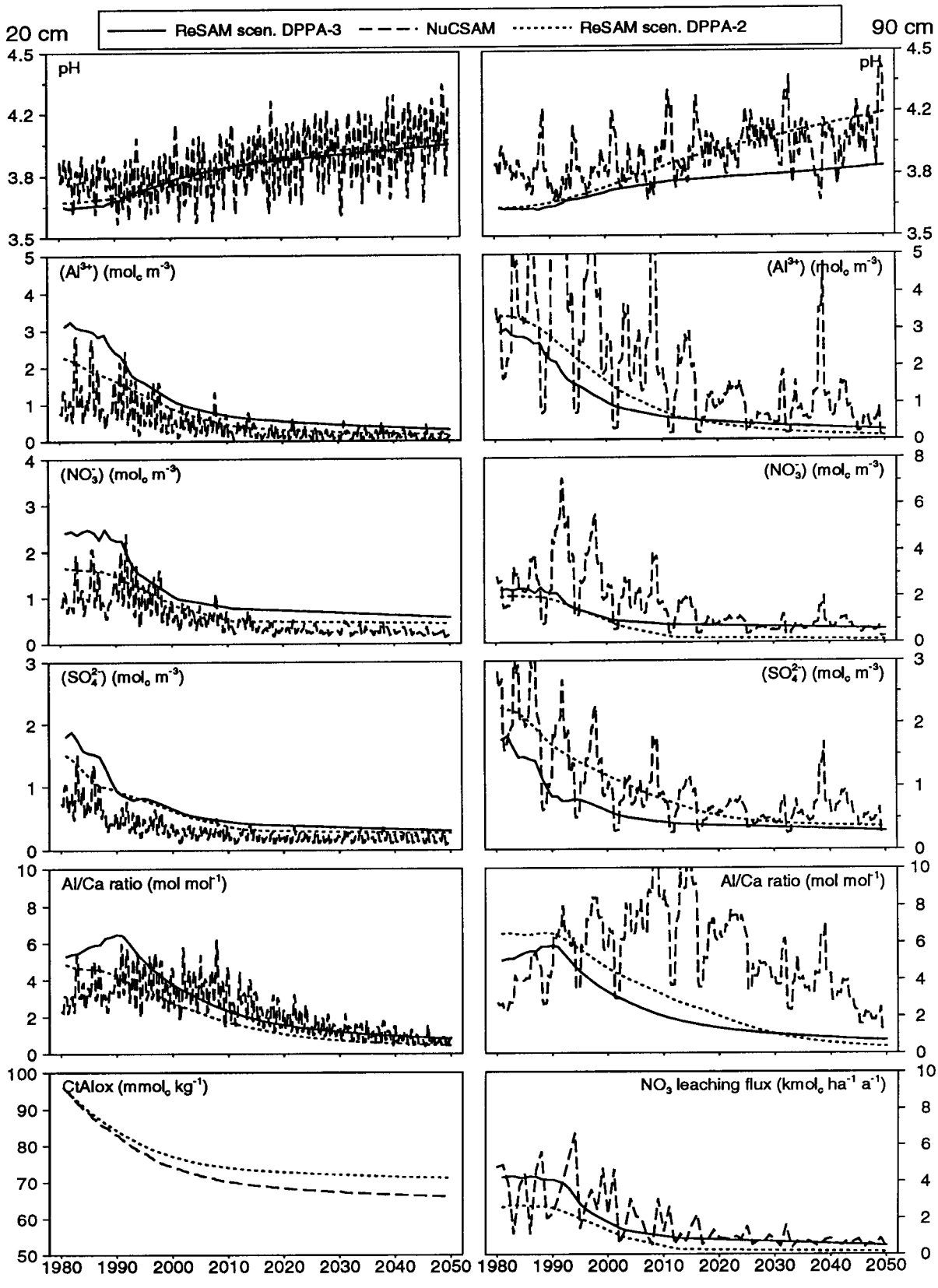

6 GENERAL DISCUSSION AND CONCLUSIONS

The effort to compare complicated models, and to apply these models to detailed observation data-sets, like the one for Speuld and the one for Solling, was a challenge. However, a first remark should be that both the Speuld data-set and the models were not really ready for this exercise to be carried out efficiently. Too much technical and practical questions arose when compiling the Speuld data-set and preparing it for the application of the three models. We feel that in the past not enough attention was paid to quality control, compilation, maintenance and distribution of the data-set *as a whole*. The same remark applies to the models. Model documentation was not finished or needed update, and the procedures for model calibration and model use were still inadequate at the onset of the exercise described here. In future research programs, more attention should be paid to quality control and to bridging the gap between models and data.

6.1 Model validation

A first conclusion is that results from ReSAM, the current tool for assessing long-term response of forest-soils to acidification abatement strategies, compared well with results from the daily based model NuCSAM. This implies that ignoring seasonal variations of weather conditions does not have a large impact for the long-term response of soil solution chemistry to deposition. As a similar comparison between SoilVeg-2 and SoilVeg-3 has not been made, conclusions pertaining to the impact of ignoring seasonal variation on the long-term assessment of effects cannot yet be drawn. A second conclusion arising from this exercise should be that the detailed DPPA-3 models have now thoroughly been tested against two common data-sets (Speuld and Solling), and that they provide a wealth of opportunities to test hypotheses about the interactions between forest, soil and atmosphere. However, it is not yet clear wether the models are suitable instruments for long-term predictions and scenario analyses. It is obvious that the Speuld data-set was too short for true model-validation. Moreover, due to the large spatial variability of throughfall, soil solution chemistry and stand structure, it was almost impossible to build a meaningful and representative data-set. A major reason for this was that the monitoring at Speuld followed a disciplinary approach, with separate subplots for hydrology, soil chemistry and forest growth. Either was the number of sampling replicates too small to calculate stand averages (soil chemistry), or it was impossible to select more or less homogeneous subplots (hydrology and biomass inventory). Furthermore, individual monitoring groups came with different data for some model parameters. Nevertheless, the models could reproduce the general magnitude of measured quantities, such as soil water contents, soil solution chemistry and stem mass increment. When it came to derived properties, the models sometimes deviated strongly (e.g. transpiration, vertical leaching fluxes, mineralization fluxes and root-uptake fluxes). In many occasions, we could derive a logical explanation from the underlying process formulations and model parameterization (e.g. nutrient cycling: root uptake, allocation, needle-fall, nitrification and mineralization). However, we could only identify and not solve the problems, as specific data to further test the underlying process formulations were usually not available. The models were not always successful in simulating measured seasonal dynamics. The most obvious problems occurred for nutrient contents in biomass compartments. Comparable conclusions were drawn from the Solling application, where long-term trends could be reproduced, but where

the models could not reproduce seasonal dynamics of nitrogen cycling. As long as we are not able to reproduce these short term dynamics, we cannot really validate the underlying processes, and long-term assessment of effects by models is bound to be uncertain.

Differences in model concepts and model parameterization became even clearer when using the models for long-term predictions and scenario analyses. For some key model outputs, all models simulated the same response to reduced deposition. Examples are the sulphate concentration in the soil solution, the aluminum chemistry and the depletion of the pool of secondary aluminum compounds. However, models were not conclusive with respect to nutrient cycling and forest growth.

All this does not mean that there is any reason to abandon the current modelling approach. Firstly, there is no true alternative for models as a tool to test hypotheses about the long-term response of the forest-ecosystems to a changing environment. Secondly, the models *do* reduce our uncertainty about the response of a forest to a manageable level. If interpreted critically, model results can provide an objective basis for taking practical measures to reduce risks for damage to forest ecosystems.

6.2 Stress assessment

The models were inconclusive with respect to effects of changing environmental conditions on forest growth and soil chemistry. This implies that the models do not (yet) give a reliable answer to questions with respect to the most important growth limiting factors. The necessity for further and more rigorous applications of the models to experimental manipulation experiments as carried out within the EXMAN project (Beier *et al.*, 1993) is beyond doubt. Nevertheless, results from this and preceding exercises (Mohren *et al.*, 1992) confirm the experimental findings (Steingröver and Jans, 1995) that direct effects of air pollution are small compared to indirect (soil mediated) effects.

SoilVeg simulates considerable reduction of nutrient uptake by high aluminum concentrations in the soil solution and low pH, whereas the effects are small for ForGro. However, with respect to these effects, we must point at the danger of getting into a vicious circle, as included stress relationships are empirical. These relationships are mainly based on laboratory experiments and pot trials with seedlings. SoilVeg uses a direct relation between nutrient uptake and aluminum concentration, whereas ForGro uses a relationship between aluminum concentration and root density as found by Keltjens and Van Loenen (1989). As long as we cannot find experimental evidence for these relationships *in the field*, model predictions remain as uncertain as the measurements themselves (see further §6.3). The same remark applies to the assumed effects of a combination of increased aluminum concentrations and summer-drought. In ForGro, the effect of drought and seasonal periodicity on fine-root growth and root-biomass as found by Olsthoorn and Tiktak (1991) seems to overshadow the effects of high aluminum concentrations. The importance of effects of enhanced nitrogen deposition is beyond discussion. All models indicate above-critical[1] nitrogen contents in the needles, and low magnesium, calcium and potassium contents. Note that nutritional imbalances caused by

[1] Refers to susceptibility to frost, plagues and diseases

increased nitrogen deposition (eutrophication) are enhanced by acidification effects, as the latter causes lower base cation availability in the soil solution. Due to nitrogen storage in standing biomass and litter, the situation of nutritional imbalances will remain for some decades. Another observed effect of increased nitrogen contents is increased respiration and water use, which together with decreased root growth make a stand more susceptible to drought stress. This effect will be most pronounced on less productive sites, in particular on sites with low water availability. On the other hand, the simulations for Drenthe indicate that decreasing nitrogen deposition may reduce forest growth in regions that already receive relatively low nitrogen deposition loads. Thus, the role of nitrogen for tree growth is ambiguous: differences of nitrogen availability between regions can lead to growth reduction due to nitrogen shortage, and growth reduction due to nitrogen surplus.

6.3 Critical values and critical loads

Critical values for the Al^{3+} concentration, the Al/Ca ratio, and the NH_4/K ratio could only partly be supported by the integrated models. These critical values are mainly derived from laboratory experiments with seedlings. Effects that were found include decreased fine-root biomass, decreased number of root tips and a decreased root uptake. A critical literature review on Al-effects (Sverdrup and Warfvinge, 1993) shows that the Al concentration criterion is anyhow unreliable, even from the laboratory experiments. The effect of the molar Al/Ca ratio (or better Al/BC ratio, with BC as the sum of the Mg, K and Ca concentrations) on seedlings appeared to differ for the various tree species. The tree species involved in this exercise were Douglas fir (Speuld, manipulation experiments and scenario analyses) and Scots pine (scenario analyses). According to Sverdrup and Warfvinge (1993), Douglas is rather insensitive to Al (a critical Al/BC value of 3.3 mol mol^{-1}), whereas Scots pine is relatively sensitive to Al (a critical Al/BC value of 0.8 mol mol^{-1}). Since Douglas fir is the main tree species involved in the modelling, this may have affected the results. On the other hand, Hendriks *et al.* (1994) also found that the vitality of trees in the field situation is hardly correlated to the Al concentration or Al/BC ratio in the soil solution. Tree species and stand age appeared to be the most important explanatory variables, while foliar nitrogen content and pH played a minor role. These results, together with the modelling efforts, imply that an exceedance of critical acid loads based on critical Al/BC ratios observed in laboratory experiments do not imply visible effects or dieback of forests. However, it does mean that the long-term sustainability of forests is affected, since an exceedance of these critical loads also causes the depletion of secondary Al compounds, as shown by the models. In general, however, it is clear that the critical loads related to other parts of the forest ecosystem (e.g. ground vegetation) are better confirmed than those derived for trees.

6.4 Scenario analyses

Scenario analyses were carried out for Douglas fir on a Cambic podzol and Scots pine on an Haplic arenosol in areas with low, intermediate and high atmospheric deposition. One must keep in mind that simulations have been carried out on the basis of one realization of weather data only. With respect to soil chemistry, the models were conclusive about general trends and differences between both forest-soil combinations. The most important trends and differences were a fast response of the sulphate and aluminum concentrations after a decrease in SO_x deposition, time-delay for the NO_3^- concentration following a

decrease in nitrogen deposition, and depletion of the pool of secondary aluminum compounds. With respect to nutrient cycling and tree growth, the models were less conclusive. Nevertheless, the two integrated models (SoilVeg and ForGro) predict high foliage and low but sufficient fine root biomass throughout the scenarios. The models further indicate that forest growth is sustained, but there are considerable differences in the magnitude of stem increment. However, it should be noted that both the applied thinning scheme and the stand age are not realistic for a production stand. Another important conclusion from both models is that after an initial fast decrease of the nitrogen content in the foliage, it takes several decades for the present high nitrogen contents to decrease.

6.5 Major uncertainties

A major uncertainty of the integrated models is found in the description of vegetation-soil linkages. For example, process formulations for nutrient uptake from soil by roots are entirely different for SoilVeg and ForGro. There is hardly any consensus on the relationships between the nutrient status of the site and tree growth. The current application also shows that the direct impact of air pollution on the forest is small, but it is not yet possible to distinguish effects of water and nutrient deficiency from effects of soil acidification. Another major shortcoming of the current (deterministic) approach is the inability, as yet, to include known catastrophic effects on stand growth and vitality like bacterial, fungal and insect infestations, bud damage due to frost, severe damage due to drought, and damage due to wind throw. Events like these will very likely occur several times within one rotation, and the susceptibility of the stand to such effects is related to the nutrient (in particular nitrogen) status, and to the biomasses of foliage and roots. Given these limitations, and acknowledging that we still cannot find experimental evidence for various stress conditions in the field, any prediction of long-term effect of air pollution on forests is bound to be uncertain.

6.6 Recommendations for future research

After application of the integrated models at the stand-level, some uncertainties still remain, and new uncertainties arose. However, despite these uncertainties tremendous progress was made. This exercise clearly shows that for further hypothesis testing and validation of the models, there is a need to continue intensive monitoring programs, but the balance between data acquisition in the various compartments of the ecosystem should be emphasized. Moreover, much more attention should be paid to bridging the gap between models and experimental data. Models should be used to select the most important parameters to be monitored. Further, models can be used to set-up sampling strategies (in particular sampling frequencies). Another major point of concern should be the issue of *quality control*. The current exercise shows that both the models and the dataset were poorly described. Perhaps the only way to guarantee that integrated data-sets become available is by building databases, which are maintained by a small group of researchers. Besides long-term monitoring of important model parameters, there is a need for measurement campaigns aimed at reducing the uncertainty in the models. However, such campaigns should be directed by the requirements of integrated models, and not follow a disciplinary line. Besides intensive monitoring programs there is a need for extensive monitoring on a larger number of locations. Such extensive monitoring programs are mandatory for calibration of regional models. However, as with the intensive monitoring

programs, much more attention should be paid to bridging the gap between models and measurements. In extensive monitoring, the need for using models to set-up measurements campaigns is even more evident than in intensive monitoring programs.

In the near future, the present models should be used to further explore available manipulation experiments, and present site calibrations could be used to assess the uncertainty of predictions for Speuld, and the deposition scenarios. Uncertainty analyses of the models should be carried out after empirical incorporation of known 'catastrophic' effects (see §6.5), and should account for variability in weather.

6.7 Major conclusions

Major conclusions of this report are:

- The models could reproduce the general magnitude of measured quantities, but when it came to derived properties, the models sometimes deviated strongly. These differences could only be identified and not solved, as specific data to further test the underlying process formulations were usually not available.
- The models were conclusive with respect to the response of aluminum chemistry to reduced deposition, and inconclusive with respect to nutrient cycling and forest growth. At present it is not clear whether the models are suitable instruments for long-term prediction of effects of atmospheric deposition and air pollution on forests.
- A major uncertainty of the integrated models is found in the descriptions of vegetation-soil linkages (e.g. nutrient uptake by roots).
- The present and preceding exercises confirm the experimental findings that direct effects of air pollution are small compared to indirect (soil mediated) effects.
- Results showed that the effects of high aluminum concentrations on fine-root development were overshadowed by effects of drought and normal fine-root periodicity. This confirms a critical literature survey by Sverdrup and Warfvinge (1993) who showed that the aluminum concentration does not have any relationship with tree functioning. Thus, the critical aluminum criterion should be regarded unreliable.
- All models point at the importance of enhanced nitrogen deposition for forest functioning. The models calculate above-critical nitrogen contents in the needles, and low magnesium, calcium and potassium contents. This situation of nutritional imbalances is enhanced by acidification effects, as acidification causes lower base cation availability in the soil solution.
- The models showed that the role of nitrogen on forest growth is ambiguous: enhanced nitrogen deposition may either increase or decrease forest growth.
- The scenario analyses showed a fast response of the sulphate and aluminum concentrations in the soil solution after a decrease of the SO_x deposition, time-delay for the NO_3^- concentration following a decrease in nitrogen deposition, and depletion of the pool of secondary aluminum compounds in regions with high deposition. The models also showed that it takes several decades for the situation of nutritional imbalances (high nitrogen contents in the needles) to improve.
- Results of the yearly based model ReSAM and the daily based model NuCSAM show general agreement. This implies that ignoring seasonal variation of weather conditions does not have a large impact on the long-term response of soil solution chemistry to deposition.

- The present modelling efforts, together with results of an inventory of 150 stands imply that an exceedance of critical Al/BC ratios do not necessarily imply visible effects or dieback of forests. However, it does mean that the long-term sustainability of forests is affected, since an exceedance of these critical values causes the depletion of the pool of secondary aluminum compounds.
- The current exercise clearly shows that for further hypothesis testing and validation of the models, there is a need to continue intensive monitoring programs, but the balance between data acquisition in the various compartments should be emphasized. For further validation, the models should be applied to experimental manipulations.

7 REFERENCES

Beier, C. and Rasmussen, L. (eds), 1993. EXMAN: Experimental Manipulation of Forest Ecosystems in Europe. Ecosystem Research Programme no. 7, Publ. EUR 14992 EN, Comm. of the European Communities.

Belmans, C., J.G. Wesseling and F.E. Feddes, 1983. Simulation model of the water balance of a cropped soil: SWATRE. J. Hydrology (63):271-286.

Berdowski, J.J.M., C. van Heerden, J.J.M. van Grinsven, J.G. van Minnen and W. de Vries, 1991. SoilVeg: A model to evaluate effects of acid atmospheric deposition on soil and forest. Volume 1: Model principles and application procedures. Dutch Priority Programme on Acidification, rep. no. 114.1-02, RIVM, Bilthoven, Netherlands, 93 pp.

Bergström, S., 1975. The development of a snow module for the HBV-2 model. Nordic hydrology (6):73-92.

Black, T.A., W.R. Gardner and G.W. Thurtell, 1969. The prediction of evaporation, drainage and soil water storage for a bare soil. Soil Sci. Soc. Am. Proc. (33):655-660.

Bouten, 1992. Monitoring and modelling forest hydrological processes in support of acidification research. Ph.D. thesis, University of Amsterdam, Amsterdam, Netherlands, pp. 218.

Bouten, W., T.J. Heimovaara and A. Tiktak, 1992. Spatial patterns of throughfall and soil water dynamics in a Douglas fir stand. Water Res. Res. (28):3227-3233.

Bredemeier, M, A. Tiktak and C. van Heerden, 1995. The Solling spruce site: Background information on the data set. In: J.J.M. van Grinsven (ed.). Modelling water, carbon and nutrient cycles in forests: application of 16 simulation models to a spruce stand at Solling, Germany. Accepted to Ecological Modelling.

Cannell, M.G.R. 1982. World forest biomass and primary production data. London, Academic Press, 391 pp.

Christophersen, N., L.H. Dymbe, M. Johanssen and H.M. Seip, 1983. A model for sulphate in streamwater at Storgama, Southern Norway. Ecol. Modelling (21):35-61.

De Visser, P.H.B., 1994. Growth and nutrition of Douglas fir, Scots pine and pedunculate oak in relation to soil acidification. Ph.D. thesis, Agricultural University, Wageningen, Netherlands, pp. 185.

De Visser, P.H.B. and W. De Vries, 1989. De gemiddelde jaarlijkse waterbalans van bos-, heide- en graslandvegetaties (The yearly average water balance of forest, heathland and grassland vegetations). STIBOKA rapport nr. 2085, Wageningen, Netherlands, 136 pp.

De Vries, W., 1988. Critical deposition levels for nitrogen and sulphur on Dutch forest ecosystems. Water Air and Soil Pollution (42):221-239.

De Vries, W., 1991. Methodologies for the assessment and mapping of critical loads and of the impact of the abatement strategies on forest soils. Winand Staring Centre, report 46, Wageningen, Netherlands, pp. 152.

De Vries, W., 1994. Soil response to acid deposition at different regional scales. Field and laboratory data, critical loads and model predictions. Ph.D. thesis, Agricultural University, Wageningen, Netherlands, pp. 487.

De Vries, W. and A. Breeuwsma, 1986. Relative importance of natural and anthropogenic proton sources in soils in the Netherlands. Water Air and Soil pollution (35):293-310.

De Vries, W., A. Hol, S. Tjalma en J.C. Voogd, 1990. Literatuurstudie naar voorraden en verblijftijden van elementen in een bosecosysteem. DLO-Staring Centrum, Rapport nr. 94, Wageningen, Netherlands, pp. 205 (In Dutch).

De Vries, W., J. Kros and C. van der Salm, 1994. The long-term impact of three emission-deposition scenarios on Dutch forest soils. Water Air and Soil Pollution (75):1-35.

De Vries, W., J. Kros and C. van der Salm, 1995a. Modelling the impact of nutrient cycling and acid deposition on forest soils. Ecological Modelling (in press).

De Vries, W., E.E.J.M. Leeters, C.M. Hendriks, W. Balkema, M.M.T. Meulenbrugge, R. Zwijnen and J.C.H. Voogd, 1992. Soil and soil solution composition of 150 forest stands in the Netherlands in 1990. In: T. Schneider (ed.). Acidification research. Evaluation and policy making. Elsevier Science Publ., Amsterdam, Netherlands, 535-536.

De Vries, W., M.M.T. Meulenbrugge, W. Balkema, J.C.H. Voogd and R.C. Sjardijn, 1995b. Rates and mechanisms of cation and silica release in acid sandy soils: 3. Differences between soil horizons and soil types. Submitted to Geoderma.

De Vries, W., M. Posch and J. Kämäri, 1989. Simulation of the long-term soil-response to acid deposition in various buffer ranges. Water Air and Soil Poll. (48):349-390.

De Vries, W., M. Posch, T. Oja, H. van Oene, J. Kros, P. Warfvinge and P.A. Arp, 1995c. Modelling critical loads for the Solling Spruce site. In: J.J.M. van Grinsven (ed.). Modelling water, carbon and nutrient cycles in forests: application of 16 simulation models to a spruce stand at Solling, Germany. Accepted to Ecological Modelling.

De Willigen, P. and M. Van Noordwijk, 1987. Roots, plant production and nutrient use efficiency. Ph.D. thesis, Wageningen Agricultural University, Wageningen, Netherlands, pp. 282.

Draaijers, G.P.J., 1993. The variability of atmospheric deposition to forests. The effects of canopy structure and forest edges. Ph.D. thesis, Univ. Utrecht, Utrecht, Netherlands, pp. 156.

Duysings, J.J.H.M., J.M. Verstraten and W. Bouten, 1986. Spatial variability in nutrient deposition under an oak/beech canopy. Zeitschr. Pflantzenernährung Bodenk. (149):718-727.
Erisman, J.W., 1990. Atmospheric deposition of acidifying compounds onto forests in the Netherlands. Throughfall measurements compared to deposition estimates from inference. National Institute of Public Health and Environmental Protection report no. 723001001, Bilthoven, Netherlands, pp. 29.
Erisman, J.W., 1991. Acid deposition in the Netherlands. RIVM report no. 723001002, Bilthoven, Netherlands, pp. 72.
Erisman, J.W., 1993. Acid deposition onto nature areas in the Netherlands. Part I. Methods and results. Water, Air and Soil pollution (71):51-80.
Erisman, J.W., G.P.J. Draaijers, E. Steingröver, H.F.G. van Dijk and A.W. Boxman, 1994. Research at the Speulder forest site: Assessment of the causal relations due to acidification and eutrophication. Dutch Priority Programme on Acidification, this volume.
Evers, P.W., W.W.P. Jans and E.G. Steingröver, 1991. Impact of air pollution on ecophysiological relations in two Douglas fir stands in the Netherlands. De Dorschkamp Research Institute for Forestry and Urban Ecology, Report no. 637, Wageningen, Netherlands, pp. 306.
Evers, P.W., C.J.M. Konsten and A.W.M. Vermetten, 1987. Acidification research on Douglas fir forests in the Netherlands (ACIFORN project). Proc. Symp. Effects of Air Pollution on Terrestrial and Aquatic Ecosystems. Grenoble, 887-909.
FAO, 1988. Soil map of the World, revised legend. World soil resources report 60, FAO, Rome, pp. 138.
Foster, N.W., I.K. Morrison and J.A. Nicolson, 1986. Acid deposition and ion leaching from a podzolic soil under hardwood forest. Water Air and Soil pollution (31):879-889.
Gash, J.H.C., 1979. An analytical model of rainfall interception by forests. Quart. J. R. Met. Soc. (105):43-55.
Gijsman, A.J. 1990. Nitrogen nutrition and rhizosphere pH of Douglas-fir. Ph.D. Thesis, State University Groningen, Netherlands, 132 pp.
Göransson, A., 1985. Effects of Aluminum on seedling growth and nutrient uptake of Norway spruce, Scots pine, and European birch at steady state nutrition. In: Indirect effects of air pollution on forest trees. Root-Rhizosphere Interactions. Proceedings CEC concerted action 'Effects of air pollution on Terrestrial and Aquatic ecosystems'. 5-6 Dec. 1985. - EAD.45.86, XII/ENV/24/86, pp. 46-56.
Groenenberg, J.E., J. Kros, C. van der Salm and W. de Vries, 1995. Application of the model NuCSAM to the Solling spruce site. In: J.J.M. van Grinsven (ed.). Modelling water, carbon and nutrient cycles in forests: application of 16 simulation models to a spruce stand at Solling, Germany. Accepted to Ecological Modelling.
Groenendijk, P., 1995. The calculation of complexation, adsorption, precipitation and weathering reactions in a soil water system with the geochemical model EPIDIM. DLO Staring Centre Report no. 70, Wageningen, Netherlands (in prep).
Heij, G.J. and T. Schneider, 1991. Acidification research in the Netherlands. Final report of the Dutch Priority Programme on Acidification. Studies in Environmental Science 46, Elsevier, Amsterdam, 771 pp.
Hendriks, C.M.A., W. de Vries and J. van den Burg, 1994. Effects of acid deposition on 150 forest stands in the Netherlands. 2. Relationship between forest vitality and the chemical composition of the foliage, humus layer and the soil solution. DLO-Staring Centre report no. 69.2, Wageningen, the Netherlands, pp. 55.
Jans, W.W.P, G.M. van Roekel, W.H. van Orden and E.G. Steingrover, 1991. Above ground biomass of adult Douglas fir. A data set collected in Garderen and Kootwijk from 1986 onwards. IBN Research Report 94/1. Institute for Forestry and Nature Research, Wageningen, Netherlands.
Janssen, B.H., 1983. Organische stof en bodemvruchtbaarheid. Landbouwuniversiteit Wageningen, intern rapport, Wageningen, Netherlands, 215 pp (in Dutch).
Janssen, B.H., 1984. A simple method for calculating decomposition and accumulation of young organic matter. Plant and Soil (76):297-304.
Janssen, P.H.M. and P.S.C. Heuberger, 1995a. Calibration of process-oriented models. In: J.J.M. van Grinsven (ed.). Modelling water, carbon and nutrient cycles in forests: application of 16 simulation models to a spruce stand at Solling, Germany. Accepted to Ecological Modelling.
Janssen, P.H.M. and P.S.C. Heuberger, 1995b. Rotated Random Scan: A simple method for set-valued calibration. RIVM report in prep. National Institute of Public Health and Environmental Protection, Bilthoven, Netherlands.
Janssen, J.J. and J. Sevenster (Eds.), 1995. Opbrengsttabellen voor belangrijke boomsoorten in Nederland. Instituut voor Bos- en Natuuronderzoek, rapport in voorbereiding, Wageningen, The Netherlands (in Dutch).
Jeffree, C., 1981. Agricultural crop damage. In: The costs and benefits of sulphur dioxide control. A methodological study, pp. 78-88. OECD, Paris.
Johnson, D.W. and D.E. Todd, 1983. Relationships among iron, aluminum, carbon, and sulfate in a variety of forest soils. Soil Sci. Soc. Am. J. (47):792-800.
Keizer, V.G. 1994. Facsimile (June 23 1994) to the Steering Committee. DGM/LE, The Hague, Netherlands.

Keltjens, W.G. and E. Van Loenen, 1989. Effects of aluminum and mineral nutrition on growth and chemical composition of hydroponically grown seedlings of five different forest tree species. Plant and Soil (119):39-50.
Keyes, M.R. and C.C. Grier, 1981. Above- and belowground net production in 40-years old Douglas stands on low and high productivity sites. Can. J. For. Res. (11):599-605.
Kleijn, C.E., G. Zuidema en W. de Vries, 1989. De indirecte effecten van atmosferische depositie op de vitaliteit van Nederlandse bossen. 2. Depositie, bodemeigenschappen en bodemvocht-samenstelling van acht Douglas opstanden. Stichting voor Bodemkartering rapport nr. 2050, Wageningen, Netherlands, pp. 96 (In Dutch).
Kros, J., J.E. Groenenberg, W. de Vries and C. van der Salm, 1994. Uncertainties in long-term predictions of forest-soil acidification due to neglecting seasonal variability. Water Air and Soil Pollution (67):353-375.
Kros, J., P.S.C. Heuberger, P.H.M. Janssen and W. de Vries, 1994. Regional calibration of a steady-state model to assess critical loads. In: J. Grasman and G. van Straten (eds). Predictability and Non Linear Modelling in Natural Sciences and Economics, pp. 541-553.
Kros, J., P.H.M. Janssen, W. de Vries and C.I. Bak, 1990. Het gebruik van onzekerheidsanalyse by modelberekeningen. Een toepassing op het regionale bodemverzuringsmodel ReSAM. Staring Centrum rapport nr. 65, Wageningen, Netherlands, pp. 127 (in Dutch).
Kros J. and P. Warfvinge, 1995. Evaluation of model behaviour with respect to biogeochemistry at the Solling Spruce site. In: J.J.M. van Grinsven (ed.). Modelling water, carbon and nutrient cycles in forests: application of 16 simulation models to a spruce stand at Solling, Germany. Accepted to Ecological Modelling.
Kuiper, L.C. and G.J.E. van Dijk, 1988. Structure and development of the root system of Douglas-fir. Dept. of Silviculture and Forest Ecology, Report D 88-06, Wageningen Agricultural University, Wageningen, Netherlands, 13 pp.
Kurz, W.A. and J.P. Kimmins, 1987. The influence of site quality on tree resource allocation to fine roots and its effect on harvestable productivity of coastal Douglas-fir stands. FRDA report no 034, Faculty of Forestry, University of British Columbia, Vancouver, Canada, pp. 103.
La Bastide, J.G.A. and P.J. Faber, 1972. Revised yield tables for six tree species in the Netherlands. Research Institute for Forestry and Urban Ecology, Report no. 11(1), Wageningen, Netherlands, pp. 64.
Landsberg, J.J., M.R. Kaufmann, D. Binkley, J. Isebrands and P.G. Jarvis, 1991. Evaluating progress toward closed forest models based on fluxes of carbon, water and nutrients. Tree Physiology (9):1-15.
Linzon, S.M., Pearson, R.G., Donnan, J.A. & Durham, F.M., 1984. Ozone effects on crops in Ontario and related monetary values. Ontario Ministry of the Environment, ARB-13-84-phyto, USA.
Makkink, G.F., 1957. Testing the Penman formula by means of lysimeters. Journ. Inst. of Water Eng. (11):277-288.
Mälkönen, E. 1974. Annual primary production and nutrient cycling in some Scots pine stands. Communicationes Instituti Forestalis Fenniae, Helsinki, 84.5, 87 pp.
Mitscherlich, G. and W. Moll, 1970. Untersuchungen über die Niederschlags- und Bodenfeuchtigkeitsverhältnisse in einigen Nadel- und Laubholzbeständen in der Nähe von Freiburg. A.F.J.Z. (141):49-60.
Mohren, G.M.J., 1987. Simulation of forest growth applied to Douglas fir stands in the Netherlands. Ph.D. thesis, Wageningen Agricultural University, Wageningen, Netherlands, 184 pp.
Mohren, G.M.J., H.H. Bartelink, I.T.M. Jorritsma and K. Kramer, 1993. A process-base growth model (ForGro) for analysis of forest dynamics in relation to environmental factors. In: M.E.A. Broekmeyer, W. Vos and H. Koop (eds.): European Forest Reserves. Proc. of the European Forest Reserves Workshop, 6-8 May 1992, The Netherlands, PUDOC, Wageningen, Netherlands, p. 273-280.
Mohren, G.M.J., I.T.M. Joritsma, A.W.M. Vermetten, M. Kropff, W.L.M. Smeets and A. Tiktak, 1992. Quantifying the direct effects of SO_2 and O_3 on forest growth. Forest. Ecol. and Management (51):137-150.
Mohren, G.M.J. and R. Rabbinge, 1990. Growth-influencing factors in dynamic models of tree growth. In: R.K. Dixon, R.S. Meldahl, G.A. Ruark & W.G. Warren (eds.): Process Modeling of Forest Growth Responses to Environmental Stress. Timber Press Inc., Portland, Oregon, USA, p229-240.
Mohren, G.M.J., J. Van den Burg and F.W. Burger 1986. Phosphorus deficiency induced by nitrogen input in Douglas-fir stands in the Netherlands. Plant and Soil 95: 191-200.
Olsthoorn, A.F.M., 1991. Fine root density and biomass of two Douglas fir stands on sandy soils in the Netherlands. I. Root biomass in early summer. Neth. J. Agric. Sci., (39): 49-60.
Olsthoorn, A.F.M. and A. Tiktak, 1991. Fine root density and biomass of two Douglas fir stands on sandy soil in the Netherlands. II. Periodicity of fine root density and root biomass and estimation of belowground carbon allocation. Neth. J. Agric. Sci., (39):61-77.
Oterdoom, J.H., J. van den Burg and W. de Vries, 1987. Resultaten van een oriënterend onderzoek naar de minerale voedingstoestand en bodem-chemische eigenschappen van acht douglasopstanden met vitale en minder vitale bomen in Midden-Nederland, winter 1984/1985. De Dorschkamp, Rapport nr. 470, Wageningen, Netherlands, pp. 47 (In Dutch).

Reddy, K.R., P.S.C. Rao and R.E. Jessup, 1982. The effect of carbon mineralization on denitrification kinetics in mineral and organic soils. Soil Sci. Soc. Am. J. (46):62-68.
Richardson, C.W. and D.A. Wright, 1984. WGEN: A model for generating daily weather variables. U.S. Dept. for Agriculture, Agric. Science, ARS-8, p.5-15.
RIVM, 1992. Milieudiagnose 1991. II. Luchtkwaliteit. RIVM rapport nr. 222101022, Bilthoven, Netherlands, 107 pp.
RIVM, 1993. Nationale Milieuverkenning 3. 1993-2015. Samson H.D. Tjeenk Willink, Alphen aan den Rijn, Netherlands, pp. 167 (In Dutch).
Roberts, J., 1983. Forest transpiration: A conservative hydrological process? J. Hydrology (66):133-141.
Roelofs, J.G.M., A.J. Kempers, A.L.F.M. Houdijk and J. Jansen, 1985. The effect of airborne ammonium sulphate on Pinus nigra var. maritima in the Netherlands. Plant and Soil (84):45-56.
Scherfose, V. 1990. Feinwurzelverteilung und Mykorhizatypen von Pinus sylvestris in verschiedenen Bodentypen. Berichte Forschungszentrum WaldÖkosystemen, Univ. Göttingen, Reihe A, Band 62, 169 pp.
Skeffington, 1988. Excess nitrogen deposition. Environmental Pollution (54):159-296.
Smeets, W.L.M., M.J. Kropff, E.M.J. Meier, E. Bakx, A.J.A. van der Zalm, 1990. Quantitative analysis of the uptake of SO_2 and O_3 by plants and effects on physiological processes and growth. Research Institute for Plant Protection, Wageningen, Netherlands, IPO rep. R-89-11, 124 pp.
Steingröver, E.G. and W.W.P. Jans, 1995. Physiology of forest-grown Douglas-fir tress: Effects of air pollution and drought. Dutch Priority Programme on Acidification rep. no. 793315-01, Bilthoven, Netherlands (in prep.).
Sverdrup, H., and P. Warfvinge, 1993. The effects of soil acidification on the growth of trees, grass and herbs as expressed by the (Ca+Mg+K)/Al ratio. Reports in Ecology and Environmental Engineering 1993.2, Lund University, Dept. of Chemical Eng. II, Lund, Sweden, pp.108.
Thornton, F.C., 1987. Effects of Aluminum on red spruce seedlings in solution culture. Environmental and experimental botany, (27):489-498.
Tiktak, A., A.H. Bakema, K.F. de Boer, J.W. Erisman, J.J.M. van Grinsven, C. van Heerden, G.J. Heij, J. Kros, F.A.A.M. de Leeuw, J.G. van Minnen, C. van der Salm, J.C.H. Voogd and W. de Vries, 1992. Scenario analysis with the Dutch Acidification Systems (DAS) model: an example for forests and forest soils. In: T. Schneider (ed.). Acidification research: evaluation and policy applications. Studies in Environmental Science 50, Elsevier, Amsterdam, 319-340.
Tiktak, A., M. Bredemeier and C. van Heerden, 1995. The Solling data-set: Site characteristics and deposition scenarios. In: J.J.M. van Grinsven (ed.). Modelling water, carbon and nutrient cycles in forests: application of 16 simulation models to a spruce stand at Solling, Germany. Accepted to Ecological Modelling.
Tiktak, A. and W. Bouten, 1990. Soil hydrological system characterization of the two ACIFORN stands using monitoring data and soil hydrological model 'SWIF'. Dutch Priority Programme on Acidification report no. 102.2-01, RIVM, Bilthoven, Netherlands, pp. 62.
Tiktak, A. and W. Bouten, 1992. Modelling soil water dynamics in a forested ecosystem. III: Model description and evaluation of discretization. Hydrol. Proc. (6):455-465.
Tiktak, A. and W. Bouten, 1994. Soil water dynamics and long-term water balances of a Douglas fir stand in the Netherlands. J. Hydrology (156):265-283.
Tiktak, A., C.J.M. Konsten, M.P. Van Der Maas and W. Bouten, 1988. Soil chemistry and physics of two Douglas-fir stands affected by acid atmospheric deposition on the Veluwe, the Netherlands. Dutch Priority Programme on Acidification, report no. 03-01, RIVM, Bilthoven, Netherlands, pp. 93.
Tiktak, A. and J.J.M. Van Grinsven, 1992. Inventory of monitored forest stands in the Netherlands. Dutch Priority Programme on Acidification, report no. 792310-01, Bilthoven, Netherlands, pp. 60.
Ulrich, B., 1983. Interaction of forest canopies with atmospheric constituents: SO_2, alkali and earth alkali cations and chloride. In: B. Ulrich and J. Pankrath (eds.). Effects of accumulation of air pollutants in forest ecosystems. Reidel, Dordrecht, Netherlands, 33-45.
Van Breemen, N. and J.M. Verstraten, 1991. Soil acidification and N cycling. In: T. Schneider and G.J. Heij (Eds.). Acidification Research in the Netherlands. Final report of the Dutch Priority Programme on Acidification. Studies in Environmental Science 46, Elsevier, Amsterdam, 289-352.
Van der Eerden, L.J., Tonneyck, A.E.G. & Wijnands, J.H.M., 1988. Crop loss due to air pollution in the Netherlands. Environm. Poll. (53):365-376.
Van der Maas, M.P. and Th. Pape, 1990. Hydrochemistry of two Douglas fir ecosystems and a heather ecosystem in the Veluwe. Dutch Priority Programme on Acidification 102.1.01, RIVM, Bilthoven, Netherlands, pp. 28 and appendixes.
Van der Salm, C., W. de Vries and J. Kros, 1994. Validation of soil acidification models with different degrees of process aggregation on an intensively monitored spruce site. In: S. Trudgill (ed.): Solute modelling in catchment systems (submitted).
Van der Zee, S.E.A.T.M., 1988. Transport of reactive contaminants in heterogeneous soil systems. Ph.D. thesis, Wageningen Agricultural University, Wageningen, Netherlands.

Van Genuchten, M. Th., 1980. A closed form for predicting the hydraulic conductivity of unsaturated soils. Soil Sci. Soc. Am. J., 44: 892-898.
Van Grinsven, J.J.M., 1988. Impact of acid atmospheric deposition on soils. Quantification of chemical and hydrological processes. Ph.D. thesis, Wageningen Agricultural University, Wageningen, Netherlands, pp. 215.
Van Grinsven, J.J.M., C.T. Driscoll and A. Tiktak, 1995. Comparison of Forest-Soil-Atmosphere models and application to the Norway spruce site in Solling (FRG). In: J.J.M. van Grinsven (ed.). Modelling water, carbon and nutrient cycles in forests: application of 16 simulation models to a spruce stand at Solling, Germany. Accepted to Ecological Modelling.
Van Grinsven, J.J.M., P.H.M. Janssen, J.G. van Minnen, C. van Heerden, J.J.M. Berdowski and R. Sanders, 1991. SoilVeg: A model to evaluate effects of acid atmospheric deposition on soil and forest. Volume 2: Uncertainty analysis. Dutch Priority Programme on Acidification report no. 114.1-03, RIVM, Bilthoven, Netherlands, pp. 61.
Van Grinsven, J.J.M., J. Kros, N. van Breemen, W.H. van Riemsdijk and E. van Eek, 1989. Simulated response of an acid forest soil to acid deposition and mitigation measures. Neth. J. Agric. Sci. (37):279-299.
Van Grinsven, J.J.M. and G.B. Makaske, 1993. A one dimensional-model for transport and accumulation of water and nitrogen, based on the Swedish model 'SOILN'. National Institute of Public Health and Environmental Protection report no. 714908001, Bilthoven, Netherlands, pp. 107.
Van Grinsven, J.J.M., N. Van Breemen and J. Mulder, 1987. Impacts of acid atmospheric deposition on woodland soils in the Netherlands. I.: Calculation of hydrological and chemical budgets. Soil Sci. Soc. Am. J. (51):1629-1634.
Van Heerden, C., J.M. van Grinsven and A. Tiktak, 1995. Simulation of forest stress for the Solling spruce site with SoilVeg. In: J.J.M. van Grinsven (ed.). Modelling water, carbon and nutrient cycles in forests: application of 16 simulation models to a spruce stand at Solling, Germany. Accepted to Ecological Modelling.
Van Heerden, C. and R.D. Yanaï, 1995. Effects of stresses on forest growth in models applied to the Solling spruce site. In: J.J.M. van Grinsven (ed.). Modelling water, carbon and nutrient cycles in forests: application of 16 simulation models to a spruce stand at Solling, Germany. Accepted to Ecological Modelling.
Van Veen, J.A., 1977. The behaviour of nitrogen in the soil: a computer simulation model. Ph.D. thesis, Free University Amsterdam, Amsterdam, Netherlands, 164 pp.
Walters, M.B. and P.B. Reich, 1989. Response of Ulmus Americana seedlings to varying nitrogen and water status. 1. Photosynthesis and growth. Tree Physiology (5):159-172.
Wesselink, L.G., 1994. Time trends and mechanisms of soil acidification. Ph.D. thesis, Wageningen Agricultural University, Wageningen, Netherlands, pp.129.
Wösten, J.H.M, G.J. Veerman en J. Stolte, 1994. Waterretentie- en doorlatendheidskarakteristieken van boven- en ondergronden in Nederland: De Staring reeks. Vernieuwde uitgave 1994. Tecnnisch document 18, SC-DLO, Wageningen, Netherlands, pp. 66 (In Dutch with English summary).